CHALMERS

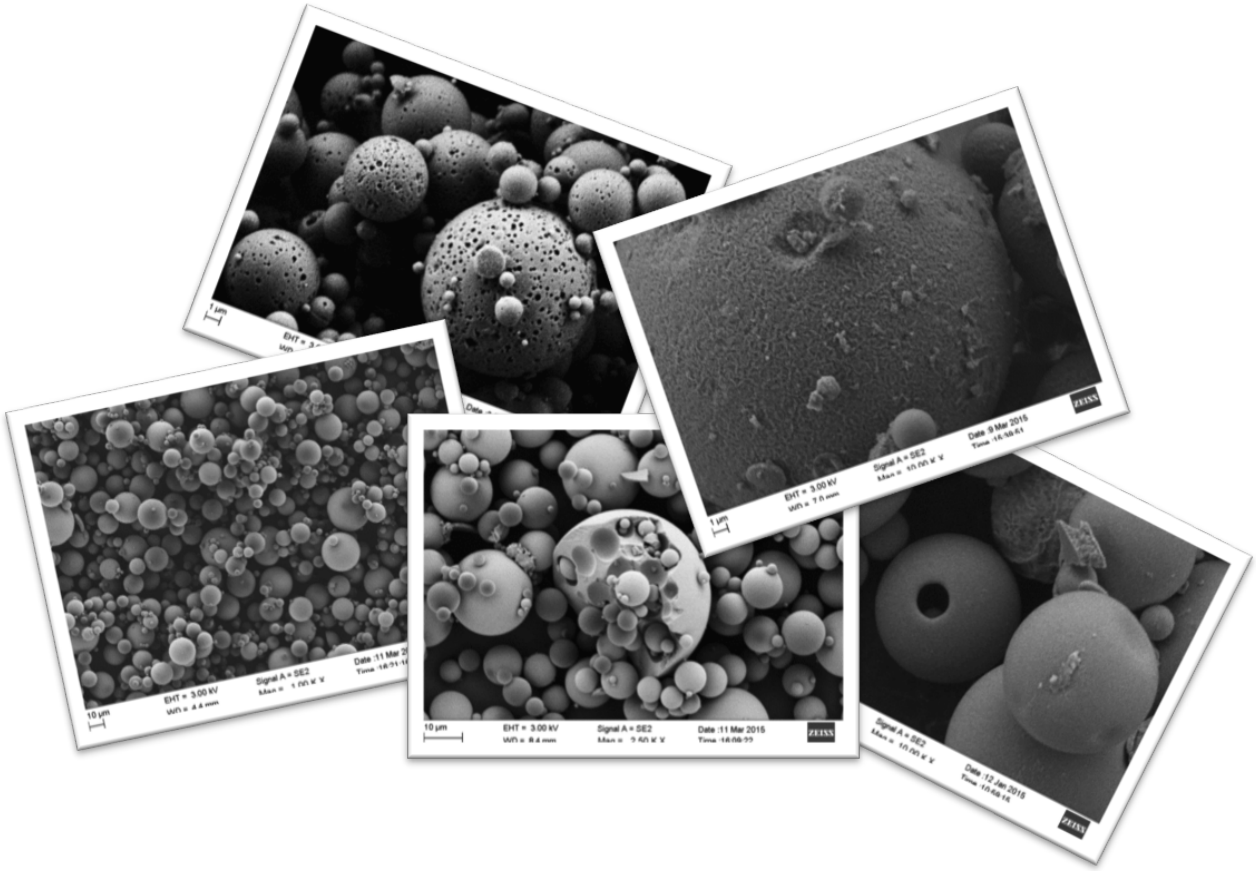

Microstructural Design of Porous Silica

Master's thesis in Materials Chemistry and Nanotechnology

JOHANNA JONSSON
MARCUS JOSEFSSON

Department of Chemistry and Chemical Engineering
Division of Applied Chemistry
CHALMERS UNIVERSITY OF TECHNOLOGY
Göteborg, Sweden 2015
Master's thesis 2015

MASTER'S THESIS IN MATERIALS CHEMISTRY AND NANOTECHNOLOGY

Microstructural Design of Porous Silica

JOHANNA JONSSON
MARCUS JOSEFSSON

Department of Chemistry and Chemical Engineering
Division of Applied Chemistry
CHALMERS UNIVERSITY OF TECHNOLOGY
Göteborg, Sweden 2015

Microstructural Design of Porous Silica
JOHANNA JONSSON
MARCUS JOSEFSSON

Master's thesis 2015
ISSN 1652-8557
Department of Chemistry and Chemical Engineering
Division of Applied Chemistry
Chalmers University of Technology
SE-412 96 Göteborg
Sweden
Telephone: +46 (0)31-772 1000

Cover:
SEM images of porous silica particles synthesized during the master thesis.

Chalmers Reproservice
Göteborg, Sweden 2015

Microstructural Design of Porous Silica
Master's thesis in Materials Chemistry and Nanotechnology
JOHANNA JONSSON
MARCUS JOSEFSSON
Department of Chemistry and Chemical Engineering
Division of Applied Chemistry
Chalmers University of Technology

Abstract

Material functionalities, such as defined diffusion properties and mass transport in general, are of great importance for the overall performance of many products today. In a sustainable society, material design will be an important research area for producing effective products specialized for its dedicated purpose. Porous silica is a material of great interest due to the natural abundance of silica, the unique properties of the material and its wide range of applications. The microstructure, such as pore size, shape and morphology, as well as total pore volume will influence the diffusion and flow properties in the material. These properties have to be optimized for a specific application and it is therefore of interest to see how the microstructure can be controlled.

In this master thesis, porous silica particles were produced by the so-called "emulsion and solvent evaporation" (ESE) method which had been optimized for the specific system. The purpose of this master thesis can be divided into two major parts; adapt the ESE-method for using a larger primary particle size and developing a toolbox for microstructural design of spherical porous silica particles of μm-size.

The ESE-method was successfully changed by using a larger primary particle and spherical porous particles were synthesized. By introducing ammonium acetate into the system the pore volume and the average pore size of the porous particles was substantially increased. A clear correlation was observed between the amount of ammonium acetate and the surface roughness of the porous particles, where a higher amount of ammonium acetate led to a rougher surface. Two types of porous particles, i.e. hollow particles and particles with well distributed voids, were synthesized with the addition of an organic template. By using a two-step synthesis and multiple sols, both with and without organic template, porous particles with a bimodal pore distribution could be obtained.

Keywords: Silica, Porous, Microstructure, Material Design, ESE, Organic Template, Toolbox

Preface

We would like to thank everyone who has helped us during this master thesis. Thank you to **Anders Mårtensson** for helping us with SEM, thanks to **Anne Wendel** for educating us on BET analysis and thanks to **Esa Väänänen** for helping us with our experimental setup.

We would like to give a great thank you to **Adjunct Prof. Michael Persson** and **Dr. Magnus Palmlöf** at AkzoNobel for giving us this oppurtunity and giving us very good ideas for the project.

Our supervisor, **Dr. Romain Bordes**, deserves a big thank you for answering our endless questions and having long discussions with us.

Göteborg, May 2015

Johanna Jonsson
Marcus Josefsson

Contents

Abbreviations

BET	Brunauer, Emmett, Teller. A method for calculating specific surface area and porosity
BJH	Barrett, Joyner, Halenda. A method for calculating pore size distribution
BzOH	Benzyl alcohol
EHEC E230	Water soluble non-ionic hydroxyethyl cellulose emulsifier
ESE	Emulsion with Solvent Evaporation
FT1	Fiber Template 1
RT	Room Temperature
SEM	Scanning Electron Microscopy
S1	Silica sol 1
S2	Silica sol 2
S3	Silica sol 3
ST1	Spherical Template 1
ST2	Spherical Template 2
ST3	Spherical Template 3

rpm	Revolutions Per Minute
vol%	Volume percent
wt%	Weight percent

1

Introduction

1.1 Background

Material functionalities, such as defined diffusion properties and mass transport in general, are of great importance for the overall performance of many products today. To mention a few, these products include food, wound care, drug delivery, diapers and cosmetics. In a sustainable society, material design will therefore be an important research area for producing effective products specialized for its dedicated purpose.

Porous materials have been used for centuries but the growing need for improved sustainability, such as energy consumption and protection of the environment, has led to a revival of research on porous materials [1]. The presence of pores inside a material increases its surface area which enhances the possibility of the material to interact with surrounding molecules and gives it unique properties that cannot exist in homogenous bulk materials [1, 2]. Porous materials can have numerous applications such as in separation, sensoring, controlled release, catalysis and more. Porous materials can be divided into three different categories depending on the pore size; microporous (pore size <2 nm), mesoporous (2-50 nm) and macroporous (>50 nm) [3]. The pore structure can either be closed or open and the pores can have different shapes [1].

Porous silica is a material of great interest due to the natural abundance of silica, the unique properties of the material and its wide range of applications [4]. The field of mesostructured silica has over the last several years attracted a lot of attention because of its multitude of possible applications [5, 6]. The main characteristics of mesoporous silica is a high surface area, high porosity and tuneable pore size. These properties are often desirable in applications such as catalysis, separation and controlled release.

The microstructure, such as pore size, shape and morphology, as well as total pore volume will influence the diffusion and flow properties in the material [7]. These prop-

erties have to be optimized for a specific application and it is therefore of interest to see how the microstructure can be controlled. For instance, in applications regarding transport and release of active molecules, diffusion rate, which is mostly controlled by the porosity, is of great importance and flow properties play a key role in separation applications.

There are a number of methods for synthesizing porous silica. In this master thesis, porous silica particles were produced by the so-called "emulsion and solvent evaporation" (ESE) method which has been optimized by Duong and Lu [8] for this specific system. The basic concept of the ESE-method is to create a water-in-oil emulsion together with a silica sol which will go into the dispersed phase, i.e. the water droplets. Upon evaporation of the water, the droplets will shrink in size and force the primary silica particles to organize in a spherical shape and eventually gel. This creates μm-sized porous silica particles. The ESE-method is further described in section *2.4.2. Emulsion and Solvent Evaporation Method*. This thesis will investigate how the microstructure of porous silica, in the aforementioned method, can be controlled by introducing new parameters.

1.2 Aim

The purpose of this master thesis could be divided into two major parts. As the first aim we will try to adapt the ESE-method used by Duong and Lu [8] for using a larger primary silica particle and build μm-sized spherical porous silica particles. The second aim is to start developing a toolbox for microstructural design of spherical porous silica particles in the μm-size range. This will be accomplished in three different ways; by induced gelling to vary the overall porosity, templating with organic particles which will be removed during calcination or by using multiple silica sols to create different types of porous structures within the particle. These three strategies will also be combined to investigate the effect on the microstructure.

1.3 Delimitations

A model system is used to develop the different microstructures in the master thesis. Porous silica particles of μm-size are produced by the ESE-method. The process conditions of the method have been optimized by Doung and Lu [8] and are therefore kept as constant as possible during the master thesis. By limiting the microstructural design to μm-sized particles many of the difficulties with defects and cracks often occurring for larger monolithic bodies can be reduced or avoided.

1.4 Overall Strategy

An overview of the experimental strategy can be seen in Figure 1.1. The project starts with synthesizing μm-sized porous silica particles from the silica sol used in previous

investigations [8] to ensure a well-functioning experimental setup. The method is then changed by using a larger primary silica particle as precursor. When this is successfully implemented, small alterations can be made to the method leading to two tracks. One track is based on the concept of silica chemistry; e.g. altering the pH value or salt concentration during the synthesis to affect the formation of the porous silica particles or by using multiple silica sols to create several pore types. The other track is based on addition of an organic template during the synthesis to form well-defined structures. The two tracks are also combined during the master thesis.

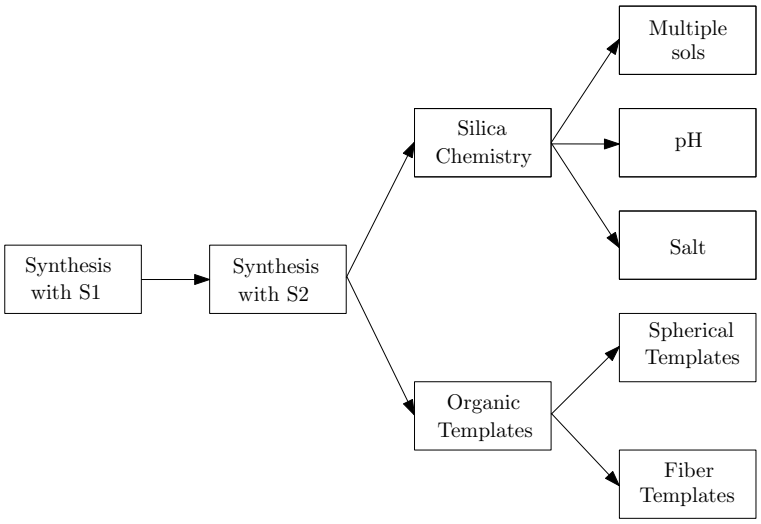

Figure 1.1: The overall strategy of the project where two main tracks are followed. S1 is a silica sol with a particle size of 7 nm and S2 a silica sol with a particle size of 22 nm. Both silica sols are stabilized by ammonium.

2

Theoretical Background

The following paragraphs will provide the knowledge necessary for understanding the model system, i.e. the ESE-method, used in the master thesis as well as the possibilities for altering the microstructure of porous silica particles based on the synthesis parameters. First the general concept of colloidal systems and emulsions will be described in more detail. This is followed by information about silica and sol-gel chemistry before the ESE-method will be presented. Finally, the characterization methods used in the master thesis are briefly described.

2.1 Colloidal Systems

A colloidal dispersion includes a collection of small particles, droplets or bubbles of one phase, having at least one dimension between 1 to 1000 nm, dispersed in a second phase [9]. The phases can either be gas, liquid, solid (crystalline or amorphous) or supercritical phase states, see Table 2.1. Colloidal particles are larger in size than atoms and also overlapping with the regime of nanoparticles. They therefore have properties that differ from those of the constituent atoms or molecules but yet also differ from macroscopic materials. The dispersed phase is very small hence the impact of gravitational forces is negligible and the interactions are mainly due to short-range forces such as van der Waals forces [10]. Colloidal particles have a high surface-area-to-volume ratio and the properties of the surface are therefore very important and leads to unique macroscopic properties [9].

Table 2.1: Common colloidal systems [9].

		Dispersed Phase		
		Liquid	*Solid*	*Gas*
Continuous Phase	*Liquid*	Emulsion	Sol, suspension	Liquid aerosol
	Solid	Sol, suspension	Solid suspension	Solid aerosol
	Gas	Foam	Solid Foam	-

There are two types of colloidal dispersions; lyophobic, thermodynamically unstable, and lyophilic, thermodynamically stable, dispersions [9]. Lyophilic colloids are thermodynamically stable and will therefore form spontaneously when the two phases are brought together. Lyophobic colloids do not form spontaneously and therefore mechanical energy needs to be added to create the colloidal dispersion. This can be obtained by some form of stirring such as that provided by a propeller-style mixer, a colloid mill or an ultrasound generator.

In this master thesis two colloidal systems are of great interest; lyophilic sols and lyophobic emulsions. A number of different sols will be used as precursors in synthesis which consist of silica nanoparticles in water solutions. An emulsion will be utilized during the synthesis step of the project.

2.2 Emulsions

An emulsion is a colloidal dispersion where a liquid is dispersed in a continuous liquid phase with another composition [9]. Emulsions can contain droplets of a bigger size than what is stated in *2.1 Colloidal Systems*. For emulsions it is common that one of the phases is aqueous and the other a hydrocarbon, referred to as the oil. In a so-called oil-in-water emulsion (O/W) oil droplets are dispersed in water, and vice versa for a water-in-oil emulsion (W/O). Most emulsions are not thermodynamically stable, however, rather stable emulsions can exist that resist phase separating for years. To increase the stability of an emulsion, an emulsifying agent (or stabilizer) can be added. This is often a surfactant, macromolecule and/or small solid particles.

2.2.1 Emulsion Stability

There are a number of processes that can cause an emulsion to collapse such as Ostwald ripening, sedimentation/creaming, aggregation and coalescence [9, 11]. Ostwald ripening is a result of the difference in solubility between the small and large droplets. The smaller emulsion droplets have a higher solubility due to the effect of curvature on surface free energy. The bigger droplets will grow at the expense of the smaller droplets which disappear over time. Sedimentation/creaming occurs as a result of differences in density

of the dispersed and continuous phase and create two separate layers with different concentrations of the dispersed phase. Aggregation is when two or more emulsion droplets clump together but keep their identity, hence the total surface area barely changes. However, the droplets lose their kinetic independence since the aggregates move as a single unit. Aggregation of emulsion droplets might cause coalescence which is when two droplets merge to form a larger particle. This will in the end result in two separated phases and a reduced surface area of the dispersed phase. The stability of the dispersion to aggregation and coalescence depends on how the dispersed species interact over time.

For lyophobic emulsions the degree of kinetic stability is very important [9]. Even though they are not thermodynamically stable, the small size and large surface area as well as the presence of an interfacial film can cause the emulsion droplets to be fairly kinetically stable. In practice emulsions can be stable enough to last for days, months or even years.

The emulsion droplets can be stabilized by either repulsion from the electric double layer or steric hindrance [9]. If the particle surface is covered with long chain molecules the steric repulsion between the particles might be significant. This repulsion is caused by osmotic effect, i.e. there is an elevated concentration of long chain molecules between the emulsion droplets. The thermodynamic driving force is to even out the concentration gradient and therefore the droplets are separated. The repulsion might also be caused by volume restriction that appears when the chains overlap and lose possible conformations.

The so-called DLVO-theory combines the attractive van der Waals forces and the repulsive forces from the electrostatic double layer and is another way of describing the stability of emulsions [11]. The electric double layer consists of a charged surface as well as an excess of counter-ions distributed close to the surface that neutralize the net charge, see Figure 2.1 [9]. It is composed of two layers; an inner layer that includes adsorbed ions and a diffuse layer where counter-ions are distributed. As particles come close to each other their electric double layers overlap which result in columbic repulsive forces that act against the destabilization process, hence increases the distance between the emulsion droplets.

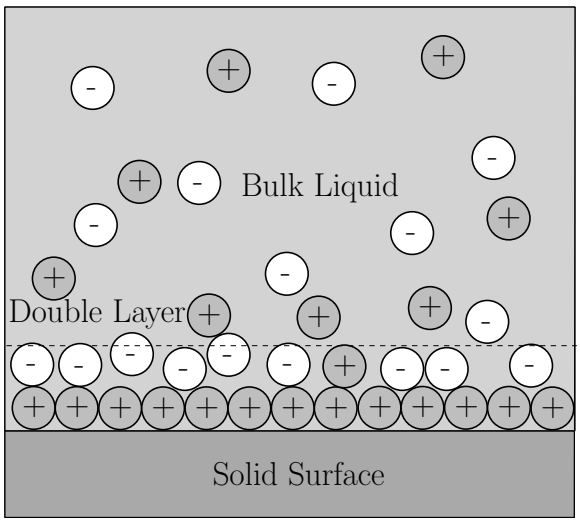

Figure 2.1: The electrical double layer at a negatively charged surface.

In this master thesis the only requirement on the stability of the emulsion was that it did not phase separate during the reaction time, i.e. less than 10 h.

2.2.2 Emulsifiers

An emulsifier, usually a surfactant, may be used to facilitate the formation of an emulsion or prevent it from collapsing [9]. The emulsifying agent is situated at the liquid-liquid interface and has a number of effects on the emulsion; it can have an influence on droplet size and distribution, the mean droplet size and therefore emulsion viscosity. The emulsifier stabilizes the emulsion by lowering the interfacial tension between the dispersed and continuous phase, increases the surface elasticity and viscosity as well as increases the electric double layer repulsion, if an ionic surfactant is used. The best result is achieved if the emulsifiers have a limited solubility in both the dispersed and continuous phase.

In this master thesis a water soluble non-ionic ethyl hydroxyethyl cellulose called EHEC E230 (AkzoNobel Performance Additives, Sweden) was used as emulsifier [12].

2.3 Silica

Silica, or silicon dioxide - SiO_2, is one of the main component of the earth crust [13]. Together with aluminium, magnesium, calcium and iron, it forms silicate minerals that make up 90 % of the earth's outer crust and constitutes one-third of all minerals. The functional unit in silica and the silicate minerals is the SiO_4 tetrahedron, where the silicon has a tetrahedral structure with four surrounding oxygen atoms [14]. Since the oxygen ion, O^{2-}, is much larger than the silicon ion, Si^{4+}, the four oxygens in the tetrahedral

SiO_4 structure will all be in mutual contact with each other and the silicon is placed in the tetrahedral hole. The tetrahedral SiO_4 building blocks are rigid but the hydroxyl groups on the silica surface, see Figure 2.2, can in a reaction form siloxane bonds, Si-O-Si, which are fairly flexible [4].

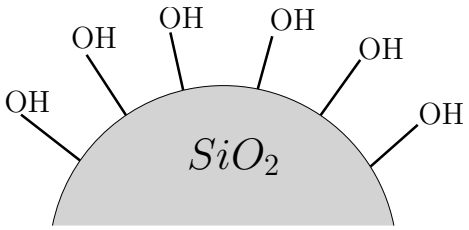

Figure 2.2: Silica particles with hydroxyl groups on the surface.

Silica has a high chemical resistivity against water and acids, only hydrofluoric acid and phosphoric acid can dissolve it [15]. Because of its high transmission of visible and ultraviolet light, silica is useful as a material for optical applications. Silica also has excellent insulating properties.

2.3.1 Collidal Silica

As described in section *2.1 Colloidal Systems*, a colloidal system has unique properties. Iler [16] has defined the term colloid silica as a stable dispersion, or a sol, of discrete particles of amorphous silica. In the 1940s stable silica sols, i.e. sols that did not gel or settle out in several years, became available. The development of synthetic ion exchange resins made it possible to synthesize uniform colloidal particles larger than 5 nm in diameter if stabilized with the right amount of base. This development has also made it possible to synthesize larger particles with a higher amount of silica in the dispersion. Because of its unique properties colloidal silica is used for various applications and with different functions such as binder, stiffener, coating material and as a stabilizing agent in the weave structure of fabrics [16, 17].

Concentrated silica sols are stabilized against interparticle siloxane bonding by either an ionic charge on the particles resulting in electrostatic repulsion or an adsorbed layer of inert material which separates the particles based on steric repulsion [16]. The most common for commercial sols is that they are stabilized by ionic charge in the presence of an alkali. The stability of a silica sol is also dependent on the concentration of silica as well as the size of the silica sol particles.

Under some conditions the stability of silica sols cannot be described by the DLVO-theory, an example is when the silica sol is in an acidic solution (pH 2), see Figure 2.4 [16]. The charge of the silica particle is then close to zero but still at a relatively slow aggregation rate. However, in an alkaline environment, when the particles are highly charged, they

are stabilized by the electrical double layer and the DLVO-theory is applicable.

2.3.2 Mesoporous Silica

The porosity of a porous material is the fraction of the bulk volume that is occupied by pores [18]. There are two types of pores, one that forms a continuous phase within the material and another that consists of closed pores or voids dispersed in the medium. The latter mentioned does not contribute to mass transport through the porous material. A mesoporous material is, by the definition of IUPAC, a porous structure where the pores are 2-50 nm in size [19]. The morphology of the pores can be different, (e.g. cylindrical, spherical and many other) and the arrangement can be varied (e.g. disordered, wormhole-like, hexagonal, cubic and lamellar mesophase), see Figure 2.3. To be classified as a mesoporous material at least one dimension needs to be in the meso range [19, 20].

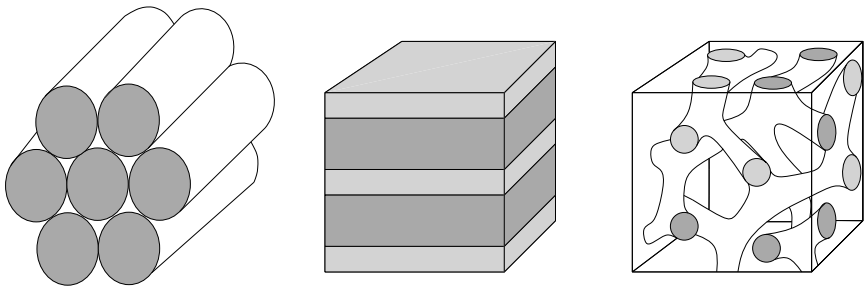

Figure 2.3: Different pore morphologies, from left to right; hexagonal, lamellar and wormhole-like/branched arrangements.

Mesoporous silica has a very high surface area as well as low density and these unique properties give it a wide range of different application areas [7]. The pore surfaces can be coated with other atoms or molecules to enhance a specific function. Mesoporous silica has been considered as a large-pore analogue of zeolites and is used for catalysis in different industrial processes [21]. Due to its high surface area and well-structured pores mesoporous silica is used as the stationary phase in High Performance Liquid Chromatography (HPLC) [7]. Mesoporous silica is used as a carrier for the active substance in drug delivery and as a biosensor in biomedical applications [22, 23].

The most common strategy for synthesis of highly ordered mesoporous silica is by using the template method [20]. Cationic surfactants are used as templates which spontaneously self-assemble and together with the silica precursor form different shapes and arrangements of a mesoporous structure. The dimensions, morphology and thermodynamics of the surfactant-silica assembly are strongly dependent of the kinetics of the sol-gel chemistry. Therefore, the mesostructure, pore size and morphology can be tailored by adjusting parameters such as the pH value of the reaction mixture, the reaction temperature, the surfactant used as well as the silica and water content.

2.4 Sol-Gel Chemistry

The two following paragraphs will describe the silica sol-gel process in general and also give a more detailed description of the method used in this master thesis. The silica sol-gel process is important since it is the process which creates the porous silica particles in the ESE-method used in the master thesis.

2.4.1 The Silica Sol-gel Process

A sol is a suspension of solid particles in a continuous liquid phase [10]. The silica sol-gel process is based on hydrolysis and condensation reactions of suitable silica precursors [4, 10]. The reaction occurs according to Reaction 2.1

$$Si(OR)_4 + H_2O \rightarrow HO - Si(OR)_3 + ROH \tag{2.1}$$

where R is either a hydrogen or another ligand [10]. Depending on the amount of water present, the reaction might go to completion or only parts of the precursor might be hydrolysed. Two partially hydrolysed molecules can react in a condensation reaction according to Reaction 2.2.

$$(OR)_3Si - OR + HO - Si(OR)_3 \rightarrow (OR)_3 - Si - O - Si - (OR)_3 + ROH \tag{2.2}$$

The reactions above can generate larger silica-based molecular networks since the hydrolysis and condensation reactions lead to formation of siloxane bonds, Si-O-Si, at the expense of the precursor silica molecules.

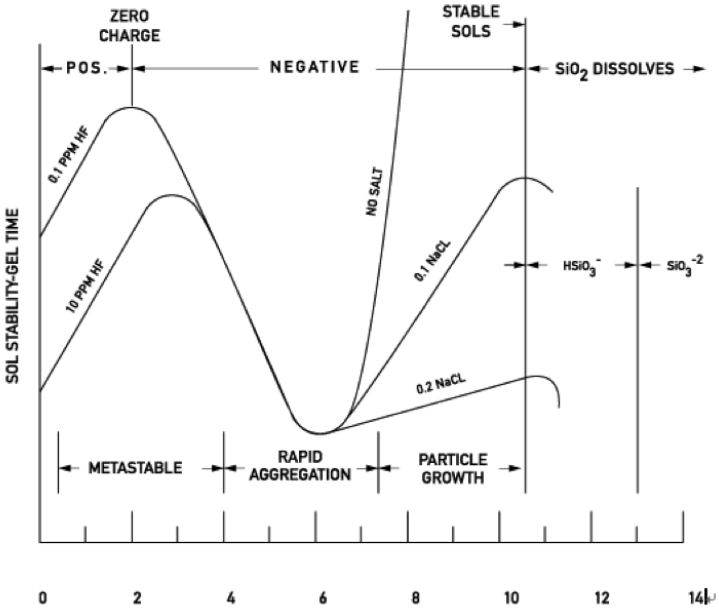

Figure 2.4: Effects of pH in the colloidal silica-water system. Copyright John Wiley & Sons. Adapted with permission [16].

Silica particles with sufficiently low surface charge can come into contact and form siloxane bonds which is the basic step in gel formation [16]. In the pH range 3 to 5 the gel time decreases with pH, see Figure 2.4, and is proportional to the concentration of hydroxyl ions which have a catalytic effect on the formation of siloxane bonds. Above pH 6, the limiting factor of gelling is no longer the lack of hydroxyl ions. Instead, particles will have a higher charge density leading to a greater electrostatic repulsion and therefore fewer collisions, thus the rate of aggregation decrease. However, as Figure 2.4 shows, rapid aggregation occurs between pH 4 and 7. Addition of salt will screen the electrical double layer and the silica particles can come closer and aggregate. The decrease in gelling time is dependent on the concentration of salt added. By changing salt concentration and pH value, there is a number of ways of altering the aggregation rate, and therefore the time of gelling.

When doing sol-gel processes with silica it is most common to start from tetraethyl orthosilicate (TEOS) [24], however, in this master thesis a precursor dispersion of silica nanoparticles was used instead, see section *3.1 Materials*.

2.4.2 The Emulsion and Solvent Evaporation Method

Controlling morphology and internal mesostructure of surfactant templated silica presents a challenge, especially when scaling up laboratory synthesis to industrial scale [25]. The emulsion and solvent evaporation (ESE) method has a number of advantages, one being easily scaled up while providing control over stoichiometric homogenity of templating sur-

factant and inorganic precursor. The ESE-method can be used to synthesize well-ordered mesostructured particles and it allows control over synthesis parameters and therefore particle properties such as particle morphology, mesostructure and pore size [26]. For instance, particle sizes and distributions can be determined by manipulating droplet size within the used water-in-oil emulsion [25].

The typical synthesis method consist of five distinct steps; *(1)* preparation of precursor solution, *(2)* emulsification of the precursor solution in oil, *(3)* aging by solvent removal, *(4)* separation of the mesostructured particles from the continuous phase, and *(5)* surfactant removal by calcination [25]. The procedure used in this master thesis was not exactly the same as described above, see Figure 2.5 for the basic steps, however, the concept remains the same.

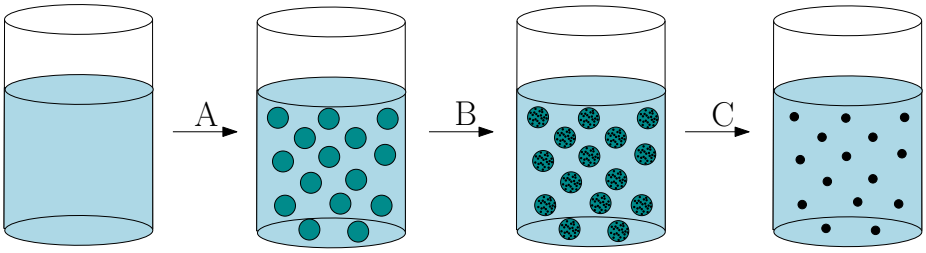

Figure 2.5: Schematic image of the ESE-method used in the master thesis. *Step A* an W/O emulsion is created, *Step B* silica sol is added to the emulsion and *Step C* the water is evaporated. This was follow by work-up of the product, i.e. filtration and calcination.

The continuous phase is an oil, commonly a hydrocarbon, and water is the dispersed phase containing the inorganic silica precursor and the templating molecules, often surfactants [25]. The oil's ability to allow transport of water out from the emulsion droplets during evaporation and tendency for not diffusing into the aqueous emulsion droplets are two important factors for the choice of oil in the continuous phase. The water-in-oil emulsion is formed in bulk by vigorous stirring which result in a rather broad particle size distribution [26, 27]. Since a narrow size distribution is often wanted, this presents a challenge [27].

As the water is evaporated from the dispersed droplets the concentration of precursor and templating material is increased and, assuming a surfactant is used as templating material, micellization occurs [27]. When the solvent is fully evaporated, the silica gels around the surfactant structures forming mesoporous particles. This is followed by calcination which removes organic materials, such as template, and a well ordered mesoporous silica material is formed.

In this master thesis, benzyl alcohol was used as the oil phase and organic particles as templating material instead of surfactants.

2.5 Characterization Methods

In the following section a short theory of the different characterization methods used in the thesis will be described. Optical microscopy was used in an early stage for controlling if synthesized particles were spherical. SEM was then used for studying the microstructure of the synthesized porous particles and BET measurements was performed to investigate the surface area and porosity.

2.5.1 Optical Microscopy

To view real-time images of a sample optical microscopy can be used [28]. The most basic parts of an optical microscope are the eyepiece, condenser, objective and the light source. The light travels from the light source into the condenser which focus the light into a small area of the sample. The diffracted light is collected by the object which produces a magnified real image close to the eyepiece. An optical microscope operates mainly in two primary modes; the transmission or reflection mode [29]. In transmission mode the light source and the objective are placed on the opposite side of the analysed sample and in reflection mode they are placed at the same side, which means that the specimen can be of any thickness. It is possible for most of the optical microscopes to operate in both modes.

2.5.2 Scanning Electron Microscopy

Scanning electron microscopy (SEM) is mostly used for studying the surface of particles larger than 5 nm [30]. The method employ an electron beam that is constricted by a magnetic lens to give a thin probe (1-10 mm) that travels point-by-point over the surface thus scanning it. The interactions between the sample and the electron beam give rise to a number of emissions such as secondary, reflected and transmitted electrons as well as X-ray radiation. These can be registered and converted to electrical signals which are amplified and fed to a cathode-ray tube resulting in images which are displayed.

An advantage of SEM is that it delivers a great amount of information [30], however, long scanning times are needed to achieve high resolution. When doing SEM, the sample needs to be conductive to prevent charge build-up of the sample [31]. If the sample is non-conductive, gold particles can be sputtered on the sample to form a conductive coating.

2.5.3 Determination of Surface Area and Porosity

The specific surface area is defined as the interstitial surface area of pores in the material and is dependent on both size and shape of the particle [9, 18]. The specific surface area is important in many applications, for instance catalysis where the surface area determine the adsorption capacity and therefore the effectiveness of the material. The porosity is defined as the fraction of the bulk volume that is occupied by pores [18].

The total surface area and the porosity of a material can be estimated by measuring the amount of gas needed to form an adsorbed monolayer by physical adsorption [9]. The process of adsorption will occur until the adsorbed layer is in thermodynamic equilibrium with the gas used for the measurements [18]. An adsorption isotherm can be created which shows the relationship between the equilibrium amount of gas adsorbed and the gas pressure at constant temperature [9]. Desorption of the gas can also be measured and presented as an isotherm. Figure 2.6 shows the two isotherms for adsorption and desorption from a BET analysis performed during the thesis.

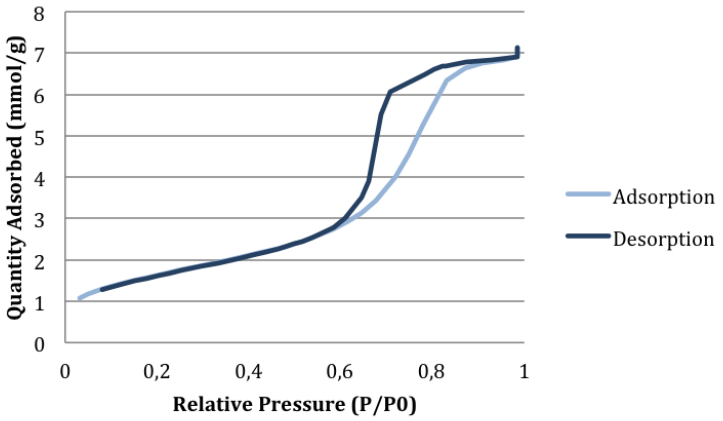

Figure 2.6: The adsorption and desorption curves measured by BET for porous silica particles synthesized during the project.

Empirical methods are used to mathematically interpret the data from the isotherms and can thereby determine the surface area and porosity [32]. In this master thesis, the BET method was used for calculating the surface area of the porous particle and the BJH method was used for obtaining information about the porosity, i.e. pore size and pore volume.

3

Experimental Procedure

The following paragraphs contain information about the materials used in the project, pre-experiments performed in continuous phase as well as the procedure for synthesis and characterisation of the porous silica particles.

3.1 Materials

As emulsifier non-ionic ethyl hydroxyethyl cellulose[1] was used. The organic solvent used was benzyl alcohol (99%, Acros Organics). Three different silica sols; S1[2], S2[3] & S3[4], were used which are described in Table 3.1. The organic templates; ST1[5], ST2[6], ST3[7] & FT1[8], used during the project are described in Table 3.2.

Other chemicals used were ammonium acetate (≥98 %, Sigma-Aldrich), acetic acid (≥99 %, Sigma-Aldrich) and sodium chloride (≥99 %, Sigma-Aldrich).

[1] EHEC E230 (AkzoNobel Performance Additives, Sweden)
[2] Experimental silica sol (Akzonobel PPC, Sweden)
[3] Bindzil (AkzoNobel PPC, Sweden)
[4] Alumina doped Bindzil (AkzoNobel PPC, Sweden)
[5] Surelease type NF 8, grade E-7-19020 (Colorcon, United Kingdom)
[6] SP CE 28 (AkzoNobel PPC, Sweden)
[7] SP AE 76 (AkzoNobel PPC, Sweden)
[8] Experimental MFC, batch 140277 (Stora Enso, Sweden)

Table 3.1: Information of the silica sols used during the master thesis.

	Stabilized by	**Surface Area** (m^2/g)	**Particle Size** (nm)	**pH**	**Comment**
Silica Sol 1 (S1)	Ammonium	400	7	9.4	
Silica Sol 2 (S2)	Ammonium	130	22	9.2	
Silica Sol 3 (S3)	Sodium	220	15	10.2	Alumina doped (1.4 wt%)

Table 3.2: Information of the organic templates used during the master thesis.

	Chemical Information	**Template Charge**	**Counter Ion**	**Density** (g/cm^3)	**Diameter** & **Length** (nm)
Fiber Template 1 (FT1)	Micro Fibrillated Cellulose	Negative	Sodium	1.6	20 & 1500
Spherical Template 1 (ST1)	Ethyl Cellulose	Negative	Ammonium	1.2	120
Spherical Template 2 (ST2)	Styrene/acrylic copolymer	Positive	Chloride	1.2	30
Spherical Template 3 (ST3)	Styrene/acrylic copolymer	Negative	Sodium	1.2	65

3.2 Continuous Phase Experiments

Pre-experiments in continuous phase were performed in order to define suitable conditions that could be implemented into the dispersed phase in the reactor. These continuous

phase experiments included compatibility tests, gelling with salts such as ammonium acetate or sodium chloride as well as gelling by lowering the pH of the silica sol.

3.2.1 Compatibility Tests

All the components, i.e. emulsifier, silica sol, templates and ammonium acetate, used in the master thesis were mixed independently to control their compatibility with each other. No visual aggregation, sedimentation or increase in viscosity should occur during mixing.

3.2.2 Gelling by Ammonium Acetate

A 2 M or 5 M ammonium acetate solution was added to a 14 wt% S2 dispersion in different amounts resulting in concentrations ranging from 0.1 to 0.6 M. The pH value was measured instantly upon addition of the ammonium acetate. The time for gelling was measured by the invert test tube technique, i.e. the sample tube was turned upside down to confirm that gelling had occurred. The pH value was also measured after (if) the sample gelled.

3.2.3 Gelling by Ammonium Acetate in Presence of Organic Template

A 2 M or 5 M ammonium acetate solution was added to a 14 wt% S2 dispersion, where 10 vol% of the silica had been exchanged for organic template ST1, in different amounts resulting in concentrations ranging from 0.35 to 0.6 M. The pH value was measured instantly upon addition of the ammonium acetate. The time for gelling was measured by the invert test tube technique. The pH value was also measured after (if) the sample gelled.

3.2.4 Gelling by Sodium Chloride

A 2 M sodium chloride solution was added to a 14 wt% S2 dispersion in different amounts resulting in concentrations ranging from 0.3 to 0.6 M. The pH value was measured instantly upon addition of the salt. The time for gelling was measured by the invert test tube technique. The pH value was also measured after (if) the sample gelled.

3.2.5 Gelling by Acetic Acid

When performing pH induced gelling experiments 1 M acetic acid was added to a 10 ml 14 wt% or 40 wt% S2 dispersions to obtain a range of pH values, see Table 4.1.

3.3 Synthesis of Porous Silica Particles

In this section the different procedures for the syntheses performed during the master thesis will be presented; the reference synthesis, synthesis with ammonium acetate,

organic templates or multiple sols as well as variations/combinations of these syntheses. Schematic images that describe the different routes are presented in *Appendix B*.

3.3.1 The Reference Synthesis

Route I 0.25 g of emulsifier was dissolved in 25 g of water (1 wt% emulsifier) and stirred until the emulsifier was fully dissolved, at least 10-15 min. Benzyl alcohol, 307.5 g, was poured into the reactor (0.5 L double-jacketed glass reactor) and the 1 wt% emulsifier dispersion was added during stirring at 450 rpm (IKA Werke, Eurostar Digital, Germany) and room temperature. The stirring was continued for 20 minutes until a water-in-oil emulsion was formed. The stirring was lowered to 350 rpm before 58.5 g of 14 wt% silica sol was added and the stirring continued for 60 min at room temperature. Stirring was lowered to 275 rpm and the first evaporation step was initiated; the reactor was heated to 65 °C by a heating circulator (Thermo Scientific, Haake B3, controller Haake DC1, USA) and the pressure in the system was lowered to 160 mbar with a vacuum pump (Büchi, V-720, vacuum controller V-850, Switzerland). The heat and reduced pressure was applied until the water was evaporated, approximately 2 h. The temperature of the heating circulator was then increased in the second evaporation step to give a reactor temperature of 80 °C for around 30 min to ensure full evaporation of the water.

The product, i.e. the porous silica particles, was collected by centrifugation (Alc International, 4233ECT, Italy) of the obtained reactor slurry for 20 min at 2500 rpm, the precipitate was dissolved in acetone and filtered (Robu Glas, Por. 3, Germany) under vacuum. The product was then washed with acetone and water and left in the fume hood over-night, dried on a hot plate for 20 min the day after and finally dried at 100 °C in an oven (Electro Helios, 28452C, Sweden) for 12 h. The dry product was calcined in a furnace (Nabertherm, controller P 330, Germany) to remove organic material such as emulsifier and template. A temperature program was used which raised the temperature from room temperature to 650 °C at constant rate during 8 h, the temperature was kept at 650 °C for 4 h and finally the system was cooled to room temperature.

3.3.2 Synthesis with Ammonium Acetate

Route IIa was performed as *Route I* with an additional step. Before the silica sol was added to the reactor it was mixed with a 5 M ammonium acetate solution for 5 min to achieve concentration 0.05 or 0.4 M in the reactor. The incubation time, i.e. the time between addition of ammonium acetate and start of evaporation, was set to 65 min. The work-up was then performed as in *Route I*.

Route IIb was performed as *Route I* with an additional step. Before evaporation was started a 5 M ammonium acetate solution was added to achieve concentrations ranging from 0.3 to 0.6 M in the reactor. The incubation time was set to 0 min. The work-up was then performed as in *Route I*.

3.3.3 Synthesis with Organic Template

Route IIIa was performed as *Route I* with an additional step. The silica sol was mixed with organic template for 30 min before it was added to the reactor. The work-up was then performed as in *Route I*.

Route IIIb was performed as *Route I* with an additional step. The emulsifier dispersion was mixed with the organic template for 20 min before addition to the reactor. The work-up was then performed as in *Route I*.

When doing synthesis where an organic template was added a certain vol% of the added silica was exchanged for the template. For templates ST1 and ST3, synthesis was performed with three different amounts of template; 10, 15 or 20 vol% and for ST2 as template, 10 vol% was used. For FT1, synthesis with 1, 2, 5, 7 or 10 vol% template was performed.

3.3.4 Synthesis with Organic Template and Ammonium Acetate

Route IVa was performed as *Route I* with two additional steps. Before the silica sol was added to the reactor it was mixed with organic template for 15 min. Thereafter a 5 M ammonium acetate solution was added and stirred with the sol and template for 5 min before addition to the reactor to achieve a concentration of 0.46 M in the reactor. The incubation time was set to 0 min. The work-up was then performed as in *Route I*.

Route IVb was performed as *Route I* with two additional steps. The silica sol was, before addition to the reactor, mixed with organic template and before evaporation was started a 5 M ammonium acetate solution was added to achieve concentrations ranging from 0.3 to 0.6 M in the reactor. The incubation time was ranging from 0 to 30 min. The work-up was then performed as in *Route I*.

When doing synthesis with both addition of ammonium acetate and organic template 10 vol% of the silica was exchanged for template ST1.

3.3.5 Synthesis with Multiple Sols

Route Va was performed as *Route I* with an exception. The added silica sol dispersion was a 14 wt% 1:1 mixture of silica sols S2 and S3.

Route Vb was a two-step synthesis where the first batch of porous silica particles were synthesized according to *Route I* until the first evaporation step was finished. Before the second step of evaporation was started the temperature was lowered to room temperature (below 30 °C), pressure returned to atmospheric pressure and stirring increased to 350 rpm. A second batch of 14 wt% silica sol was added and stirred for 1 h. Evaporation at 65 °C and 160 mbar was then performed for 2 h before evaporation was continued at

80 °C for 30 min. The work-up was then performed as in *Route I*.

Route Vc was a two-step synthesis where the first batch of porous silica particles were synthesized according to *Route I* until the first evaporation step was finished. Before the second step of evaporation was started the temperature was lowered to room temperature (below 30 °C), pressure returned to atmospheric pressure and stirring increased to 450 rpm. A second batch of 1 wt% emulsifier dispersion was added and stirred for 20 min. Stirring was lowered to 350 rpm and a second batch of 14 wt% silica sol was added and stirred for 1 h. Evaporation at 65 °C and 160 mbar was then performed for 2 h before evaporation was continued at 80 °C for 30 min. The work-up was then performed as in *Route I*.

Route Vd was a two-step synthesis where the first batch of porous silica particles were synthesized according to *Route I* until half the amount of water had been evaporated in the first evaporation step. Before the evaporation was continued the temperature was lowered to room temperature (below 30 °C), pressure returned to atmospheric pressure and stirring increased to 350 rpm. A second batch of 14 wt% silica sol was added and stirred for 1 h. Evaporation at 65 °C and 160 mbar was then performed for 2 h before evaporation was continued at 80 °C for 30 min. The work-up was then performed as in *Route I*.

3.3.6 Synthesis with Multiple Sols and Organic Template

Route VIa was a two-step synthesis where the first batch of porous silica particles were synthesized according to *Route I* until the first evaporation step was finished. Before the second step of evaporation was started the temperature was lowered to room temperature (below 30 °C), pressure returned to atmospheric pressure and stirring increased to 450 rpm. A second batch of 1 wt% emulsifier dispersion was added and stirred for 20 min. Stirring was lowered to 350 rpm and a second batch of 14 wt% silica sol, mixed with organic template for 30 min, was added and stirred for 1 h. Evaporation at 65 °C and 160 mbar was then performed for 2 h before evaporation was continued at 80 °C for 30 min. The work-up was then performed as in *Route I*.

Route VIb was a two-step synthesis where the first batch of porous silica particles were synthesized according to *Route IIIa* until half the amount of water had been evaporated in the first evaporation step. Before the evaporation was continued the temperature was lowered to room temperature (below 30 °C), pressure returned to atmospheric pressure and stirring increased to 350 rpm. A second batch of 14 wt% silica sol was added and stirred for 1 h. Evaporation at 65 °C and 160 mbar was then performed for 2 h before evaporation was continued at 80 °C for 30 min. The work-up was then performed as in *Route I*.

When doing synthesis with multiple sols and organic template 10 or 15 vol% of the silica was exchanged for ST3 in the second batch sol, for *Route VIa*, and in the first batch sol, for in *Route VIb*.

3.4 Characterization of Porous Silica Particles

The following methods were used for characterizing the synthesized silica particles.

3.4.1 Optical Microscopy

When looking at the particles in an optical microscope (Zeiss, Scope A1 Axio, AxioCam MRc5, Germany) the product was dispersed in distilled water. Magnification ranging from 10 to 40x was used.

3.4.2 Scanning Electron Microscopy

SEM (Zeiss, LEO Ultra 55, Germany) was performed to get a better understanding about the microstructure of the porous silica particles. Both non-crushed and crushed samples were studied to investigate both the surface and internal structure of the particles. The samples were placed as powders on the sample holders by conductive tape, followed by sputtering with gold in argon (Edward Sputter Coater S150 B, United Kingdom). A secondary ion beam detector and EDX detector were used for the analysis.

3.4.3 Determination of Surface Area and Porosity

The surface area, pore volume and pore size were determined by BET. 100 to 300 mg of sample was weighed in and dried (Micromeritics, Smartprep, USA) under nitrous atmosphere at 225 °C for 3 hours before mounting in the instrument (Micromeritics, Tri-star, USA). The surface area was calculated by the BET model and the porosity, i.e. average pore size and pore volume, was calculated by the BJH method.

3.4.4 Determination of Mean Particle Size and Size Distribution

For determining the mean size and size distribution of the synthesized particles an image recognition programme was used in Matlab. The images used were obtained by optical microscopy of calcined particles dispersed in slightly basic water (pH 9). At least 2000 particles were taken into account during the size characterization.

4

Results and Discussion

The following paragraphs will present the results from the master thesis. First the results from continuous phase experiments will be presented and thereafter the results from the syntheses. For the synthesized particles optical microscopy was used in an early stage to determine if the particles were spherical. SEM was used to study the surface and microstructure of the particles more closely. Results from BET measurements will show information about the surface area, average pore size and total pore volume of the synthesized particles.

4.1 Continuous Phase Experiments

Alteration of the aggregation rate of the silica particles, by changing salt concentration or pH, might create new porous structures in the silica particle. Due to this, some gelling experiments were performed in a continuous silica sol phase, i.e. no emulsion was used, to find suitable pH values and salt concentrations which could later be integrated into the synthesis, i.e. in dispersed phase. Compatibility tests of emulsifier, silica sols and organic templates respectively were also performed. The aim of these tests was to make sure that introducing new components to the system would not cause major emulsion failure in the reactor.

It is important to note that the gelling time of the experiments performed in continuous phase are not directly transferable to syntheses performed in dispersed phase since the environment in the emulsion droplets will be different. For example, in the reactor there was a good controlled continuous mixing and the reactor was heated which will decrease the gelling time. The continuous experiments performed were used as guidelines for finding the initial conditions to apply to the syntheses in the reactor.

4.1.1 Compatibility Tests

To get a good dispersion of silica sol in all the droplets of the emulsion during the synthesis it would be an option to first stir and then add the silica sol with the emulsifier.

However, when mixing a 1 wt% emulsifier dispersion with a 14 wt% S2[1] dispersion a viscous and lumpy mixture was formed why it was determined to add these in separate stages to the reactor as done in previous work [8].

When mixing a 14 wt% S2 dispersion with the organic templates used in the project no complications arose except for when the silica sol was mixed with template ST2[2] where aggregation and sedimentation occurred due to them having opposite charge. When mixing different sols no problems could be observed based on appearance of the mixture.

4.1.2 Gelling by Ammonium Acetate

Ammonium acetate was chosen for salt studies due to that ammonium is already present in the system as sol stabilizer and acetate is volatile and will therefore leave the system during evaporation and calcination. As seen in Figure 4.1, additions of 2 M or 5 M stock solution of ammonium acetate resulted in decreased gelling times.

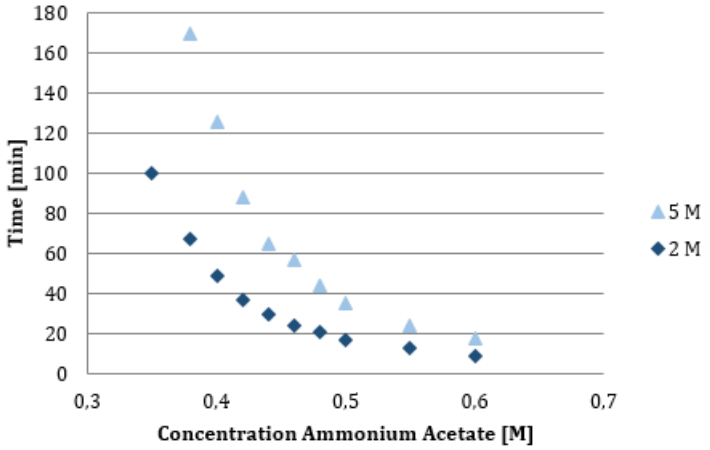

Figure 4.1: Gelling of a 14 wt% S2 dispersion with 2 M or 5 M ammonium acetate.

Ammonium acetate acts as a screening agent but also as a buffer and therefore the salt concentration as well as the pH value of the solution was affected when adding ammonium acetate, i.e. gelling time decreased due to both parameters. The pH value was measured upon addition of the ammonium acetate to investigate the effect and the results showed that the pH value was affected almost linearly of the added amount of ammonium acetate according to Figure 4.2. Since the pKa value of ammonium acetate is around 7 and the pH of the silica sol is above 9, addition of ammonium acetate will have buffering effect on system. This could be the reason for the initial drop in pH when ammonium acetate was added.

[1]Silica sol 2, 22 nm, ammonium stabilized
[2]Spherical template 2, positively charged, counter ion: chloride

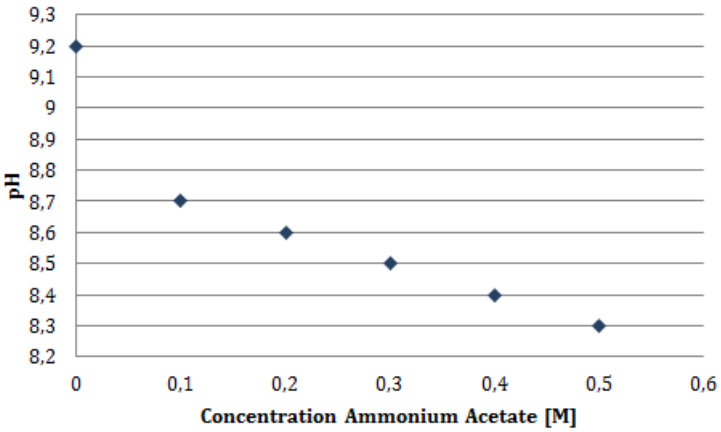

Figure 4.2: pH as a function of addition of a 2 M ammonium acetate solution to a 14 wt% S2 dispersion.

4.1.3 Gelling by Ammonium Acetate in Presence of Organic Template

Gelling experiments were also performed by addition of 2 M or 5 M ammonium acetate stock solution to a 14 wt% S2 dispersion with 10 vol% of the silica volume exchanged for template ST1[3], see Figure 4.3.

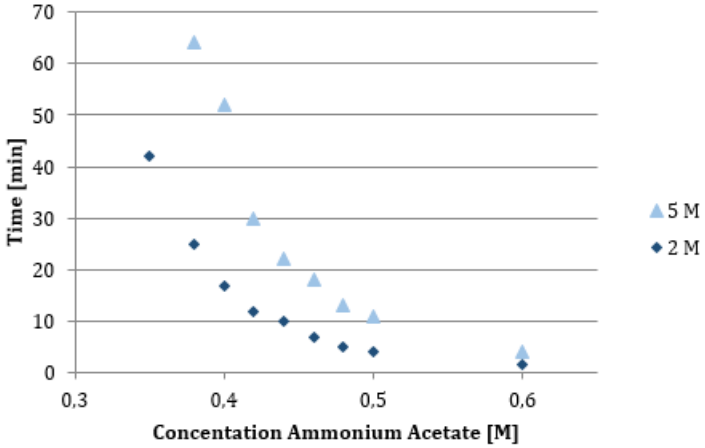

Figure 4.3: Gelling of 14 wt% S2 dispersion with 10 vol% of the silica volume exchanged with ST1 with 2 M or 5 M stock solutions of ammonium acetate.

When comparing these results with the results without added ST1, see Figure 4.1, it can be seen that the gelling time has been decreased substantially by the addition of

[3]Spherical template 1, negatively charged, counter ion: ammonium

the organic template. The introduction of ST1 will increase the ionic strength which would lead to a faster gelling. Also, Ji and Walz [33] has shown that the combination of nanoparticles and polymers has a synergistic effect of induced flocculation. The result above indicates that the combination of the small silica particles and the larger ST1 particles follows this concept and hence have synergistic effects of induced gelling.

4.1.4 Gelling by Sodium Chloride

In order to study only the effect of salt concentration on the gelling time, sodium chloride was used. The experiments showed that addition of sodium chloride did not decrease the gelling time as much as the additions of ammonium acetate, or ammonium acetate and ST1, at the same concentration, compare Figures 4.1, 4.3 and 4.4. A reason for this could be that the gelling with sodium chloride was not induced by simultaneous lowering of the pH value as for ammonium acetate. Therefore, the gelling was only affected by the increased screening effect induced by sodium chloride, i.e. the ionic strength.

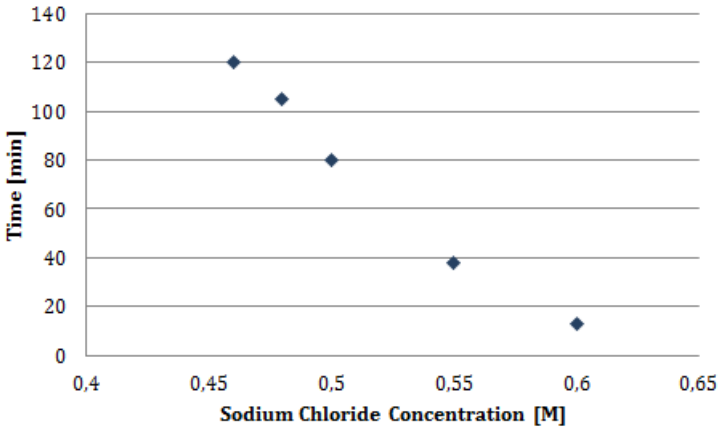

Figure 4.4: Gelling of a 14 wt% S2 dispersion with 2 M sodium chloride solution added.

The pH was measured after addition of sodium chloride showing that the pH was reduced compared to the original sols, i.e. pH 8.6 instead of 9.2. The pH value was lowered even though there was no buffer effect from the sodium chloride. An explanation for this is the result of condensation during the formation of siloxane bonds, see Reaction 2.2.

Samples with lower sodium chloride concentrations, 0.35 M to 0.4 M, were also prepared but the gelling time of these samples were long, and no exact gelling time was estimated.

4.1.5 Gelling by Acetic Acid

To investigate the effect of pH, gelling experiments were performed with acetic acid. When performing gelling experiment with acetic acid, 1 M acid was added to 10 ml 14

wt% or 40 wt% S2 dispersion to achieve a range of pH values, see Table 4.1.

Table 4.1: The additions of 1 M acetic acid to a 14 wt% or 40 wt% S2 dispersion and the resulting pH values.

Sample	**Silica Sol**	**Acetic Acid** (ml)	**pH**
Silica Sol	14 wt% S2	0	9.4
0	14 wt% S2	0.1	9.0
1	14 wt% S2	0.2	6.6
2	14 wt% S2	0.25	5.7
3	14 wt% S2	0.3	5.5
4	14 wt% S2	0.5	5.0
5	14 wt% S2	1.5	4.2
6	40 wt% S2	0.7	7.3
7	40 wt% S2	1.1	5.5
8	40 wt% S2	3.5	4.3

None of the samples above prepared from 14 wt% S2 dispersion gelled within a month. However, the turbidity of the samples differed, see Figure 4.5, which indicates that the samples have obtained various degree of aggregation. Samples having a higher turbidity scatter light more indicating that these samples should contain bigger or more aggregates. The most turbid samples, made from a 14 wt% silica sol, were samples 3 and 4 having pH values of 5.5 and 5 respectively. These samples were the only samples to gel within a couple of months. According to Iler [16], the most rapid aggregation occurs around pH 5.5, see Figure 2.4. This rapid aggregation in samples having a pH close to 5.5 might result in different arrangements and structures compared to the samples with different pH giving these samples other properties, e.g. light scattering properties. This could be a reason for why samples 3 and 4 have another visual appearance than the other samples.

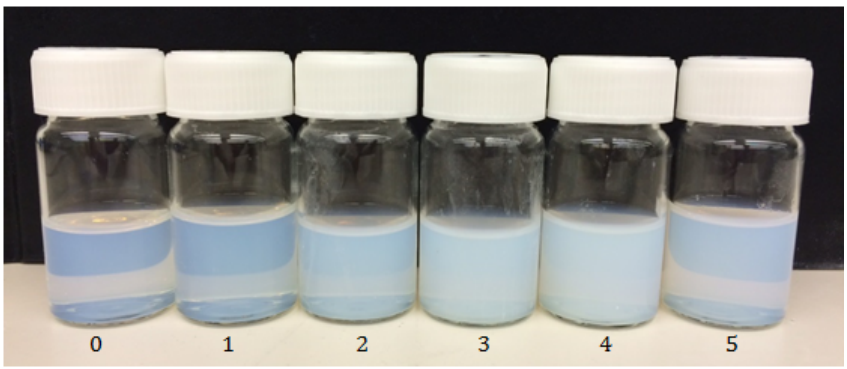

Figure 4.5: Gelation of 14 wt% S2 dispersion with acetic acid. The pH values of the samples range from 9 to 4.3.

According to Iler [16], a silica sol of higher concentration should gel faster than one with a lower concentration. Therefore, gelling tests were also performed on a 40 wt% S2 dispersion since an option might be to increase sol concentration to decrease gelling time. Three samples; sample 6, 7 and 8 were prepared according to Table 4.1. The samples gelled within days and as for the 14 wt% S2 dispersion a difference in turbidities could be seen, see Figure 4.6.

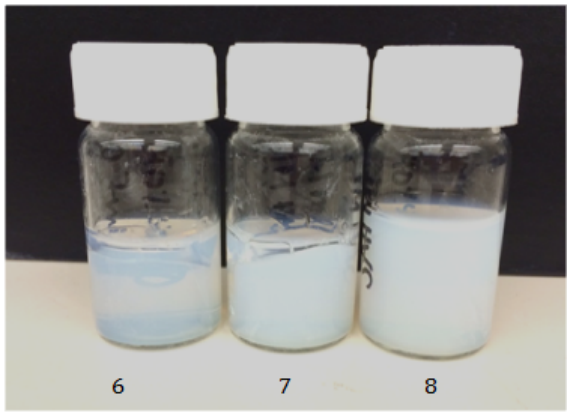

Figure 4.6: Gelation of 40 wt% S2 dispersion with acetic acid. From left to right; pH 7.3, 5.5 and 4.3.

Since the gelling time for the pre-experiments in continuous phase where acetic acid was used to induce gelling was too long, no experiments were performed with acetic acid in dispersed phase in the reactor.

4.2 Synthesis of Porous Silica Particles

Porous silica particles was synthesized by the ESE-method according to different routes, see section *3.3 Synthesis of Porous Silica Particles*. First results from the reference synthesis will be presented, follow by results from synthesis with addition of ammonium acetate and/or organic template. Thereafter the results for synthesis with multiple sols as well as multiple sols and organic template are presented. All the experiments performed in the reactor are described in more detail in *Appendix A*. Results from BET measurements for the synthesized spherical porous particles are presented in *Appendix C*. Finally, results for determining the particle size from the different syntheses of porous particles are presented in *Appendix D*.

4.2.1 The Reference Synthesis

Synthesis of μm-size silica particles was performed with a 14 wt% S1[4], S2[5] or S3[6] dispersion according to *Route I*. A schematic image of the reference synthesis with S2 dispersion can be seen in Figure 4.7.

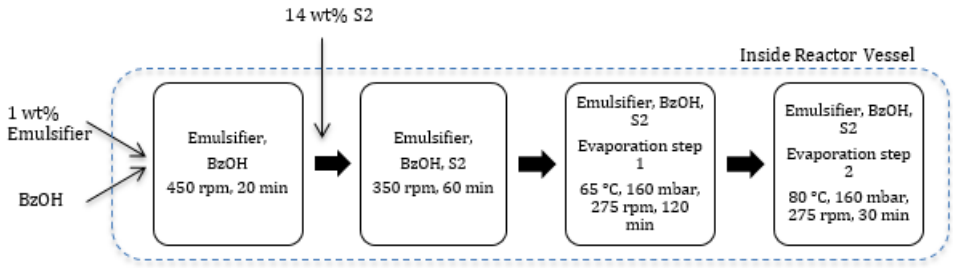

Figure 4.7: Schematic image describing *Route I* with S2 dispersion. When S1 or S3 were used as silica precursor the addition was made in the same manner as for S2.

Synthesis with each silica sol dispersion resulted in spherical porous particles which was confirmed by optical microscopy and SEM. Figure 4.8 show the results from synthesis with S2 dispersion as silica precursor. An optical microscopy image is shown in **A**, Figure 4.8, and images **B-D** show SEM images with increasing magnification. The surface of the particles was smooth which indicates a good packing of primary silica particles. However, as can be seen in images **C**, where a particle has been crushed, the cross-section of the particle was quite rough which is typical for porous materials. Therefore, even if the particles was smooth and seem to have a good packing of primary particles the final particles was highly porous.

[4]Silica sol 1, 7 nm, ammonium stabilized
[5]Silica sol 2, 22 nm, ammonium stabilized
[6]Silica sol 3, 15 nm, sodium stabilized, alumina doped

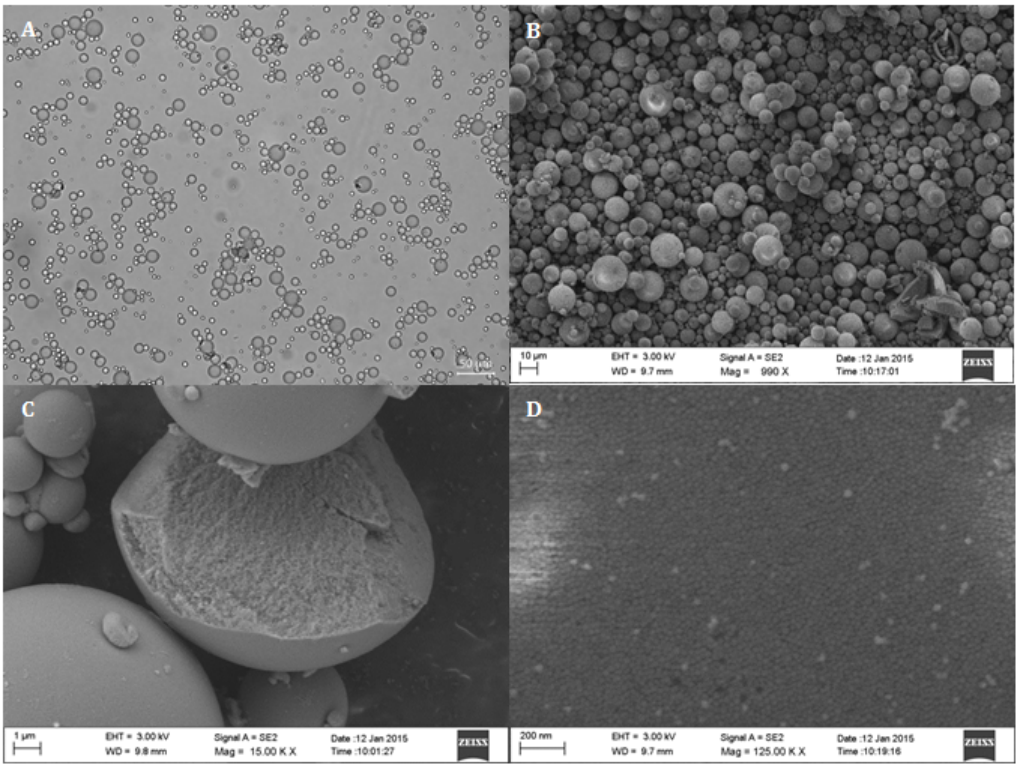

Figure 4.8: Porous particles synthesized according to *Route I* with a S2 dispersion. **A** shows an image from optical microscopy and **B-D** shows SEM images with increasing magnification. Image **C** shows the cross-section of a porous particle and in **D** the primary particles are visible.

This porosity was also confirmed by BET measurements, see Table 4.2, for particles synthesized with all silica sols by *Route I*. The results show that the pore volume decreases when using a silica sol with a larger primary particle size. The measured surface area for S1 and S2 was a little higher than expected, this could mean that the calcination conditions used were not optimal. The size of the primary particle seems to have a small impact on the mean size of the final porous particle.

Table 4.2: BET results for particles synthesized by *Route I* with silica sols S1, S2 and S3. The mean particle size and polydispersity for the particles are also shown.

	BET Surface Area (m^2/g)	**Average Pore Size** (Å)	**Pore Volume** (cm^3/g)	**Mean Particle Size** (μm)	**Polydispersity** (μm)
S1	400.6	43.6	0.5861	7.9	4.0
S2	134.6	59.2	0.2541	7.1	4.1
S3	186.5	44.3	0.2966	6.6	4.1

4.2.2 Synthesis with Ammonium Acetate

Synthesis was performed with addition of ammonium acetate to see how this affected the microstructure of the formed porous silica particles. The ammonium acetate concentration range was based on the experiments performed in continuous phase, see section *4.1.2 Gelling with Ammonium Acetate*, in an attempt to control the gelling time of the system. In order to make small changes to the gelling time in the droplets a new parameter was introduced called incubation time. In this master thesis, the incubation time was defined as the time from addition of ammonium acetate to the silica dispersion until initiating of the evaporation. In *Route IIa*, the silica sol and ammonium acetate was mixed for 5 min before addition to the reactor to ensure that a homogeneous mixture was obtained. Thereafter, the reactor components were mixed for 60 min before starting evaporation. The incubation time was therefore 65 min.

When doing synthesis according to *Route IIa* with 0.4 M ammonium acetate no, or very few, spherical particles were formed, see image **C** in Figure 4.9. This could be due to that the incubation was too long, i.e. 65 min. It might be possible that mm-sized gel beads had formed which were unable to form spherical porous particles and were so big that they were crushed by the impeller. But as can be seen in image **A**, spherical particles were formed when an ammonium acetate concentration of 0.05 M was used.

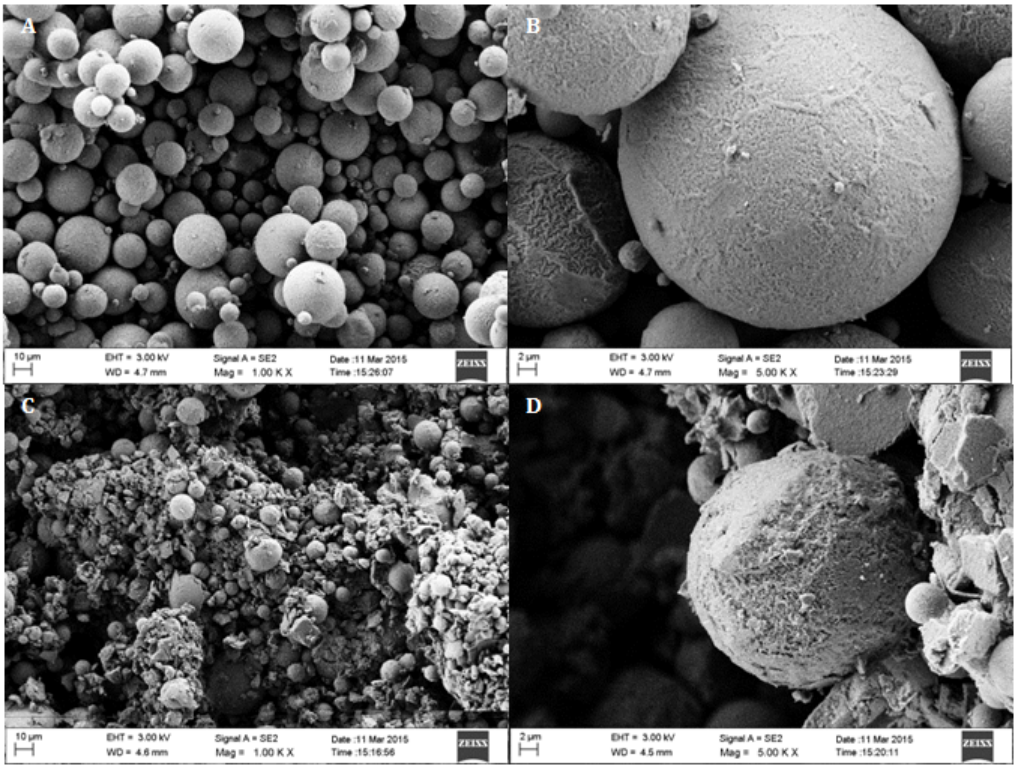

Figure 4.9: SEM images showing porous particles synthesized by *Route IIa* with different concentrations of ammonium acetate in the reactor and an incubation time of 65 min. **A-B** 0.05 M ammonium acetate and **C-D** 0.4 M ammonium acetate.

When doing synthesis according to *Route IIa* the emulsion had a different appearance compared to when synthesizing particles according to *Route I*. At 0.4 M ammonium acetate, gel beads of mm-size formed and sedimented in the reactor which was more apparent as the evaporation prolonged.

Route IIb was performed to see how the synthesized particles would be affected if the ammonium acetate was added in a later stage of the synthesis, i.e. when the silica sol already was well dispersed in the emulsion droplets. Therefore the ammonium acetate was added just prior to the initiation of the evaporation, i.e. the incubation time was 0 min. Synthesis according to *Route IIb* with ammonium acetate concentrations in the reactor ranging from 0.3 to 0.6 M was performed. For the high concentration of ammonium acetate the system should gel in an early stage of the evaporation, while for the low concentration the gelling should be affected at a later stage of the evaporation. According to Figure 4.1, 0.6 M ammonium acetate in the reactor should gel the system within 20 min, if a stock solution of 5 M was used. At that time, the temperature in the reactor will still be increasing, therefore the evaporation will nearly have begun and the amount of water evaporated will be low.

Synthesis according to *Route IIb* resulted in spherical porous particles, however, more defects can be seen in these particles than in particles synthesized according to *Route I*, i.e. fewer and less spherical particles were formed, see Figure 4.10.

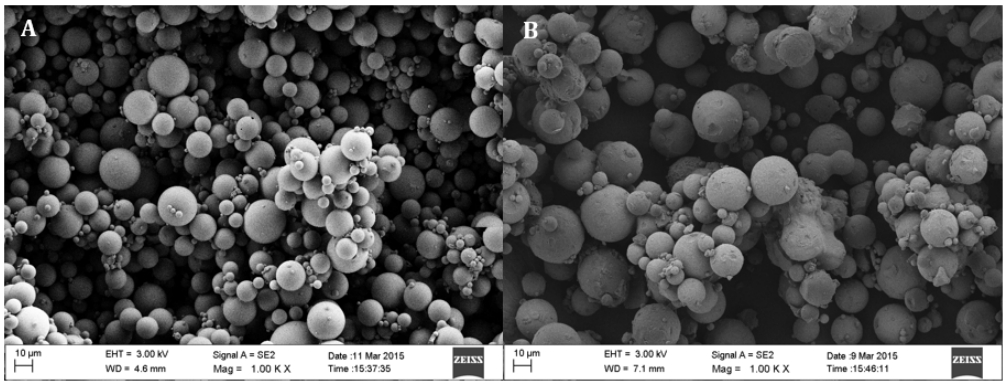

Figure 4.10: SEM images showing porous particles synthesized by **A** *Route I* and **B** *Route IIb* with 0.46 M ammonium acetate.

When studying the SEM images in Figure 4.11 more closely it can be seen that particles synthesized with a higher concentration of ammonium acetate had a rougher surface than particles synthesized with a lower concentration. This increased roughness should arise due to bigger silica aggregates forming before the final porous particles are formed during evaporation. Therefore the silica particles are not built up by only primary particles but instead irregular silica aggregates made of a relatively small number of primary particles creating a rougher surface.

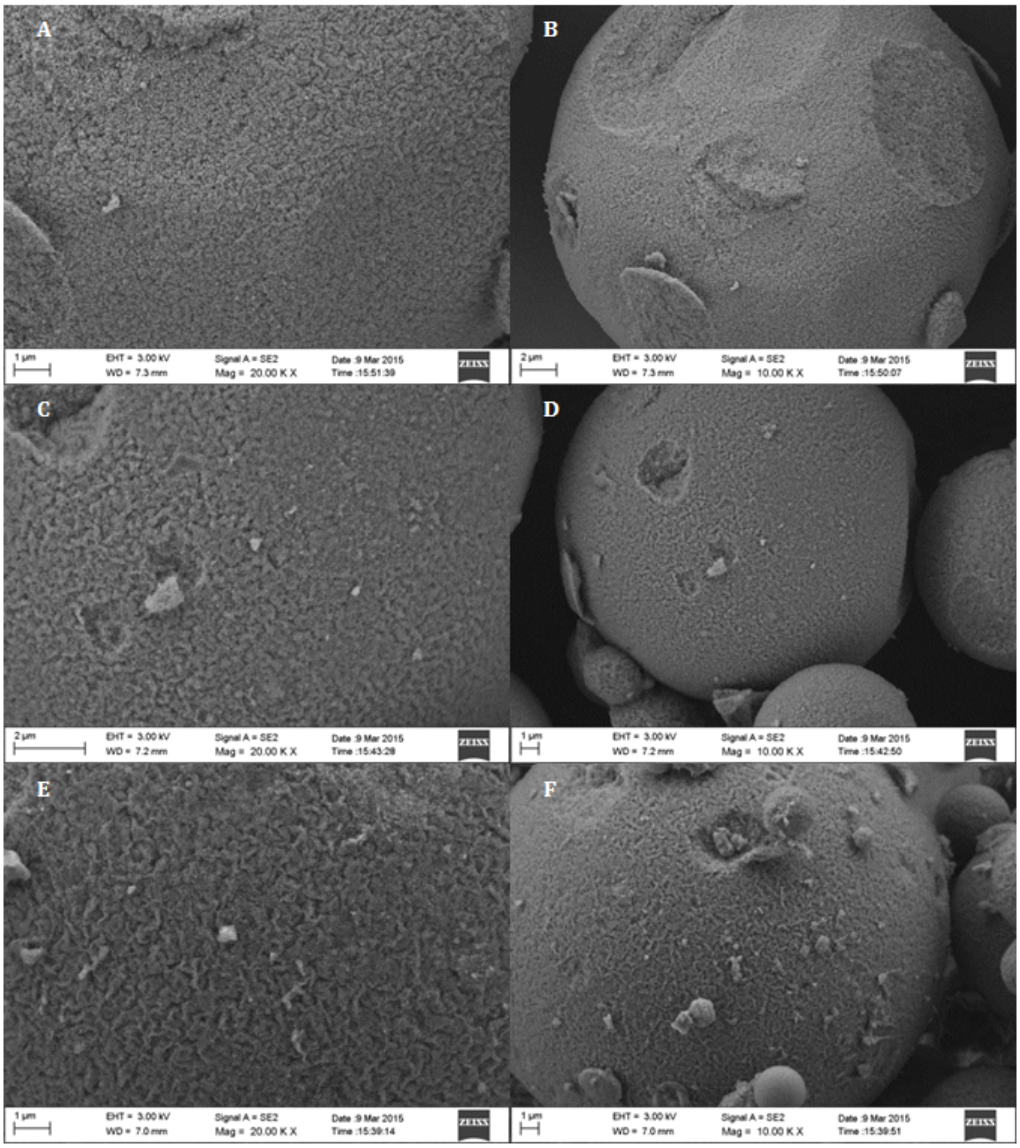

Figure 4.11: SEM images showing porous particles synthesized by *Route IIb* with different concentrations of ammonium acetate in the reactor and an incubation time of 0 min. **A-B** 0.3 M ammonium acetate, **C-D** 0.46 M ammonium acetate and **E-F** 0.6 M ammonium acetate.

When doing synthesis with addition of ammonium acetate by *Route IIb* the emulsion had a different appearance compared to synthesis by *Route I*. As for *Route IIa*, mm-sized gel beads formed and sedimented during some synthesis. The reason for this in *Route IIb* could be that so-called hot spots were formed during addition of the ammonium acetate to the reactor, i.e. locally there was an increased concentration of ammonium acetate which caused rapid aggregation resulting in big aggregates which sedimented or were

crushed by the impeller. The quality of the emulsion, based on amount of aggregation and sedimentation, for synthesis by *Route IIb* with 0.3, 0.46 or 0.6 M ammonium acetate varied. During synthesis with 0.46 M ammonium acetate, no aggregation or sedimentation occurred. For synthesis with 0.3 M ammonium acetate small gel beads formed and sedimented, for 0.6 M ammonium acetate bigger gel beads formed and sedimented.

From the results for *Routes IIa-b*, the quality of the emulsion does not seem to be only dependent on the concentration of ammonium acetate. One of the parameters that differs between the syntheses was the time of addition of the ammonium acetate to the reactor which could be the crucial parameter. The time of addition, in this project ranging from 30 to 120 s, needs to be optimized to get a better emulsion. However, this was not controlled during the master thesis and therefore the time of addition was mostly dependent on the experimentalist.

For particles synthesized in the presence of ammonium acetate, it seems likely that the sphericity of the particles is dependent on the ammonium acetate concentration in the reactor as well as the time where the primary silica particles are in contact with the ammonium acetate before the evaporation has started, i.e. the incubation time.

The surface area, average pore size and pore volume for porous particles synthesized by *Route IIa-b* were calculated from BET measurements and the results are presented in Table 4.3. Since the particles synthesized according to Route IIa with 0.4 M ammonium acetate were not spherical, no BET measurement was performed on those particles. When comparing the results for particles synthesized with ammonium acetate, by both routes, with results for particles synthesized by *Route I* a large increase can be seen in both average pore size and pore volume. Therefore we can conclude that addition of ammonium acetate to the system could be a way to increase the pore size or pore volume.

Table 4.3: Result from BET measurement for synthesis with ammonium acetate according to *Route IIa-b*. The surface area was calculated with the BET model while the average pore size and pore volume were calculated with the BJH method for the desorption curve. BET measurements for particles synthesized by *Route I* with S2 is shown as a reference.

	Salt concentration in reactor (M)	**Surface Area** (m^2/g)	**Average Pore Size** (Å)	**Pore Volume** (cm^3/g)
Route I	0	134.6	59.2	0.2541
Route IIa	0.05	132.2	129.9	0.5000
Route IIb	0.3	117.0	133.0	0.4544
Route IIb	0.46	133.6	124.8	0.4819
Route IIb	0.6	127.1	117.9	0.4302

No clear trend can be seen in the BET results for *Route IIb* which is difficult to explain. To clarify this, experiments should be performed where, for instance, the conditions for addition of ammonium acetate is controlled and a lower concentration range is tested.

4.2.3 Synthesis with Organic Template

One of the aims with this project was to create pore structures by introducing organic templates during synthesis which could then be removed during calcination. A number of templates were used; one fiber and three spherical, see Table 4.4.

Table 4.4: Information of the organic templates used during the master thesis.

Organic Template	**Chemical Information**	**Template Charge**	**Counter Ion**	**Glass Transition Temp.,** (T_g) °C	**Diameter** & **Length** (nm)
Fiber Template 1 (FT1)	Micro fibrillated cellulose	Negative	Sodium	N/A	20 & 1500
Spherical Template 1 (ST1)	Ethyl Cellulose	Negative	Ammonium	60	120
Spherical Template 2 (ST2)	Styrene/acrylic copolymer	Positive	Chloride	70	120
Spherical Template 3 (ST3)	Styrene/acrylic copolymer	Negative	Sodium	74	65

4.2.3.1 Fiber Template

For synthesis by *Route IIIa* with template FT1 mostly spherical particles were obtained, see Figure 4.12. As can be seen in image **A** and **C**, increased addition of FT1 during synthesis decreased the number of spherical particles and the amount of non-spherical artefacts increased.

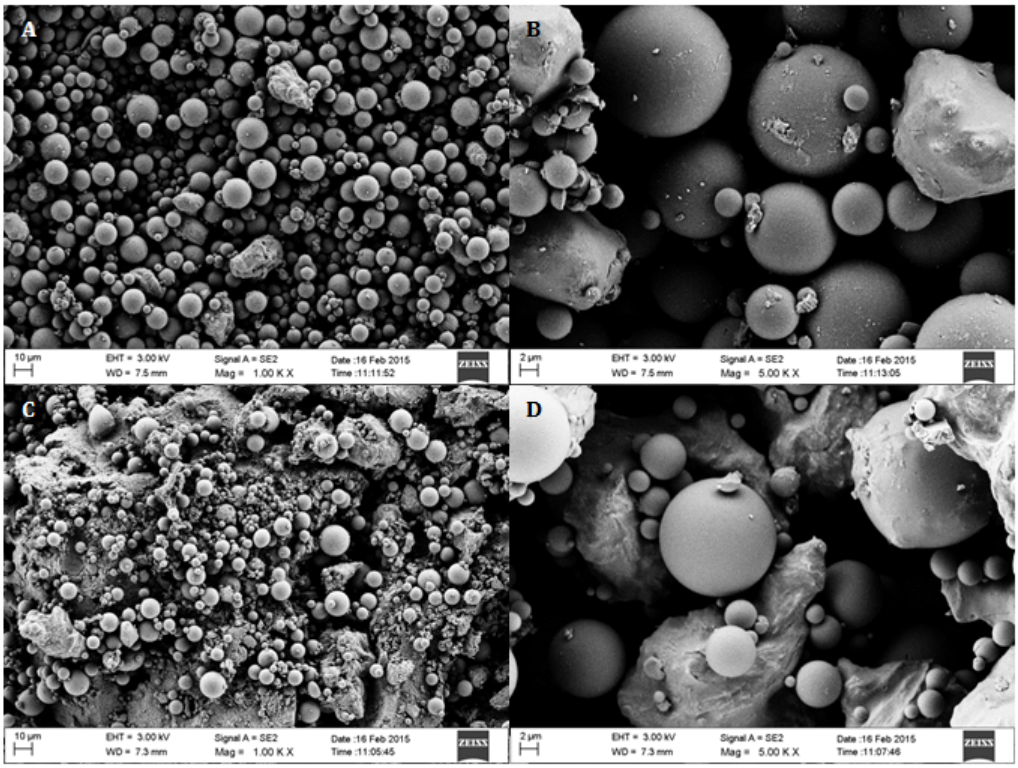

Figure 4.12: SEM images of porous particles synthesized with FT1 as organic template. **A-B** 5 % FT1 and **C-D** 10 % FT1.

Figure 4.12 seems to indicate that the template was not integrated into the silica particles and no new features can be seen. It might be possible that the stock dispersion of FT1 contain large clusters of entangled template fibers. The fibers need to be better disentangled before synthesis to be able to integrate them into the silica gel structure, but to disentangle these would required more optimization of the process conditions. Also, the BET measurements did not show any difference in pore volume or surface area compared to non-templated silica particles, see *Appendix C*, and therefore no further synthesis were performed with FT1 as template.

4.2.3.2 Spherical Templates

When performing synthesis according to *Route IIIa* with the spherical template ST1 the SEM images showed that many spherical particles were obtained, see Figure 4.13, but a lot of non-spherical artefacts could also be seen. SEM images **B** and **D** in Figure 4.13 show that some hollow particles have formed and it is reasonable that the non-spherical artefacts are crushed hollow particles. The reason for hollow particles forming could be that all or most of the added ST1 has aggregated in the centre of the emulsion droplet surrounded by the silica primary particles. Initially the ST1 is negatively charged and

ammonia stabilized, however, as heating is applied during the synthesis ammoniac will evaporate and the ST1 will be destabilized. This could lead to aggregation of ST1 in the droplets. Another interesting property of the template was the low glass transition temperature, T_g, at 60 °C. This means that the template will start to transform from its rigid glassy state to a more flexible state during evaporation. This could affect the shape and properties of the template and could be the reason for coalescence, after the destabilization, of template particles at the centre of the emulsion droplets. Since the silica shell seems to have a smooth surface on both the outer and inner layer, the surface of the coalesced ST1 particles should be smooth as well. The possible explanation could be that the low T_g and the coalescence of ST1 creates a smooth particle in the middle of the droplets.

The solid silica wall does not seem to be affected by the ST1 since no imprint of the template can be observed. The cross-section of the silica wall in image **C**, Figure 4.13, seems to have a similar structure to the core of the particles synthesized with the reference synthesis in Figure 4.8.

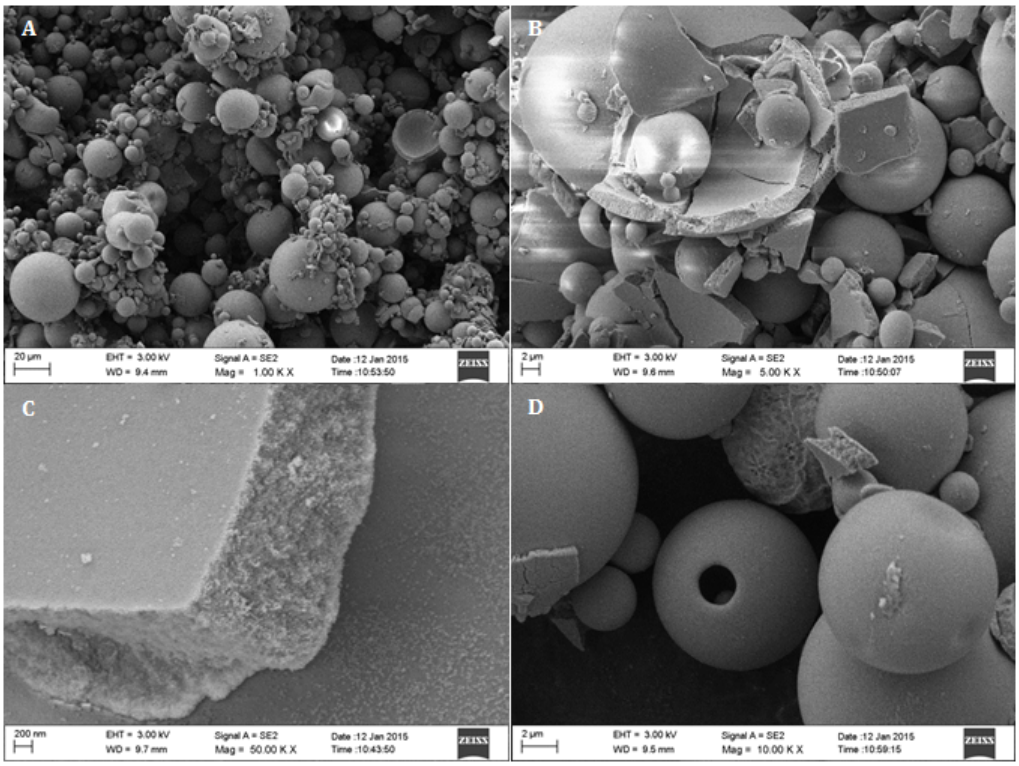

Figure 4.13: SEM images of porous particles synthesized with ST1 as organic template. **A** 15 vol% ST1, **B** 10 vol% ST1, **C** 10 vol% ST1 and **D** 15 vol% ST1.

To investigate the proportion of hollow silica particles, they were embedded into an epoxy

resin, sliced with a microtome and analysed with SEM. The results can be seen in Figure 4.14. From the SEM images it can be seen that not all particles were hollow and no clear pattern or trend can be seen regarding if the big or small particles are hollow. Since all porous particles were not hollow, this could indicate that the aggregation of the organic template did not necessarily occur in the center of the emulsion droplet and therefore the template did not integrate into the final porous silica particle.

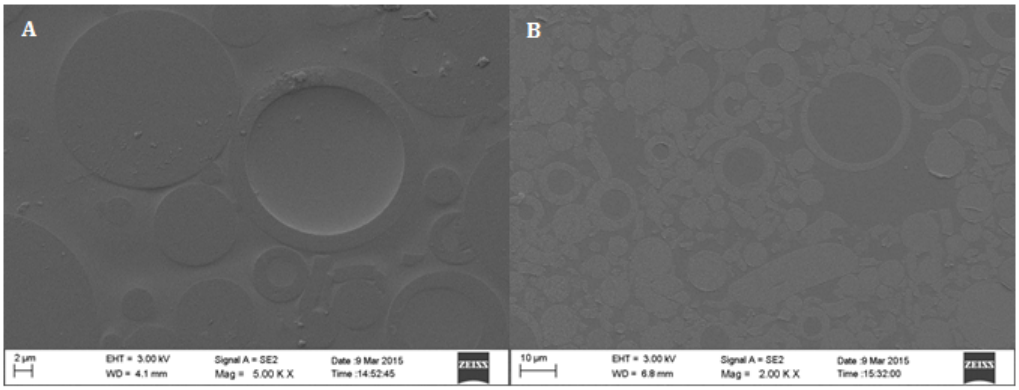

Figure 4.14: SEM images of the sliced epoxy embedded particles. **A** dried particles and **B** calcined particles from *Route IIIa* with 10 vol% ST1.

Synthesis was also performed by *Route IIIa* using organic template ST2 and ST3. When performing synthesis with the ST2 no spherical particles were obtained and hence no further experiments were performed with this template. Synthesis using ST3 as template resulted in spherical porous particles, see Figure 4.15, with well dispersed voids. The size and frequency of the voids appears to be correlated to the amount of template added, compare images **A-C** in Figure 4.15.

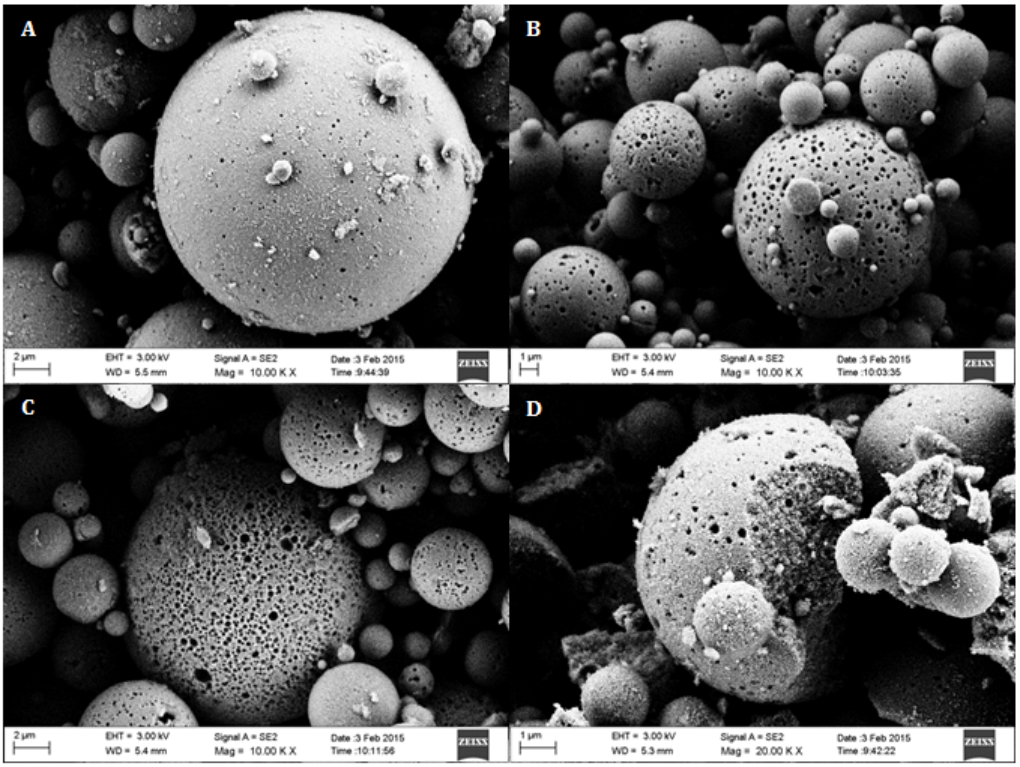

Figure 4.15: SEM images of porous particles synthesized according to *Route IIIa* with ST3 as organic template. **A** 10 vol% ST3, **B** 15 vol% ST3, **C** 20 vol% ST3 and **D** 15 vol% ST3.

The distribution of voids seems to vary among the porous particles and this could be an indication of that the gelling process was not homogeneous within the emulsion droplets during the synthesis. Also the sizes of the holes on the surface vary quite much and they are rather big compared to the size of ST3 (65 nm), some of them as big as 500 nm. Therefore it is likely to believe that the voids are created by aggregated ST3 template. To investigate the macroscopic homogeneity of the template within the porous particle, fluorescent ST3 was used, see image **A-C** in Figure 4.16. The ST3 template was rendered fluorescent by the introduction of a fluorescent monomer, 1 %, in the template particle synthesis. The fluorescence from the porous particles indicates a uniform distribution of the template and image **D** also show this by SEM.

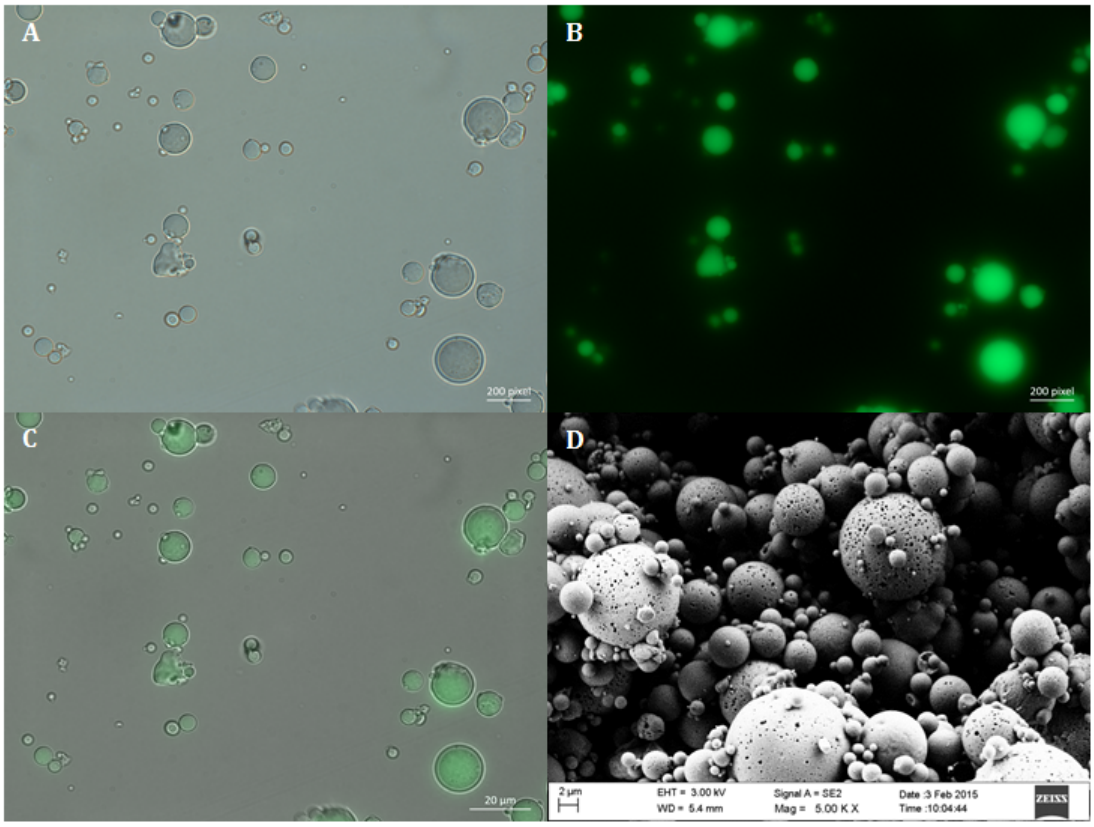

Figure 4.16: **A** show a microscopy image of porous particles synthesized according to *Route IIIa* with fluorescent ST3 as organic template, **B-C** show the fluorescence from porous silica particles and **D** display well dispersed pores created by the template. All imaged particles are synthesized with 15 vol% ST3.

The spherical templates behave rather differently during the syntheses. Both ST1 and ST3 start of as negatively charged particles, however, as evaporation is prolonged ST1 loses its negative charge in contrast to ST3. The ST3 particles repel each other during the whole synthesis hindering them from aggregating at the centre of the emulsion droplet as ST1 does. The organic template ST2 was positively charged and since the silica primary particles are negatively charged the system will precipitate which hinders the formation of spherical porous particles.

4.2.3.3 Spherical Template and Ammonium Acetate

When performing synthesis with the organic template ST1 the template particles aggregated at the centre of the emulsion droplets resulting in hollow particles, see section *4.2.3.2 Spherical Templates*. To avoid this, the template particles aggregation could be hindered by locking their positions in the emulsion droplet. An option was, with help of ammonium acetate, to quickly gel silica around one or a few template particles

hindering them from aggregating and creating a big void in the centre of the porous silica particle after calcination. The ammonium acetate concentrations used was based on the results from the experiments conducted in continuous phase, see section *4.1.3 Gelling by Ammonium Acetate in Presence of Organic Template*, in an attempt to control the gelling rate of the system.

In *Route IVa* the ammonium acetate was mixed with the silica sol and organic template for 5 min before addition to the reactor. The silica, template and ammonium acetate was then stirred in the reactor for 1 h before the evaporation was started to get a homogeneous mixture. Synthesis was performed by *Route IVa* with 0.46 M ammonium acetate and an incubation time of 65 min which did not result in spherical particles. However, when performing *Routes IIa-b* at lower ammonium acetate concentrations a higher number of spherical particles were obtained why it would be reasonable to believe that performing *Routes IVa* at lower concentrations would also result in increased amount of spherical particles.

In *Route IVb* the template was mixed with the silica sol before addition to the reactor. The sol and the template were then stirred in the reactor for 1 h to obtain a good dispersion of silica and template in all the emulsion droplets before the ammonium acetate was added. When performing synthesis according to *Route IVb* only a few spherical particles was obtained, see Figure 4.17. The reason for not getting only spherical particles might be the same as for when doing synthesis with only ammonium acetate in *Route IIb*. For instance, it was possible that hot spots formed which caused aggregation and sedimentation. Also, the quality of the emulsion was not as good as when performing syntheses according to *Route I*.

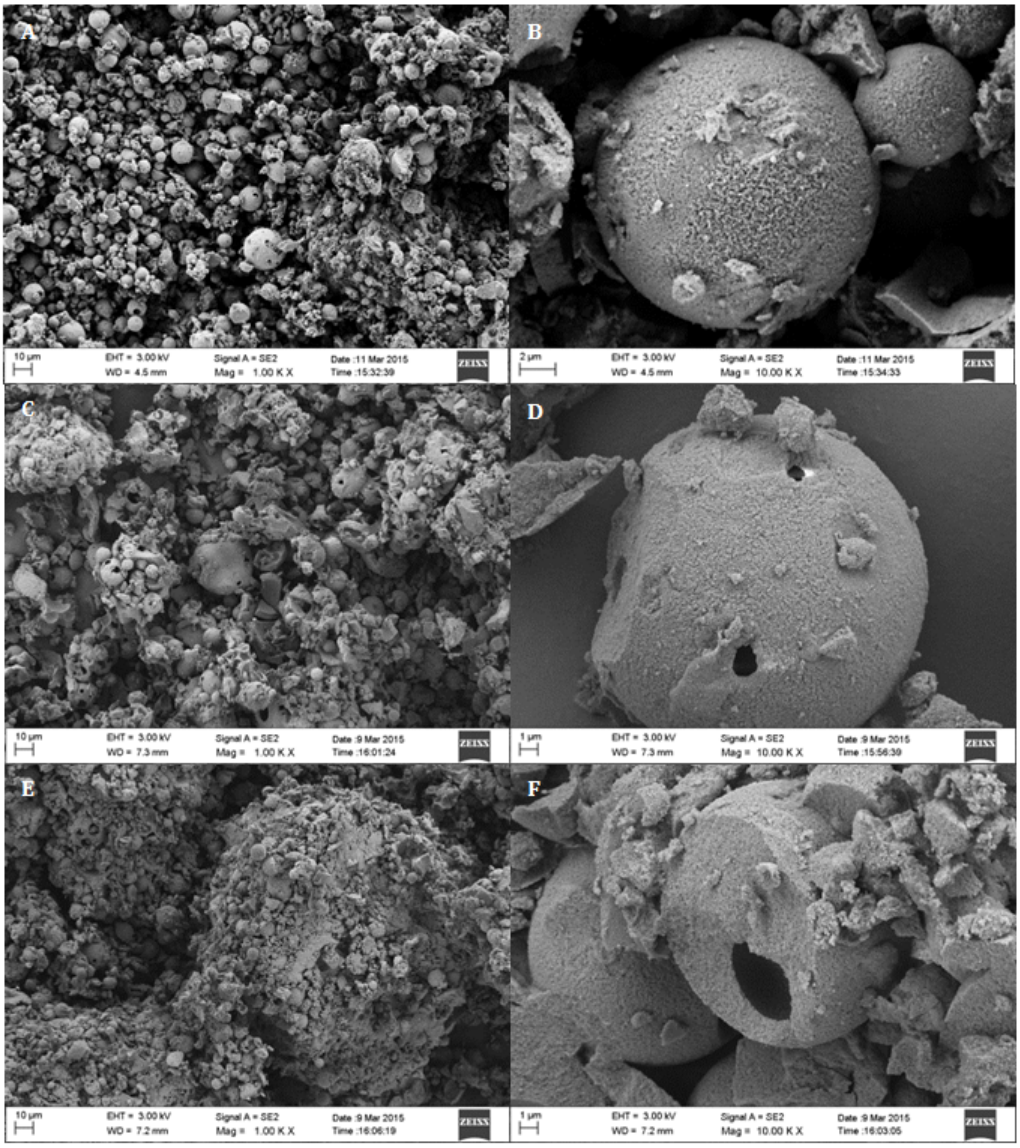

Figure 4.17: SEM images showing particles synthesized according to *Route IVb* with different concentrations of ammonium acetate in the reactor. **A-B** 0.3 M ammonium acetate, **C-D** 0.46 M ammonium acetate and **E-F** 0.6 M ammonium acetate. The incubabation time was in A-D 0 min and in E-F 20 min.

Synthesis by *Route IVb* with both ammonium acetate and template resulted in hollow particles similar to those synthesized by *Route IIIa* when using only ST1, see Figure 4.17. However, they do seem to have a higher frequency of holes on the surface of the particles than particles synthesized by *Routes IIIa* with ST1. This could indicate that some template aggregates have been locked in different places in the emulsion droplet as

the silica particles are formed, creating voids.

From Figure 4.17 it can also be seen that increasing the ammonium acetate concentration decreases the number or spherical particles. To get a high number of spherical particles the ammonium acetate concentration has to be optimized. It is a balance to enhance gelling with ammonium acetate in order to immobilize the template particles without creating a too weak silica structure.

For the synthesis with 0.46 M ammonium acetate and ST1 by *Route IVa*, experiments were performed with the incubation time 0, 10, 20 and 30 min. However, the result shows that the incubation time had a minor impact on the final porous silica particles. Instead, the concentration of ammonium acetate seems to be the crucial parameter.

4.2.4 Synthesis with Multiple Sols

The idea of using multiple sols was to create particles with new porous structures. Synthesis with multiple sols was performed by four different routes, see section *3.3.5 Synthesis with Multiple Sols*. In *Route Va* the silica sols were mixed before addition to the reactor to achieve a homogenous mixture of the primary particles within the final porous particle. By performing a two-step synthesis in *Route Vb-d* the goal was to create layered particles with a core particle of the first batch primary particles and a shell of the second batch primary particles, i.e. a core-shell structure. Figure 4.18 show how the different sols should ideally be distributed within the porous particles. In order to establish where in the final particles the different sols are situated and if they are well distributed in every particle or in only a few, the S3 dispersion was doped with alumina. Ideally by using elemental analysis by SEM (EDX), the alumina could be traced and the location of S3 could be established.

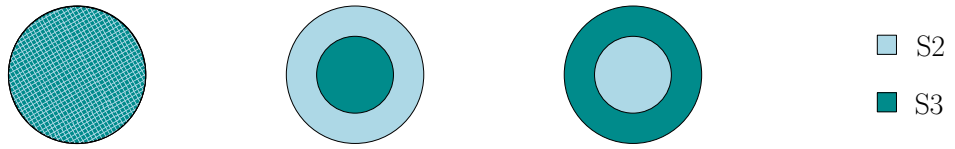

Figure 4.18: Schematic image showing the structures wanted by mixing silica sols in a one or two-step synthesis.

Figure 4.19 shows a schematic image of *Route Vc*.

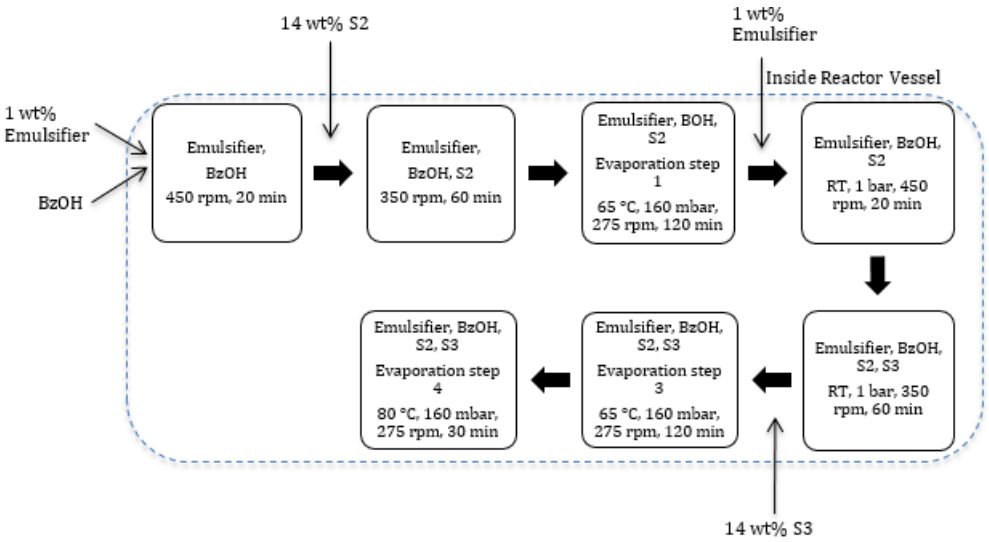

Figure 4.19: Schematic image describing the two-step synthesis according to *Route Vc* with 1st batch S2 dispersion and 2nd batch S3 dispersion.

Regardless of which route that was used the syntheses resulted in spherical particles. SEM images from syntheses made from Route *Va-d* can be seen in Figure 4.20.

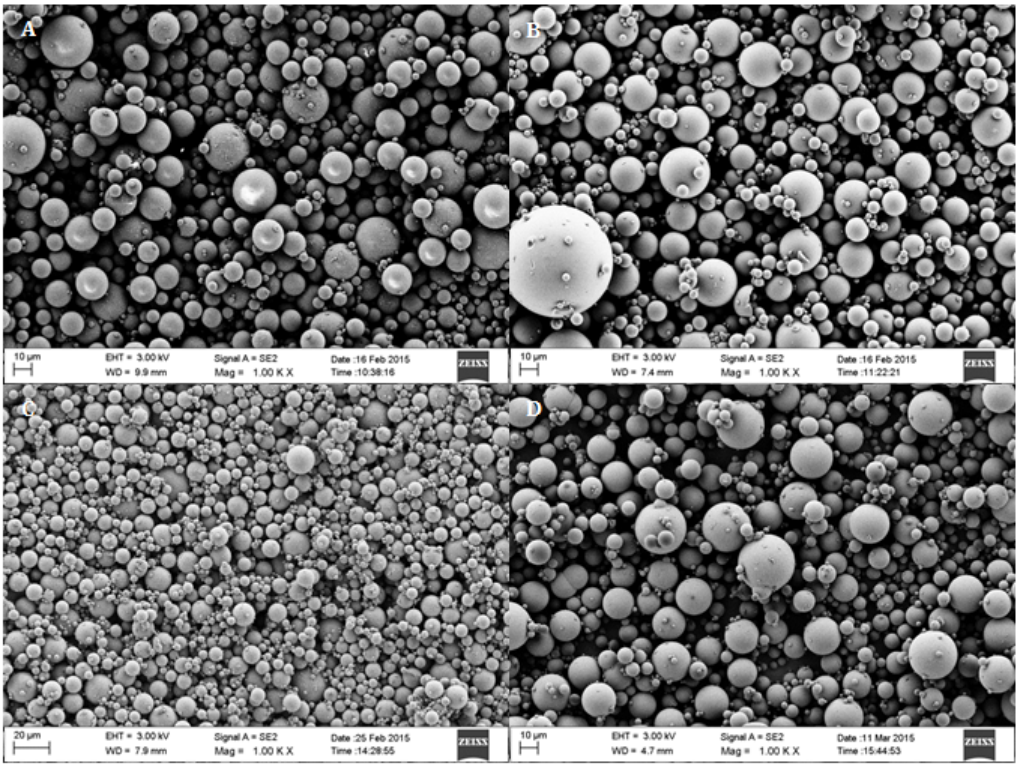

Figure 4.20: SEM images of porous particles synthesized with multiple sols according to *Routes Va-d*. **A** *Route Va* with a 1:1 mixture of S2 & S3, **B** *Route Vb* with 1st S3 & 2nd S2, **C** *Route Vc* with 1st S2 & 2nd S3 and **D** *Route Vd* with 1st S2 & 2nd S3.

One could first notice that when performing *Route Vb* some very large particles were obtained, see image **B** in Figure 4.20. During this synthesis no additional emulsifier was added before the addition of second batch of sol. The presence of very large particles could indicate aggregation of first batch porous silica particles which have been coated by the second batch of primary particles that formed an outer layer, however this was difficult to confirm. To avoid possible aggregation of the first batch porous silica particles synthesis according to *Route Vc* with a second addition of emulsifier was performed, see image **C** in Figure 4.20. This resulted in porous particles of more similar sizes. It was difficult to tell if the second batch primary particles had coated the first batch particles or if two populations of particles were obtained. However, due to the size of the particles it was likely to believe that two populations were formed; one from the first batch and the other from the second batch.

Route Vd was designed to avoid formation of two populations of particles. By arresting the first evaporation step when half the amount of water had been evaporated, emulsion droplets containing the first batch of silica sol will still be present. Upon addition of the second batch of silica sol, the silica dispersion should merge with the

existing droplets instead of creating a new population. The result from synthesis according to *Route Vd* can be seen in image **D**, Figure 4.20. However, it was difficult to draw any further conclusions from the SEM images other than that the particles were spherical and of regular size. Another synthesis with fluorescent template particles in the first batch silica dispersion were performed similar to *Route Vd* to determine if it was possible to coat the first batch of porous silica particles with a second batch of silica particles, see result in section *4.2.5 Synthesis with Multiple Sols and Organic Template*.

The great challenge in the analysis of the porous particles from multiple sol two-step syntheses was to determine if the second batch of silica coats the first batch of porous silica particles, as wanted, or if two populations were created. Since it was difficult to draw any conclusion from only observing the SEM images, EDX analysis was performed as an attempt to trace the alumina in S3. However, due to the low amount of alumina in S3 the Al-signal could not be registered with the EDX detector during the SEM analysis.

BET measurements were also performed on the particles synthesized from multiple sols, the BET isotherms for syntheses performed by *Route Va-d* are available in *Appendix C*. BET results showed that porous particles synthesized according to *Route Va* had a monomodal pore distribution, i.e. only one type of pore has formed, see image **A** in 4.21. This indicates that the synthesized porous particles had a homogeneous mixture of the two sols. When performing synthesis according to *Route Vb-d*, i.e. a two-step synthesis, bimodal pore structures were observed from the BET measurements, see **B-C** in Figure 4.21. This could be due to the fact that the primary particles of the different sols have different sizes and when they are not homogeneously distributed within the particles they will create two different types of porous structures. Even though a bimodal pore structure was desired for these types of syntheses, one cannot tell from the BET result if the two types of pores are in the same particle, i.e. the second batch sol coats the first sol, or if the two different pores correlates to two population of porous particles.

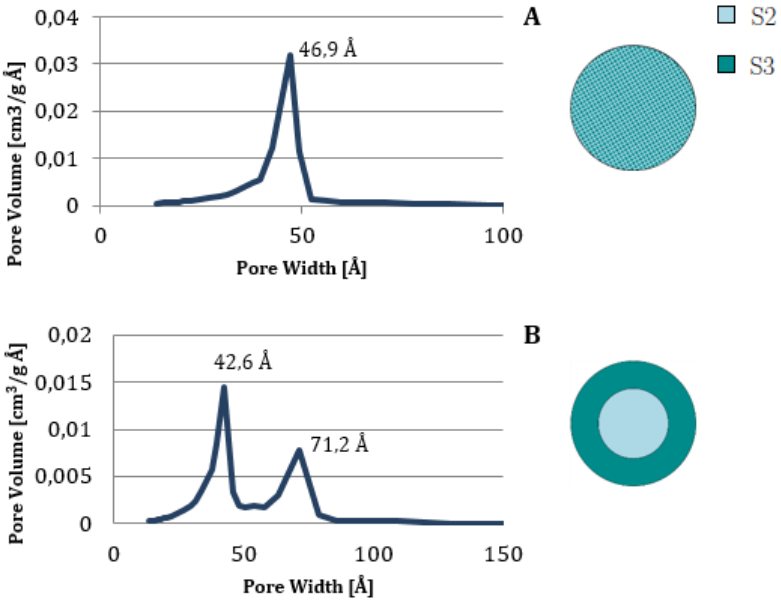

Figure 4.21: Pore size distribution of the pores in particles synthesized by **A** *Route Va* with 1:1 mixture of S2 & S3 and **B** *Route Vb* with 1st S2 & 2nd S3. Porous particles synthesized by *Route Vc-d* showed a bimodal pore size distribution similar to the one in image **B**. The images to the right show how the different silica primary particles should ideally be distributed within the porous particle.

The BET surface area, BJH pore volume and BJH average pore size from the BET measurements for the particles synthesized according to *Route Va-d* with different sols can be seen in Table 4.5.

Table 4.5: BET results from synthesis with multiple sols according to *Route Va-d*. The surface area were calculated with the BET model while the average pore size and pore volume were calculated with the BJH method for the desorption curve. BET measurements for particles synthesized by *Route I* with silica sols S1, S2 and S3 are shown as references.

	Silica Sol	**Surface Area** (m^2/g)	**Pore Size** (Å)	**Pore Volume** (cm^3/g)
Route I	S1	400.8	43.6	0.5861
Route I	S2	134.6	59.2	0.2541
Route I	S3	186.5	44.3	0.2966
Route Va	1:1 mixture of S2 and S3	169.8	46.9	0.2537
Route Vb	1^{st} S2, 2^{nd} S3	163.6	42.6 and 71.2	0.3022
Route Vb	1^{st} S3, 2^{nd} S2	159.2	48.3 and 56.6	0.3000
Route Vc	1^{st} S2, 2^{nd} S3	150.4	43.0 and 64.2	0.2634
Route Vd	1^{st} S2, 2^{nd} S3	151.7	48.9 and 58.7	0.2792
Route Vd	1^{st} S1, 2^{nd} S2	257.5	43.7 and 71.9	0.3900

The surface area of the particles synthesized by *Route Va-d* was in line of what was expected compared to the references synthesized by *Route I*. The pore volume of particles synthesized by *Route Vb* was a bit higher than for the particles synthesized by the other routes, this could be a result of coalesced porous particles from the first batch. The pore sizes in the particles with bimodal pore structure correlate quite well with the result for the average pore size for each silica sol.

4.2.5 Synthesis with Multiple Sols and Organic Template

A two-step synthesis with multiple sols where an organic template was added into one of the batches of silica sol was performed to try to create a core-shell structure. By using a two-step synthesis the idea was to create a dense core with the first batch of primary particles and by adding an organic template to the second batch, coat the dense core with a highly porous shell where the higher porosity would result from both the different primary particle size and the presence of a sacrificial organic template, i.e. core-shell structure.

Synthesis according to *Route VIa* with S2 dispersion as the first batch and S3 dispersion + ST3 in the second batch resulted in spherical particles, see Figure 4.22.

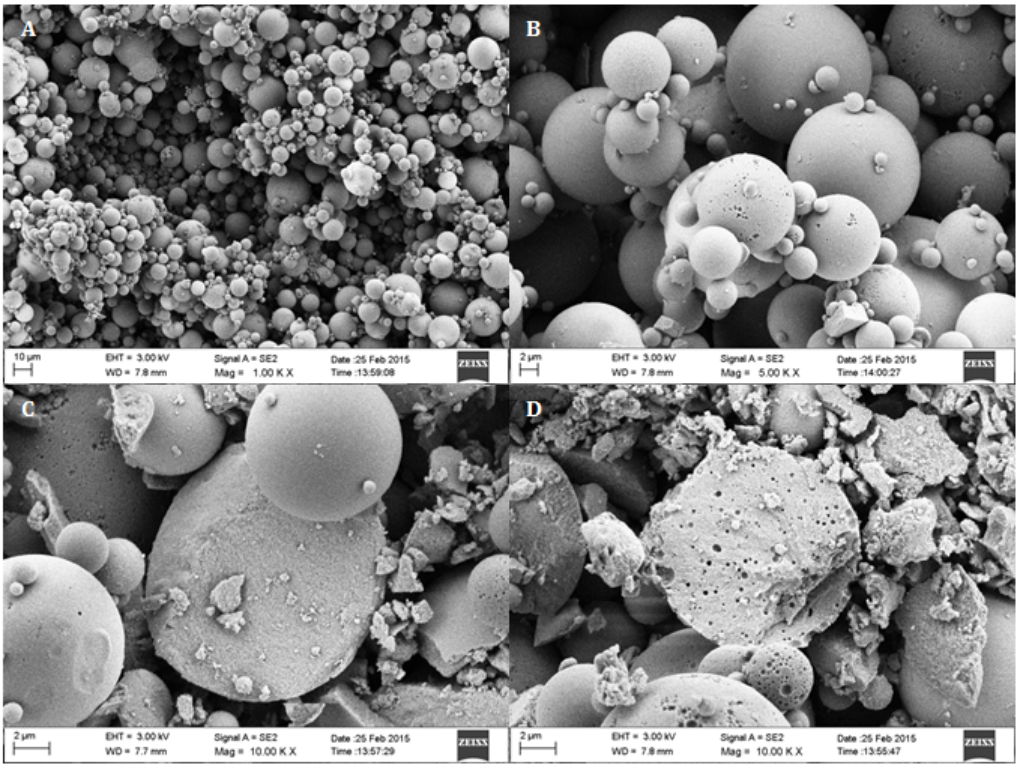

Figure 4.22: SEM images of porous particles synthesized according to *Route VIa* with multiple sols and organic template. **A-D** 1st S2 and 2nd S3+15 vol% ST3.

As can be seen in image **B** traces of the organic template cannot be found in every particle. Some particles had many voids on the surface while other did not have any. In order to distinguish whether a core-shell structure had been created or not the particles were crushed before SEM analysis to be able to see the cross-section of a porous particle. Images **C** and **D** show the cross-section of two different porous particles and it was clear that no core-shell structure was created. Image **C** show no trace of organic template in any spot of the particle while in image **D** the holes from the organic template was well distributed in the whole particle. This result indicates that two different population of particles was created; one with the first batch of silica dispersion and one with the second batch of silica dispersion together with the organic template. However, the analysis was not good enough to determine that no mixture of the two silica batches was obtained at all.

It is likely that addition of the second batch of emulsifier creates new droplets instead of adding to the existing first batch of porous silica particles. Upon addition of the second batch of silica sol the particles will distribute themselves into the new droplets and two populations will be formed. A way to avoid this problem could be to not add a second batch of emulsifier as in *Route Vb*. This resulted in some very large particles which could be coalesced porous particles of the first batch with a coating layer of second batch

particles, indicating that one population of particles were formed. Therefore, it could be of interest to perform a similar synthesis with an organic template in one of the batches.

Another approach to the problem could be a synthesis performed where the first evaporation step was arrested when half the amount of water was evaporated, similar to *Route Vd*, and therefore *Route VIb* was designed. Since the first batch of porous particles still contain water and no new batch of emulsifier was added, the second batch silica particles should find their way into the existing droplets creating one population. Synthesis according to *Route VIb* with S2 and fluorescent ST3 in the first batch and S3 in the second batch was performed, the result can be seen in Figure 4.23.

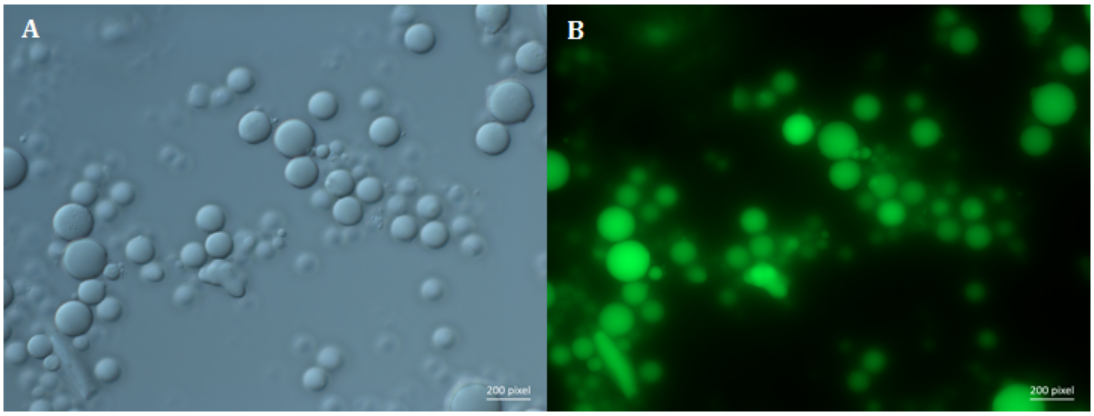

Figure 4.23: Porous particles synthesized according to *Route VIb* with 1st S2 + 10 vol% fluorescent ST3 and 2nd S3. Microscopy images with **A** normal light and **B** fluorescent light.

Since the first batch includes the fluorescent template the idea was to distinguish the two different batches by having a porous particle with a fluorescent core and a non-fluorescent shell. But as can be seen when comparing image **A** and **B** in Figure 4.23, it was difficult to distinguish between the core and shell of the porous particles when switching between fluorescent and normal light. However, it is important to notice that all particles fluoresce, indicating that one population of porous particles were formed. The question is if a porous silica core have been formed from the first batch of silica before the second batch was added, or if the two batches mixed upon addition of the second batch silica. Since *Route VIb* was very similar to *Route Vd*, except for that an organic template was added in the first batch, it would be likely that this synthesis also would result in porous particles with bimodal pore size distribution. This would mean that the mixture of the sols within the porous particle should be inhomogeneous. According to estimations, based on the amount of added silica, the coating layer should be quite thin and therefore light scattering and focus issues could be the reason for not being able to differentiate between the two batches when using fluorescence microscopy. However, a inhomogeneous particle does not mean a core-shell particle.

One approach for synthesizing a core-shell structure could be to evaporate more than half of the water from the first batch before addition of the second batch of silica sol. This would, in contrast to when evaporating less water, result in a more gelled core before the second addition hence would more likely give a core-shell structure. It is important to note that the gelling is not reversible upon dilution. The approach of evaporating more than half of the water applies for syntheses performed according to *Route VIb* as well as *Route Vd*.

The results above shows that porous particles with multiple sols and template can be formed but the microstructure of the particles could not be completely defined in this master thesis.

5

Conclusions

From the pre-experiments in continuous phase it was concluded that there was a clear correlation between the amount of added salt and the gelling time. If also a negatively charged organic template was introduced to the silica sol and ammonium acetate system, an even lower gelling time was observed than when performing gelling with only ammonium acetate but the correlation stayed the same.

The ESE-method was successful in producing μm-sized porous particles from a larger primary particle than used in previous work. It was also successful in synthesizing porous particles from a sodium ion stabilized, alumina doped primary particle.

By introducing ammonium acetate into the system the pore volume and the average pore size of the porous particles could be substantially increased. A clear correlation could be observed between the amount of ammonium acetate and the surface roughness of the porous particles, where a higher amount of ammonium acetate led to a rougher surface. However, no other trend was seen regarding the amount of ammonium acetate and the effect of the microstructure.

Two types of porous particles were synthesized with the addition of an organic template; hollow particles when ST1 was used and particles with well distributed voids when ST3 was used. An attempt to spread ST1 in the porous particle was performed by adding ammonium acetate during the synthesis to lock the template particles in the emulsion droplet before they could aggregate. However, it was difficult to get, at the same time, spherical particles and a well dispersed template.

By using a two-step synthesis and multiple sols, both with and without organic template, porous particles with a bimodal pore distribution could be obtained. If these pores are located in one or two populations of porous particles seems to be dependent on the type of synthesis route. If a second batch of emulsifier is added it seems to create two populations of particles corresponding to the two batches of silica sol. But if only half the amount of water was evaporated before addition of the next batch of silica sol is added,

one population of particles seems to form. However, to create a core-shell structure more water needs to be evaporated.

A trend throughout the master thesis was that the quality of the emulsion had a major impact on the resulting porous particles. If, for instance gelling occurred in a too early stage, less spherical particles could be seen.

6

Future Work

Since the addition of salt seem to have significant effect on the quality of the emulsion, the addition technique needs to be further investigated and developed to be able to create nice spherical particles in every synthesis.

Organic template FT1 did not contribute to any results in this master thesis, but it cannot be ruled out as a potential template. Instead more preparation of the template needs to be performed before it could be added to the synthesis. Since the template seems to be highly entangled in the stock dispersion, the fibers needs to be dispersed before the synthesis in order to include them uniformly into the emulsion droplets and hence in the porous particle. Synthesis with organic template ST1 resulted in hollow particles and these might be useful in applications such as drug delivery or as micro-capsules for e.g. pesticides. Since the conditions used in this master thesis seems to lead to a mixture of dense and hollow particles, some optimization should be performed to get the template well-dispersed into all emulsion droplets and making all the porous particles hollow.

To get the ST1 particles more distributed within the porous particle with help of ammonium acetate, optimization must be performed regarding ammonium acetate concentration and which process parameters that should be used for obtaining spherical particles. However, the additional effect of ammonium acetate on the particles could be interesting since the roughness of the surface as well as the porosity could be modified. This could be useful for applications where transport and controlled release of a substance is important.

The strong attraction between the silica particle and organic template ST2 could be solved by, for instance, coating the template with silica before the synthesis. The template would then be stabilized against rapid aggregation with the silica sol. For ST3 more work could be performed to avoid aggregation of template particles in the emulsion droplet resulting in smaller, more well distributed voids.

For particles synthesized by two-step synthesis with multiple sols, with or without

template, further investigations needs to be performed regarding if the different routes yield one or two populations of porous particles. In syntheses were only half the amount of the water was evaporated before addition of the second silica batch was probably the best way of synthesizing layered particles. However, more work needs to be done concerning if a core-shell particle has formed or if the porous particle was homogeneous. Synthesis should also be performed where more than half of the water has been evaporated in the first evaporation step to increase the probability of gelling the first batch of silica before adding the second batch. This would most likely result in a core-shell particle.

Bibliography

(1) Zdravkov, B. D.; Čermák, J. J.; Šefara, M.; Janku, J. *Central European Journal of Chemistry* **2007**, *5*, 385–395.

(2) Li, W.; Zhao, D. *Chem. Commun.* **2013**, *49*, 943–946.

(3) Carter, C. B.; Norton, M. G., *Ceramic materials: science and engineering*; Springer Science & Business Media: 2007.

(4) Cademartiri, L.; Ozin, G. A., *Concepts of nanochemistry*; Wiley-VCH: Weinheim, 2009.

(5) Sundblom, A. Formation of mesostructured silica based on non-ionic interactions., Ph.D. Thesis, Chalmers University of Technology, 2010.

(6) Shiba, K.; Shimura, N.; Ogawa, M. *J Nanosci Nanotechnol* **2013**, *13*, 2483–94.

(7) Giraldo, L. F.; López, B. L.; Pérez, L.; Urrego, S.; Sierra, L.; Mesa, M. *Macromolecular Symposia* **2007**, *258*, 129–141.

(8) Duong, C.; Lu, C. The effect of synthesis parameters on mesoporous silica particle morphology and size distribution., MA thesis, Chalmers University of Technology, Applied Surface Chemistry, 2014.

(9) Schramm, L. L., *Emulsions, Foams and Suspensions*; Weinheim:Wiley-VHC: 2005.

(10) Brinker, C. J.; Scherer, G. W., *Sol-gel science: the physics and chemistry of sol-gel processing*; Academic Press: Boston, 1990.

(11) Holmberg, K., *Surfactants and polymers in aqueous solution*, 2nd ed.; John Wiley & Sons: Chichester, West Sussex, England, 2003.

(12) Additives, A. P. Bermocoll.

(13) Daintith, J., *A dictionary of chemistry*, 6th ed; Oxford paperback reference; Oxford University Press: New York, 2008.

(14) Bergna, H. E.; Roberts, W. O., *Colloidal silica: fundamentals and applications*; CRC Taylor and Francis: Boca Raton, FL, 2006; Vol. 131.

(15) Schaeffer, H. A In *Concise encyclopedia of advanced ceramic materials*, Brook, R. J, Ed., 1st ed; Pergamon Press: Oxford, 1991, pp 416–419.

(16) Iler, R. K., *The chemistry of silica: solubility, polymerization, colloid and surface properties, and biochemistry*; Wiley: New York, 1979.

(17) Pulp, A.; Chemicals, P. Industrial Applications.

(18) Dullien, F. A. L, *Porous media: fluid transport and pore structure*; Academic Press: New York, 1979.

(19) Johansson, E. M. Controlling the Pore Size and Morphology of Mesoporous Silica., Ph.D. Thesis, Linköping University Electronic Press, 2010.

(20) Wu, S.-H.; Mou, C.-Y.; Lin, H.-P. *Chem Soc Rev* **2013**, *42*, 3862–75.

(21) Pasqua, L., *Update on Silica-Based Mesoporous Materials for Biomedical Applications*; Smithers Rapra Technology: 2011.

(22) Slowing, I. I.; Trewyn, B. G.; Lin, V. S.-Y.; Giri, S. *Advanced Functional Materials* **2007**, *17*, 1225–1236.

(23) Wu, S.-H.; Hung, Y.; Mou, C.-Y. *Chem Commun (Camb)* **2011**, *47*, 9972–85.

(24) Vincent, B. *Adv Colloid Interface Sci* **2012**, *170*, 56–67.

(25) Andersson, N.; Kronberg, B.; Corkery, R.; Alberius, P. *Langmuir* **2007**, *23*, 1459–64.

(26) Sörensen, M. H.; Zhu, J.; Corkery, R. W.; Hayward, R. C.; Alberius, P. C. A. *Microporous and Mesoporous Material* **2009**, *120*, 359–367.

(27) Carroll, N. J.; Rathod, S. B.; Derbins, E.; Mendez, S.; Weitz, D. A.; Petsev, D. N. *Langmuir* **2008**, *24*, 658–61.

(28) Murphy, D. B.; Davidson, M. W., *Fundamentals of light microscopy and electronic imaging*, 2nd ed; Wiley-Blackwell: Hoboken, N.J., 2013.

(29) Grubb, D. In *Polymer Science: A Comprehensive Reference*, Möller, K. M., Ed.; Elsevier: Amsterdam, 2012, pp 465 –478.

(30) Sergeev, G. B; Klabunde, K. J., *Nanochemistry*, 2nd edition.

(31) Newbury, D. E., *Advanced scanning electron microscopy and X-ray microanalysis*; Plenum Press: New York, 1986.

(32) Lowell, S; Lowell, S, *Characterization of porous solids and powders: surface area, pore size, and density*; Particle technology series, Vol. 16; Springer: Dordrecht, 2006.

(33) Ji, S.; Walz, J. Y. *The Journal of Physical Chemistry B* **2013**, *117*, 16602–16609.

A

Details of the Syntheses

Appendix A holds the details about how each synthesis was performed.

Table A.1: Details about all the syntheses made during the project. When doing synthesis with ammonium acetate a 5 M stock solution was used.

Sample	**Silica Sol**	**Template**	**Ammonium Acetate Concentration in the Reactor (M), Incubation Time (min)**	**Route**	**Comments**
Test 1	14 wt% S1			I	The impeller stopped a few times during the synthesis.
Test 2	14 wt% S1			I	
MJJJ_1	14 wt% S2			I	The impeller stopped at one point.
MJJJ_2	14 wt% S2			I	
MJJJ_3	14 wt% S2			I	The emulsion was taken out of the reactor and added again before the sol was added.
MJJJ_4	14 wt% S2			I	
MJJJ_5_ST1	14 wt% S2	10 vol% of the silica volume was exchanged for ST1.		IIIb	
MJJJ_6_ST1	14 wt% S2	15 vol% of the silica volume was exchanged for ST1.		IIIb	
MJJJ_7_ST1	14 wt% S2	10 vol% of the silica volume was exchanged for ST1.		IIIa	
MJJJ_8_ST1	14 wt% S2	15 vol% of the silica volume was exchanged for ST1.		IIIa	
MJJJ_9_ST1	14 wt% S2	20 vol% of the silica volume was exchanged for ST1.		IIIa	

Sample	**Silica Sol**	**Template**	**Ammonium Acetate Concentration in the Reactor (M), Incubation Time (min)**	**Route**	**Comments**
MJJJ_10_FT1	14 wt% S2	1 vol% of the silica volume was exchanged for FT1.		IIIa	The impeller stopped at one point.
MJJJ_11_FT1	14 wt% S2	2 vol% of the silica volume was exchanged for FT1.		IIIa	It was more difficult to dry the product during filtration.
MJJJ_12_FT1	14 wt% S2	3 vol% of the silica volume was exchanged for FT1.		IIIa	
MJJJ_13_FT1	14 wt% S2	10 vol% of the silica volume was exchanged for FT1.		IIIa	Resulted in very little product which was lumpy.
MJJJ_14_FT1	14 wt% S2	5 vol% of the silica volume was exchanged for FT1.		IIIa	
MJJJ_15_FT1	14 wt% S2	7 vol% of the silica volume was exchanged for FT1.		IIIa	
MJJJ_16_ST3	14 wt% S2	10 vol% of the silica volume was exchanged for ST3.		IIIa	
MJJJ_17_ST2	14 wt% S2	10 vol% of the silica volume was exchanged for ST2.		IIIa	Product looked very different, white and fluffy instead of white opaque and compact.
MJJJ_18_ST3	14 wt% S2	15 vol% of the silica volume was exchanged for ST3.		IIIa	
MJJJ_19_ST3	14 wt% S2	20 vol% of the silica volume was exchanged for ST3.		IIIa	
MJJJ_20_ST1salt	14 wt% S2	10 vol% of the silica volume was exchanged for ST1.	0.46 M 20 min	IVb	As evaporation was performed, gel beads formed and sedimented.

Sample	**Silica Sol**	**Template**	**Ammonium Acetate Concentration in the Reactor (M), Incubation Time (min)**	**Route**	**Comments**
MJJJ_21_ST1salt	14 wt% S2	10 vol% of the silica volume was exchanged for ST1.	0.46 M 30 min	IVb	As evaporation was performed, gel beads formed and sedimented.
MJJJ_22_ST1salt	14 wt% S2	10 vol% of the silica volume was exchanged for ST1.	0.6 M 20 min	IVb	As evaporation was performed, gel beads formed and sedimented.
MJJJ_23_ST1salt	14 wt% S2	10 vol% of the silica volume was exchanged for ST1.	0.46 M 10 min	IVb	As evaporation was performed, gel beads formed and sedimented.
MJJJ_24_ST1salt	14 wt% S2	10 vol% of the silica volume was exchanged for ST1.	0.46 M 0 min	IVb	
MJJJ_25_S2_S3	1^{st} addition: 14 wt% S2, 2^{nd} addition: 14 wt% S3			Vb	
MJJJ_26_S3_S2	1^{st} addition: 14 wt% S3, 2^{nd} addition: 14 wt% S2			Vb	
MJJJ_27_salt	14 wt% S2		0.46 M 0 min	IIb	The salt was added a bit too late, i.e. when the temperature of the water bath had been increased but not reached 80 °C.
MJJJ_28_S2_S2ST3	1^{st} addition: 14 wt% S2, 2^{nd} addition: 14 wt% S2	15 vol% of the silica volume was exchanged for ST3.		VIa	
MJJJ_29_S2S3	1:1 mixture of 14 wt% S2 and 14 wt% S3			Va	
MJJJ_30_S2_S3	1^{st} addition: 14 wt% S2, 2^{nd} addition: 14 wt% S3			Vc	
MJJJ_31_ST1salt	14 wt% S2	10 vol% of the silica volume was exchanged for ST1.	0.46 M 20 min	IVb	As evaporation was performed, gel beads formed and sedimented.

Sample	**Silica Sol**	**Template**	**Ammonium Acetate Concentration in the Reactor (M), Incubation Time (min)**	**Route**	**Comments**
MJJJ_32_ST1salt	14 wt% S2	10 vol% of the silica volume was exchanged for ST1.	0.46 M 0 min	IVa	As evaporation was performed, gel beads formed and sedimented. Very little product was obtained which was very difficult to filtrate.
MJJJ_33_S2_S3ST3	1^{st} addition: 14 wt% S2, 2^{nd} addition: 14 wt% S3	15 vol% of the silica volume was exchanged for ST3.		VIa	
MJJJ_34_salt	14 wt% S2		0.4 M 0 min	IIa	The salt/sol solution had an increased viscosity before it was added to the reactor. The emulsion was very lumpy. After 2 h of evaporation, the emulsion was more transparent than previously.
MJJJ_35_salt	14 wt% S2		0.6 M 0 min	IIb	As evaporation was performed, small gel beads formed and sedimented, but not as much as when also using ST1.
MJJJ_36_salt	14 wt% S2		0.3 M 0 min	IIb	As evaporation was performed, small gel beads formed and sedimented but not as much as when using a higher salt concentration or using salt and ST1.
MJJJ_37_flST3	14 wt% S2	15 vol% of the silica volume was exchanged for fluorescent ST3.		IIIa	
MJJJ_38_salt	14 wt% S2		0.46 M 0 min	IIb	
MJJJ_39_salt	14 wt% S2		0.05 M 0 min	IIa	
MJJJ_40_S3	14 wt% S3			I	
MJJJ_41_S2_S3	1^{st} addition: 14 wt% S2, 2^{nd} addition: 14 wt% S3			Vd	There was a problem with the vacuum hence the pump had to be turned, off for a short period of time.
MJJJ_42_S1_S2	1^{st} addition: 14 wt% S1, 2^{nd} addition: 14 wt% S2			Vd	
MJJJ_43	14 wt% S2			I	
MJJJ_44_S2flST3_S3	1^{st} addition: 14 wt% S2, 2^{nd} addition: 14 wt% S3	15 vol% of the silica volume was exchanged for fluorescent ST3.		VIb	

B

Synthesis Routes

Appendix B holds schematic images of all the different routes for synthesizing porous silica particles used during the master thesis.

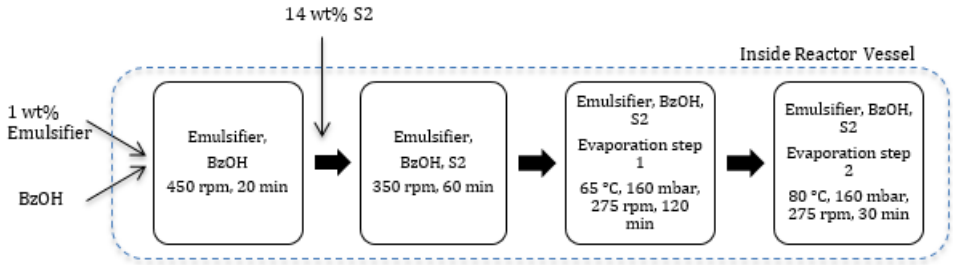

Figure B.1: Synthesis procedure according to *Route I*.

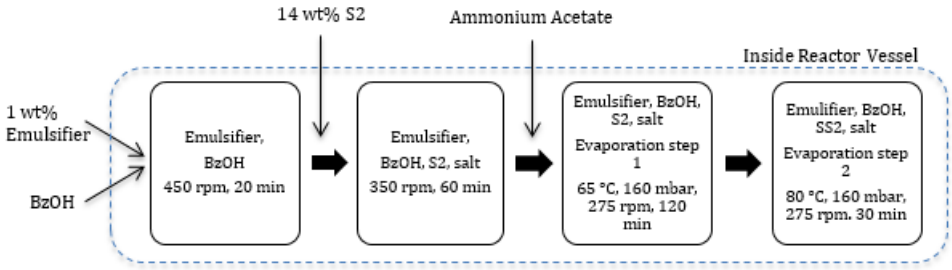

Figure B.2: Synthesis procedure according to *Route IIa*.

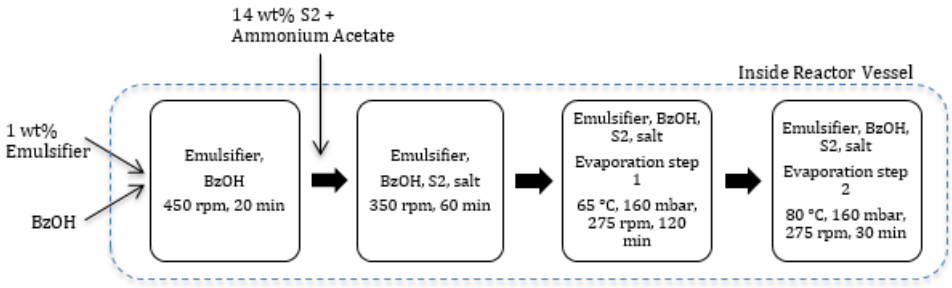

Figure B.3: Synthesis procedure according to *Route IIb*.

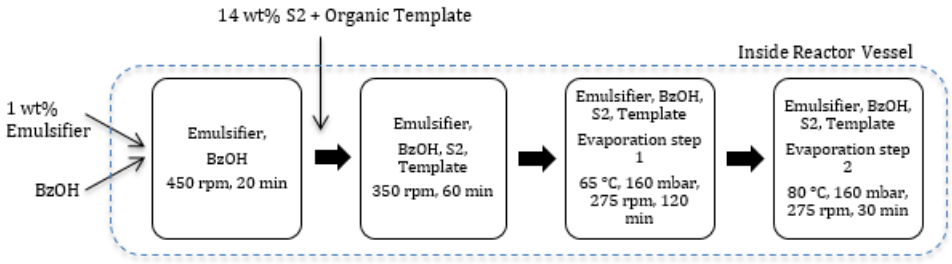

Figure B.4: Synthesis procedure according to *Route IIIa*.

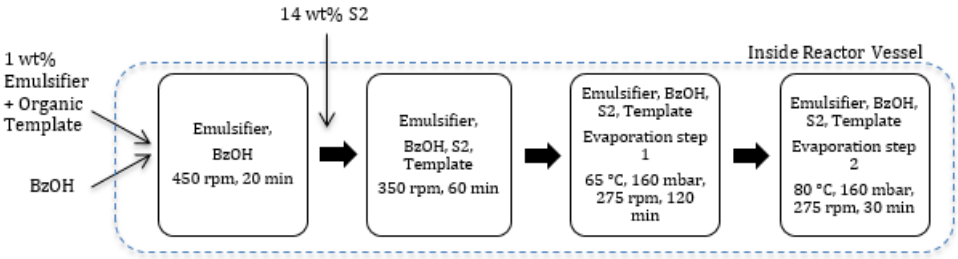

Figure B.5: Synthesis procedure according to *Route IIIb*.

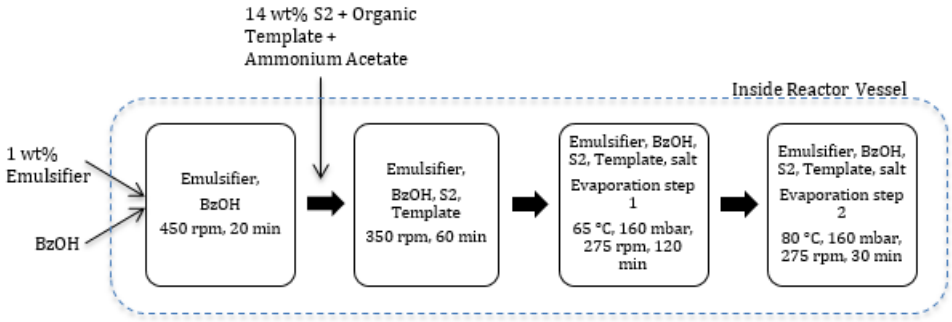

Figure B.6: Synthesis procedure according to *Route IVa*.

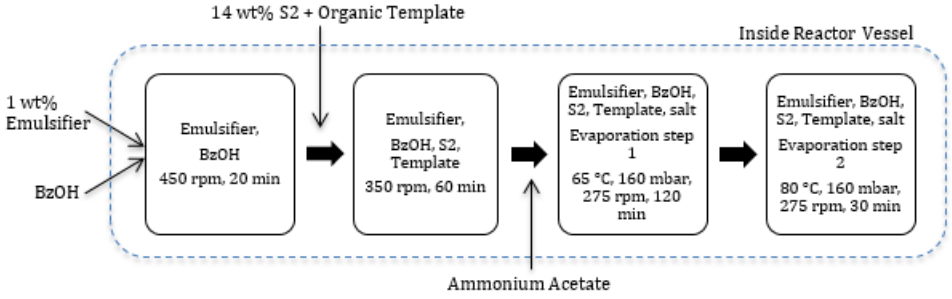

Figure B.7: Synthesis procedure according to *Route IVb*.

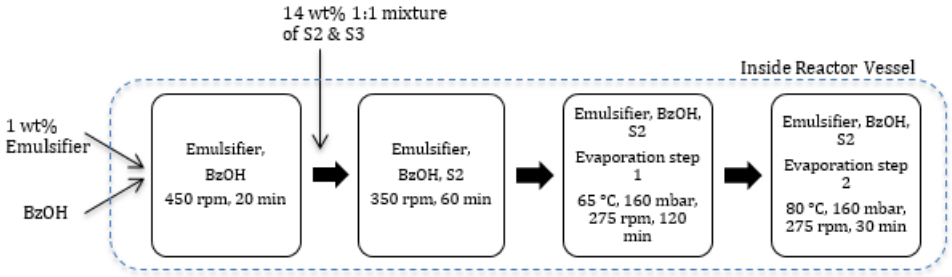

Figure B.8: Synthesis procedure according to *Route Va*.

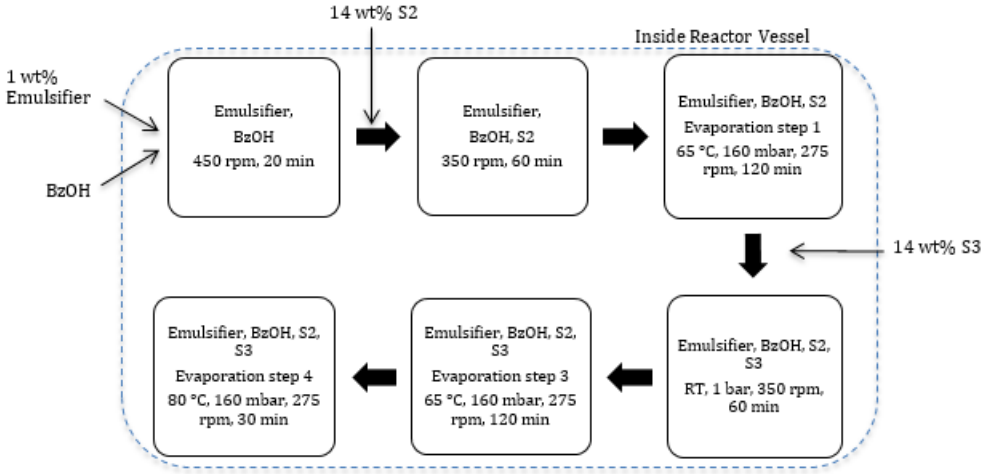

Figure B.9: Synthesis procedure according to *Route Vb*.

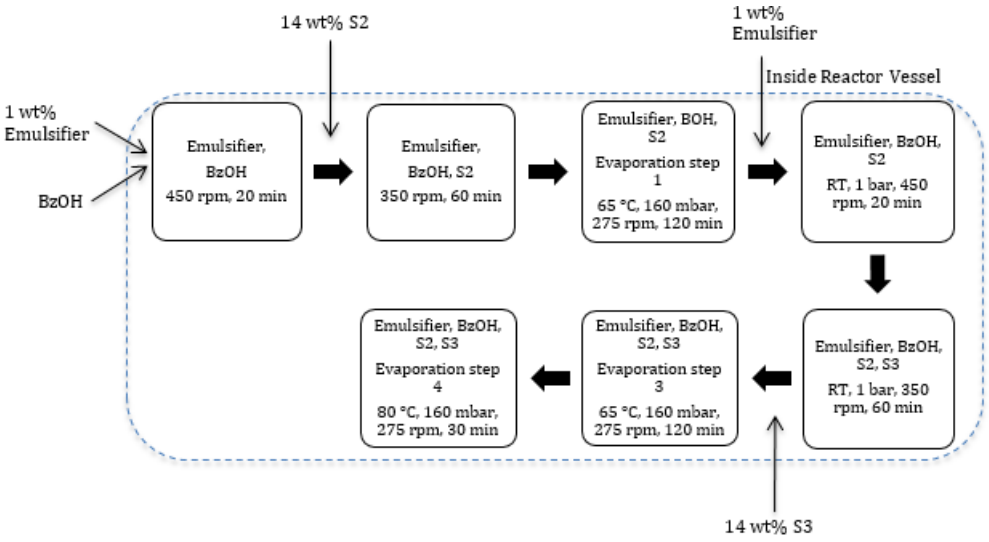

Figure B.10: Synthesis procedure according to *Route Vc*.

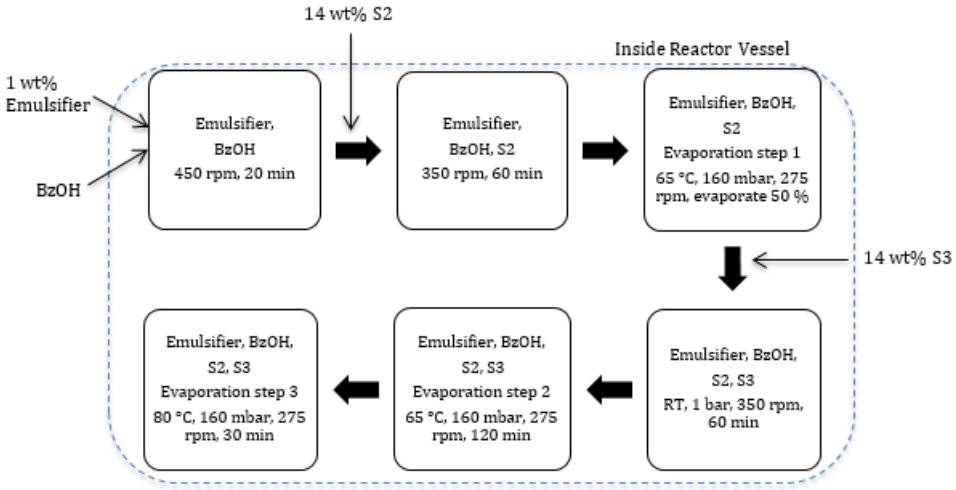

Figure B.11: Synthesis procedure according to *Route Vd*.

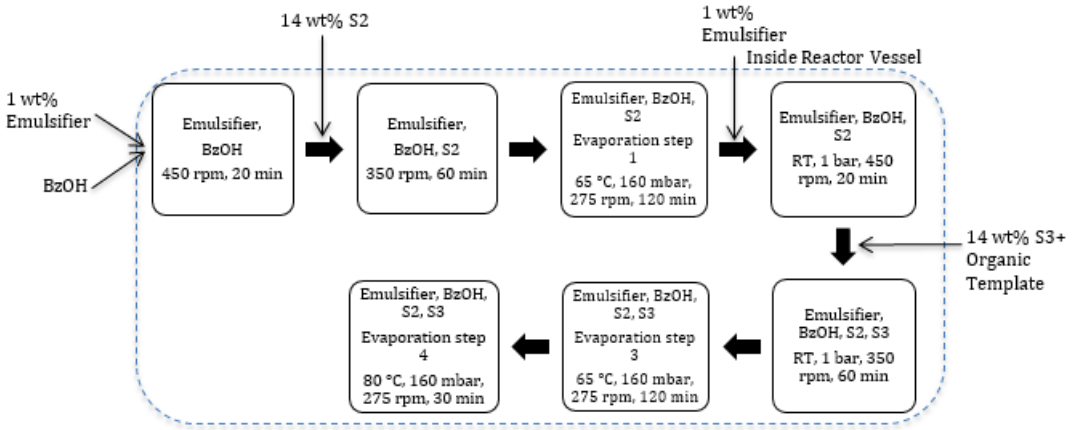

Figure B.12: Synthesis procedure according to *Route VIa*.

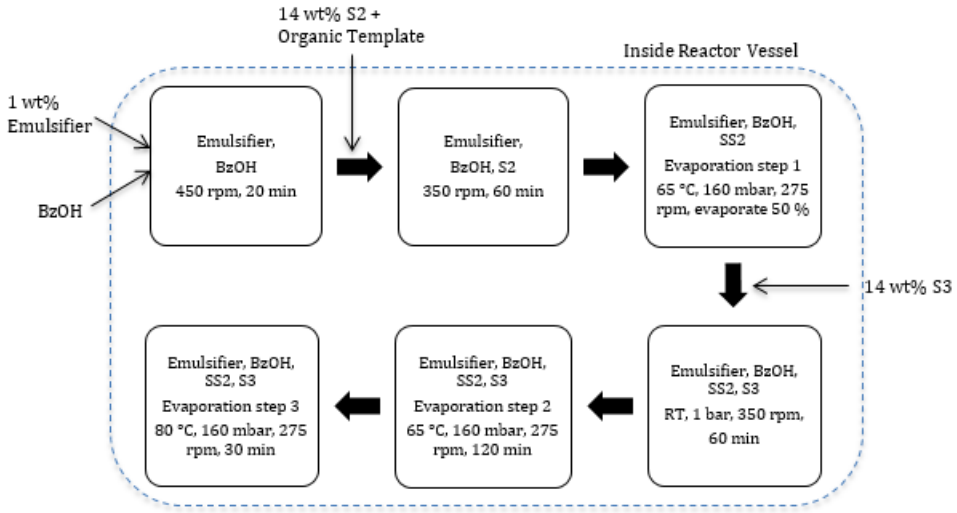

Figure B.13: Synthesis procedure according to *Route VIb*.

C

BET Results

Appendix C holds the results from the BET measurements.

Table C.1: The results from the BET measurements.

Sample	**BET Surface Area** (m^2/g)	**BJH desorption Pore volume** (cm^3/g)	**BJH adsorption average pore width** (Å)	**BJH desorption average pore width** (Å)
Test 2	400.5710	0.586316	41.537	43.553
MJJJ_1	133.8779	0.250352	56.751	58.508
MJJJ_2	136.2600	0.271819	59.428	61.932
MJJJ_7_ST1	131.7326	0.2425.42	55.165	56.246
MJJJ_9_ST1	134.7397	0.254609	56.811	59.146
MJJJ_10_FT1	133.7240	0.256664	57.329	60.060
MJJJ_12_FT1	133.3392	0.289440	64.986	68.839
MJJJ_13_FT1	131.0258	0.276986	63.606	66.598
MJJJ_19_ST3	131.9891	0.381871	89.433	94.022
MJJJ_25_S2_S3	163.5820	0.302194	53.932	52.633
MJJJ_26_S3_S2	159.2343	0.303495	55.972	54.269
MJJJ_27_salt	134.3734	0.313920	70.957	75.543
MJJJ_28_S2_S2ST3	134.8951	0.312456	70.459	75.482
MJJJ_29_S2S3	169.7754	0.253667	43.493	42.601
MJJJ_30_S2_S3	150.3964	0.263411	51.233	49.669
MJJJ_33_S2_S3ST3	151.3448	0.320939	63.331	62.523
MJJJ_35_salt	127.1088	0.430196	105.361	117.860
MJJJ_36_salt	116.9927	0.454434	120.482	133.010
MJJJ_38_salt	133.5527	0.481910	112.460	127.767
MJJJ_39_salt	132.1541	0.500167	118.448	129.934
MJJJ_40_S3	186.5173	0.296615	45.776	44.275
MJJJ_41_S2_S3	151.6778	0.279186	54.100	52.119
MJJJ_42_S1_S2	257.5018	0.390509	43.456	45.854
MJJJ_43	134.4650	0.254085	56.400	59.219

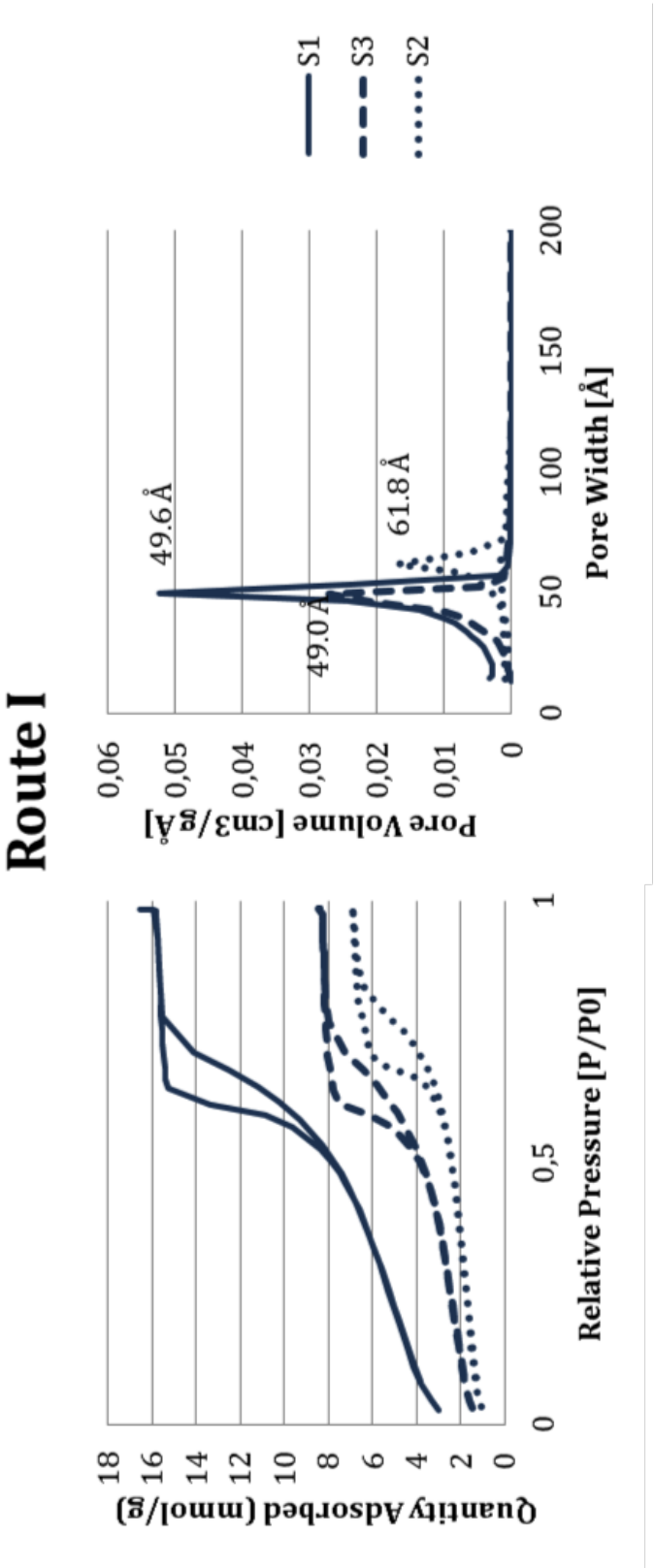
Route I
Quantity Adsorbed (mmol/g)
Relative Pressure [P/P0]
Pore Volume [cm3/gÅ]
Pore Width [Å]
49.6 Å
49.0 Å
61.8 Å
S1
S3
S2

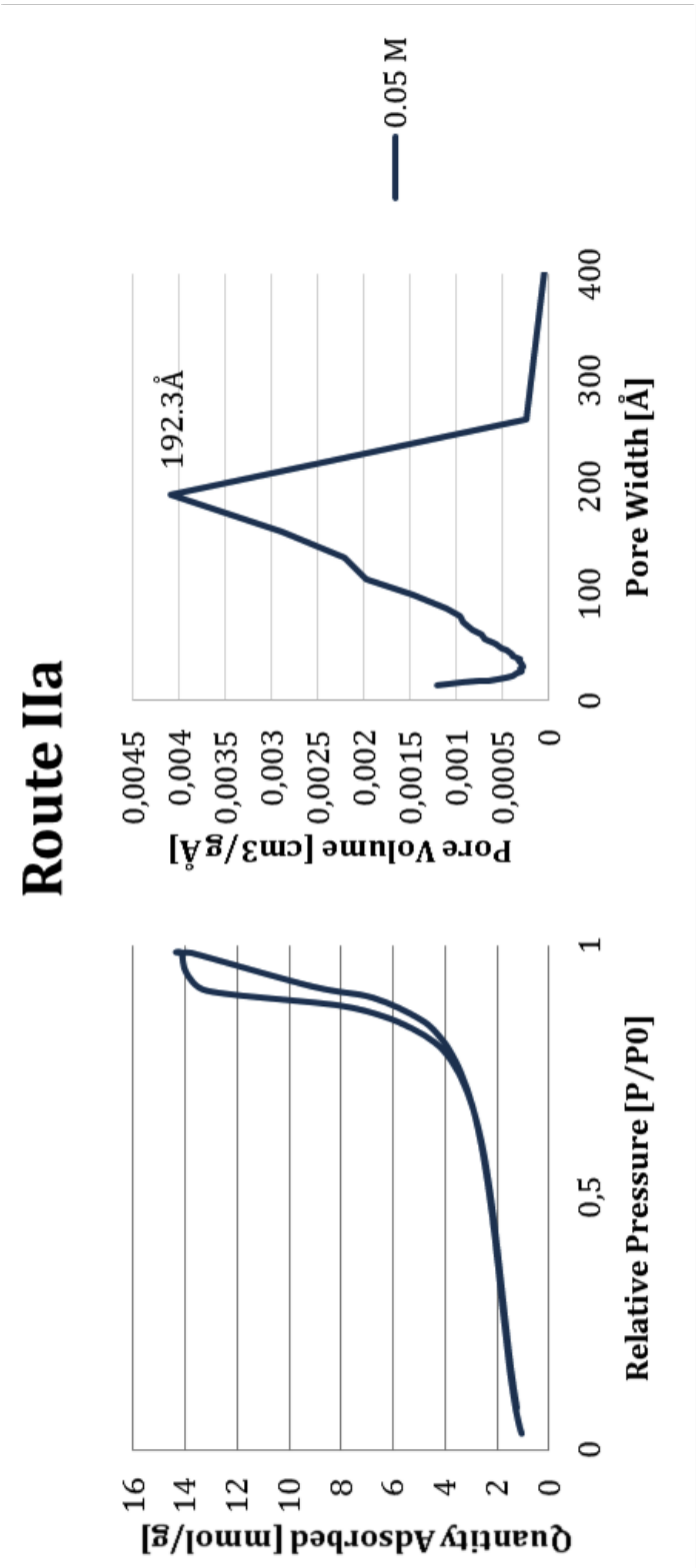
Route IIa
0.05 M
192.3Å
Pore Volume [cm3/g Å]
0,0045
0,004
0,0035
0,003
0,0025
0,002
0,0015
0,001
0,0005
0
0
100
200
300
400
Pore Width [Å]
Quantity Adsorbed [mmol/g]
16
14
12
10
8
6
4
2
0
0
0,5
1
Relative Pressure [P/P0]

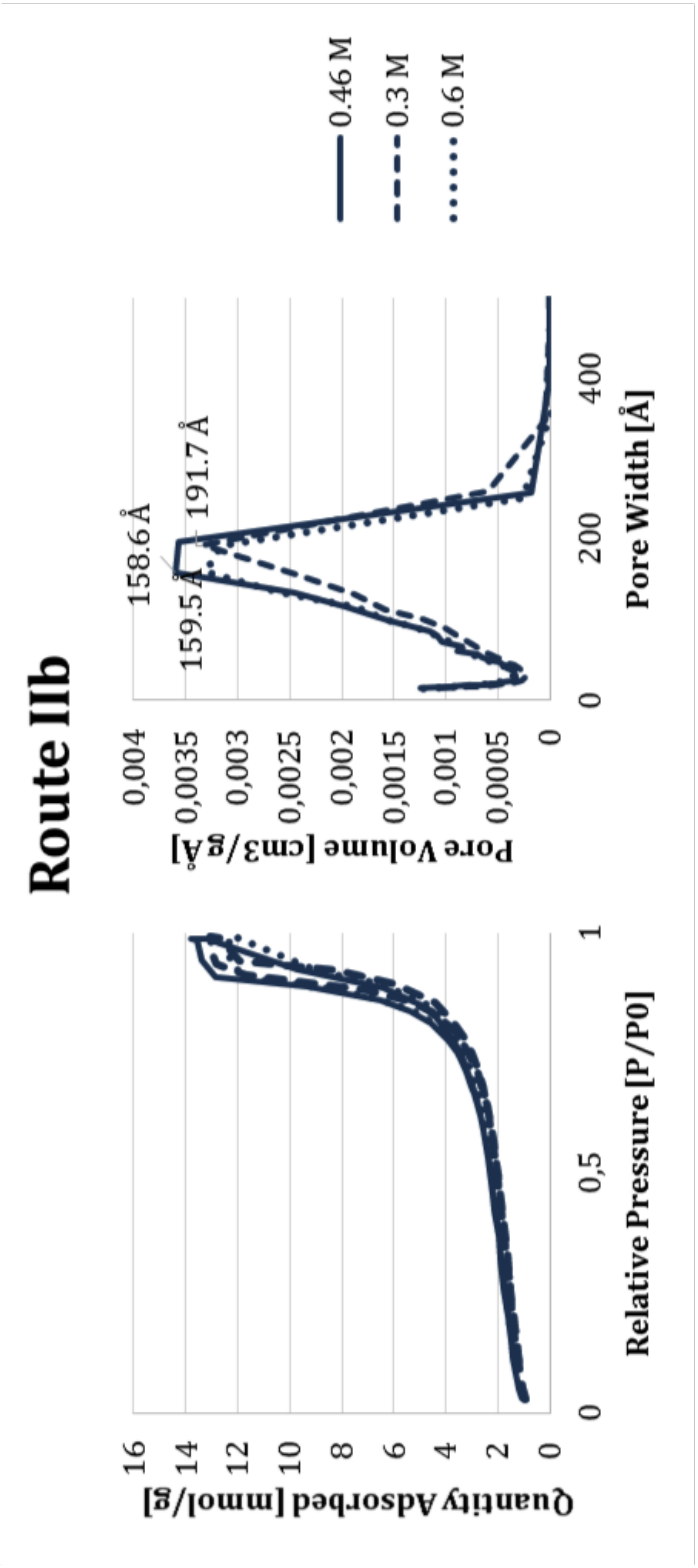
Route IIb
Quantity Adsorbed [mmol/g]
16
14
12
10
8
6
4
2
0
0
0,5
1
Relative Pressure [P/P0]
Pore Volume [cm3/gÅ]
0,004
0,0035
0,003
0,0025
0,002
0,0015
0,001
0,0005
0
158.6 Å
159.5 Å
191.7 Å
0
200
400
Pore Width [Å]
0.46 M
0.3 M
0.6 M

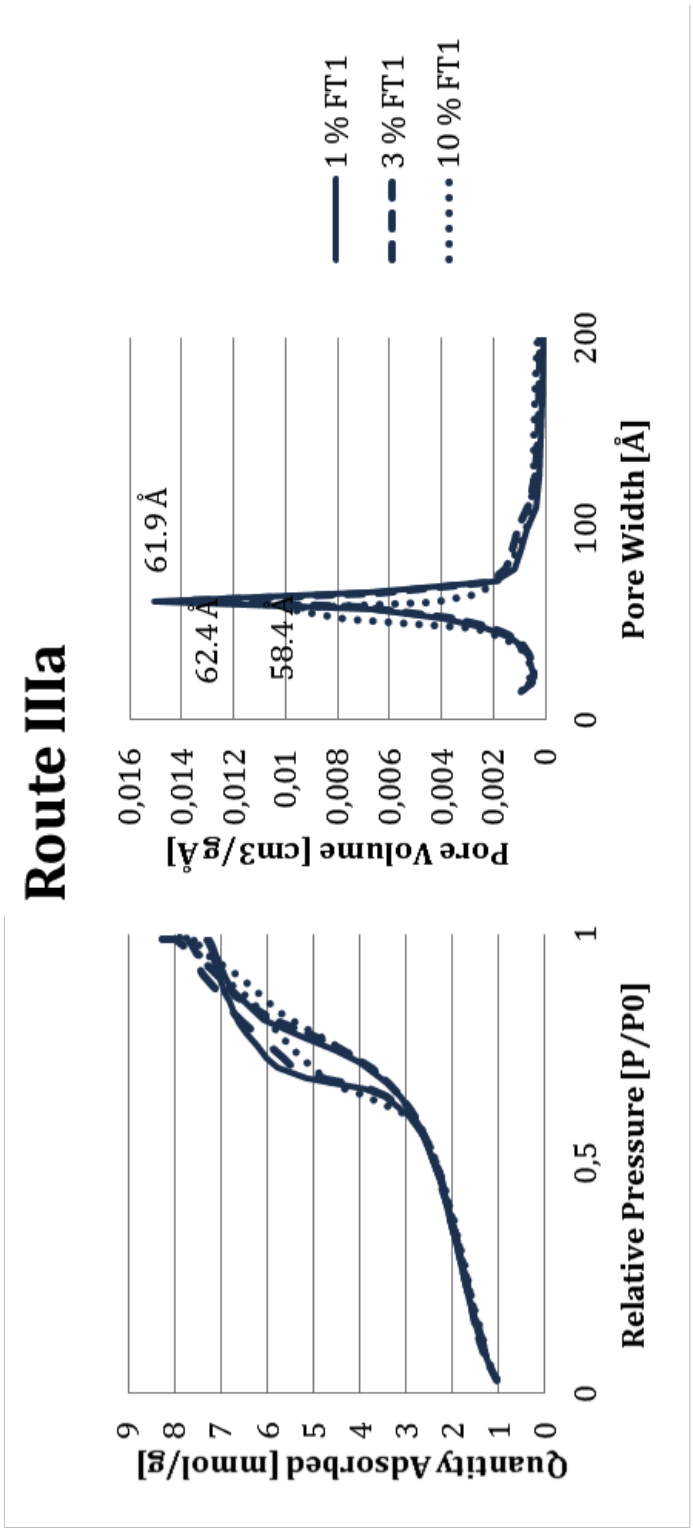
Route IIIa
Quantity Adsorbed [mmol/g]
Relative Pressure [P/P0]
Pore Volume [cm3/gÅ]
Pore Width [Å]
61.9 Å
62.4 Å
58.4 Å
1 % FT1
3 % FT1
10 % FT1

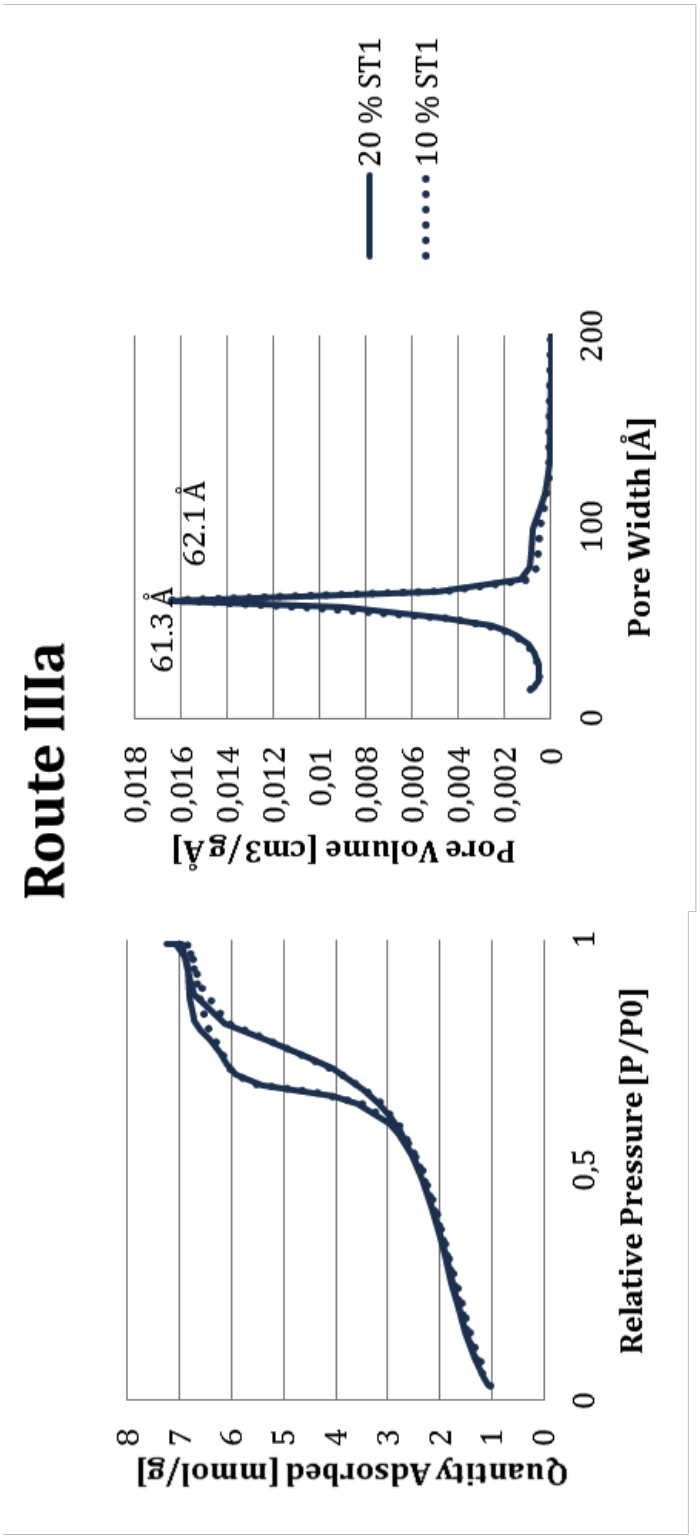
Route IIIa
Quantity Adsorbed [mmol/g]
Relative Pressure [P/P0]
Pore Volume [cm3/gÅ]
Pore Width [Å]
61.3 Å
62.1 Å
20 % ST1
10 % ST1

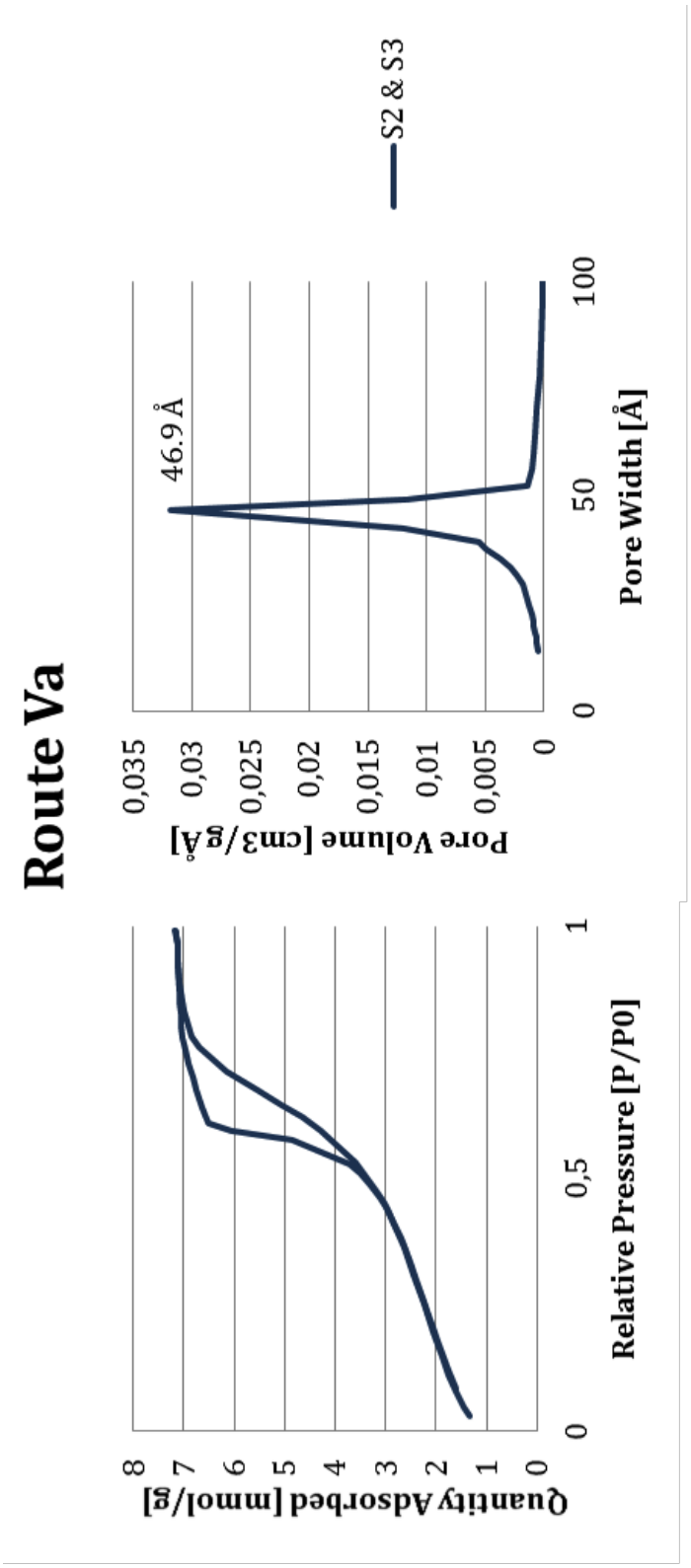
Route Va
Quantity Adsorbed [mmol/g]
0
1
2
3
4
5
6
7
8
0
0,5
1
Relative Pressure [P/P0]
Pore Volume [cm3/gÅ]
0
0,005
0,01
0,015
0,02
0,025
0,03
0,035
46.9 Å
0
50
100
Pore Width [Å]
S2 & S3

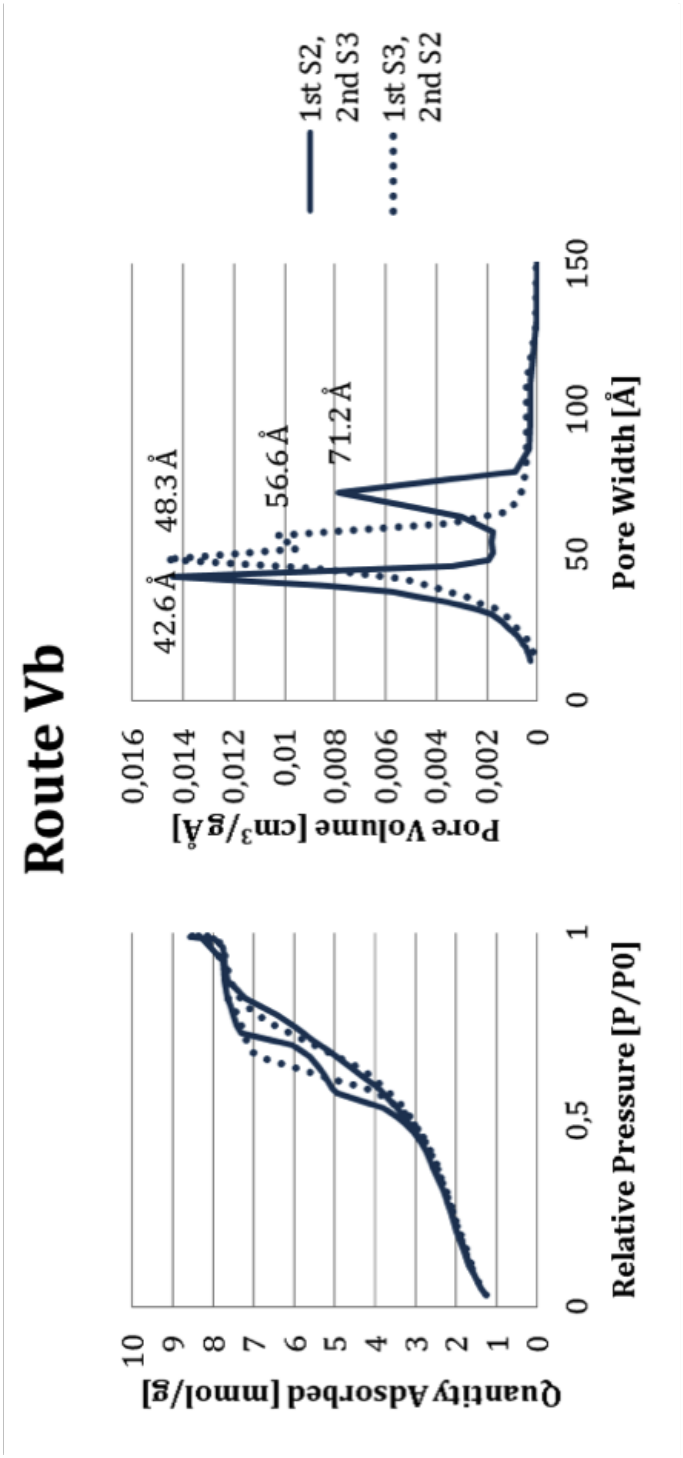
Route Vb
Quantity Adsorbed [mmol/g]
Relative Pressure [P/P0]
Pore Volume [cm³/g Å]
Pore Width [Å]
42.6 Å
48.3 Å
56.6 Å
71.2 Å
1st S2, 2nd S3
1st S3, 2nd S2

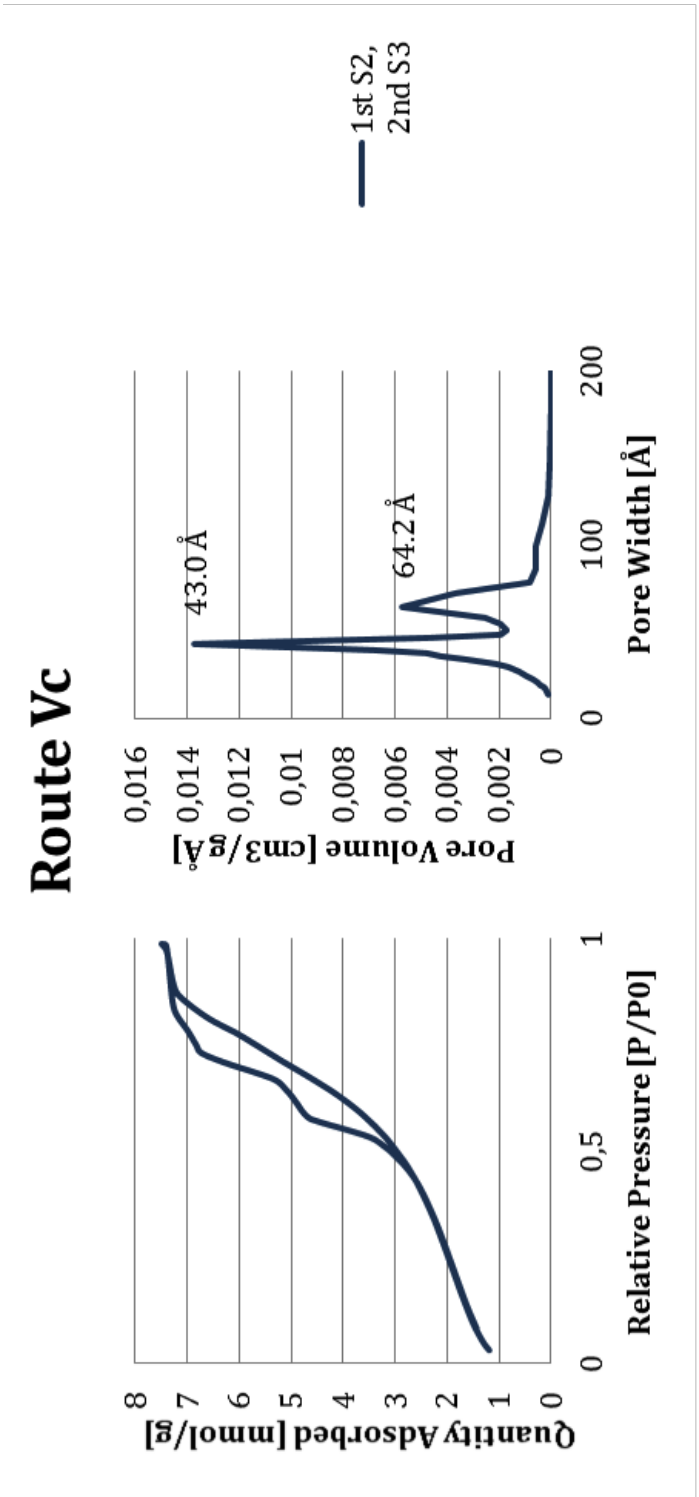
Route Vc
1st S2,
2nd S3
Quantity Adsorbed [mmol/g]
0
1
2
3
4
5
6
7
8
0
0,5
1
Relative Pressure [P/P0]
Pore Volume [cm3/gÅ]
0,016
0,014
0,012
0,01
0,008
0,006
0,004
0,002
0
43.0 Å
64.2 Å
0
100
200
Pore Width [Å]

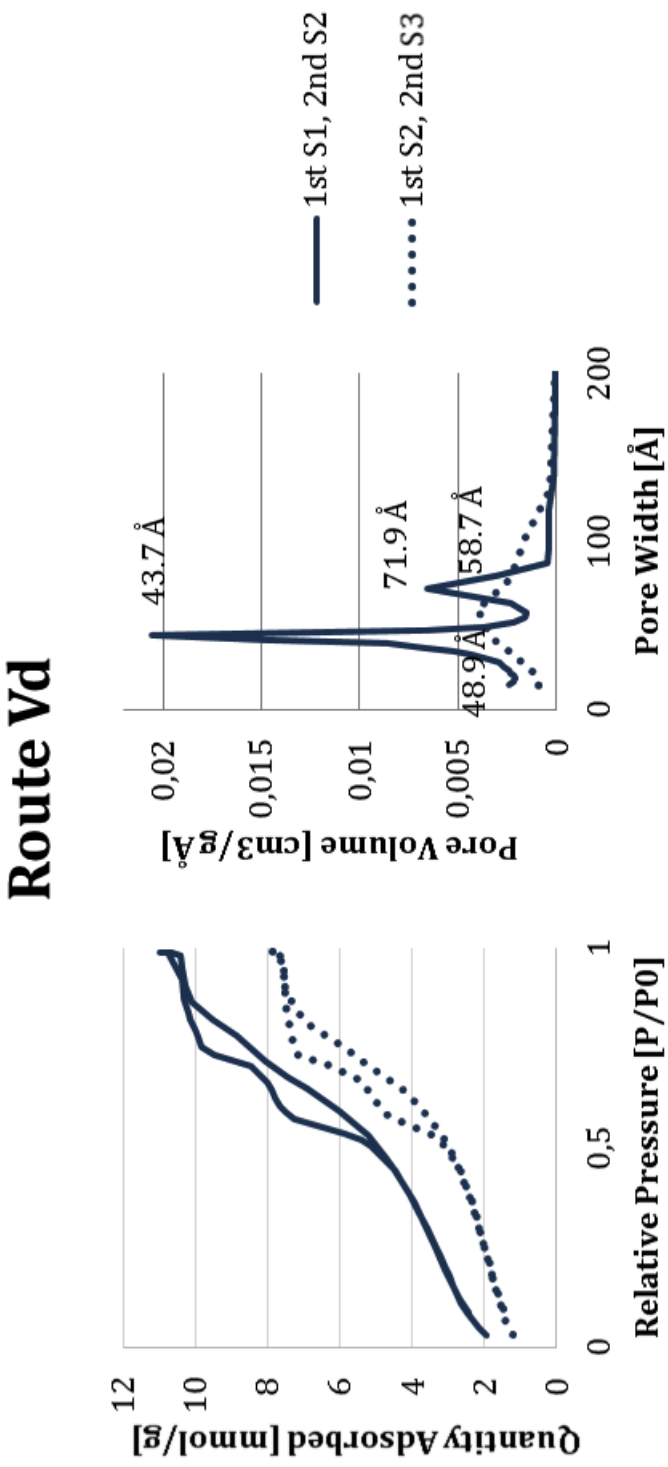
Route Vd
1st S1, 2nd S2
1st S2, 2nd S3
43.7 Å
71.9 Å
58.7 Å
48.9 Å
Pore Volume [cm3/gÅ]
0,02
0,015
0,01
0,005
0
0
100
200
Pore Width [Å]
Quantity Adsorbed [mmol/g]
12
10
8
6
4
2
0
0
0,5
1
Relative Pressure [P/P0]

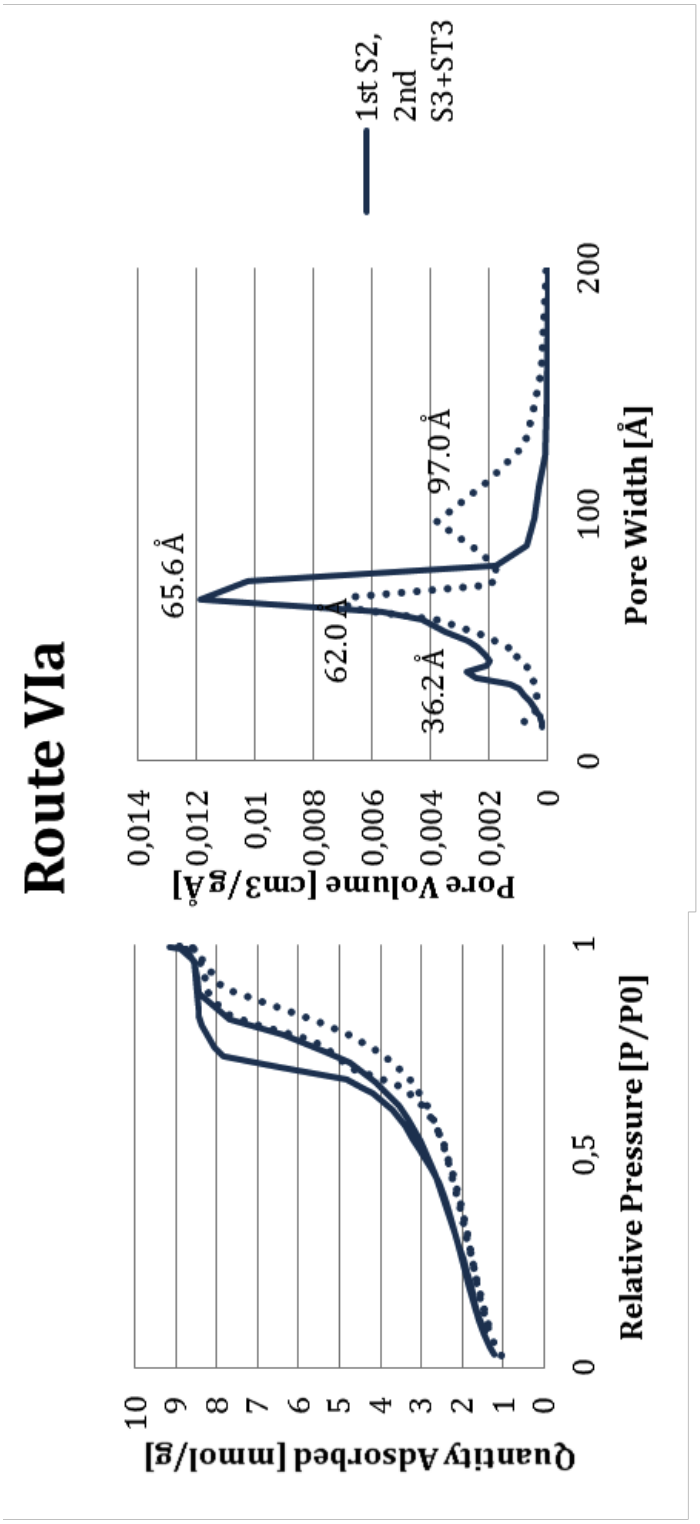
Route VIa
Quantity Adsorbed [mmol/g]
Relative Pressure [P/P0]
Pore Volume [cm3/gÅ]
Pore Width [Å]
65.6 Å
62.0 Å
36.2 Å
97.0 Å
1st S2,
2nd
S3+ST3

D

Size Determination of Porous Silica Particles

Appendix D holds the information about the particle size distribution for the syntheses made. Not all the samples where sized during the project since it would not give representative results. An example is when doing synthesis with ST1 and ammonium acetate, few spherical particles were obtained and the particle size could not be determined. Determination of particle size was not performed when the program made obvious miscalculation, for instance was unable to find the biggest particles.

Table D.1: Particle Size distributions of some of the silica particles.

Sample	**Average Particle Size** (μm)
Test 2	7.9
MJJJ_1	6.1
MJJJ_2	7.4
MJJJ_3	8.3
MJJJ_4	11.0
MJJJ_5_ST1	7.8
MJJJ_6_ST1	7.9
MJJJ_10_FT1	7.6
MJJJ_11_FT1	7.5
MJJJ_12_FT1	6.5
MJJJ_13_FT1	6.4
MJJJ_14_FT1	8.5
MJJJ_15_FT1	6.4
MJJJ_16_ST3	5.2
MJJJ_18_ST3	5.4
MJJJ_19_ST3	5.5
MJJJ_27_salt	4.8
MJJJ_28_S2_S2ST3	4.4
MJJJ_29_S2S3	6.2
MJJJ_30_S2_S3	6.0
MJJJ_33_S2_S3ST3	6.5
MJJJ_35_salt	6.2
MJJJ_40_S3	6.6
MJJJ_41_S1_S2	6.8
MJJJ_43	7.1

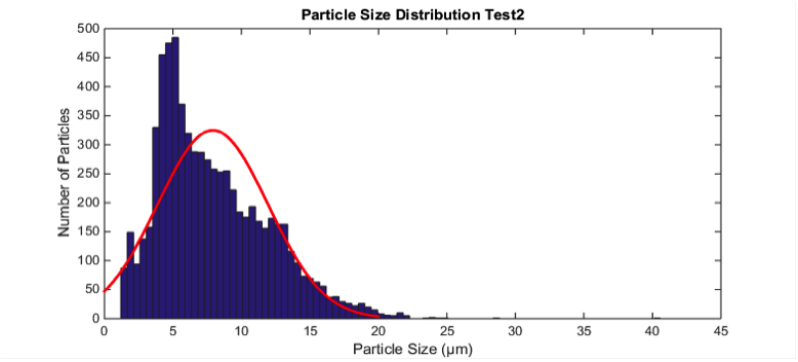

Figure D.1: Particle size distribution of particles synthesized by *Route I* with S1.

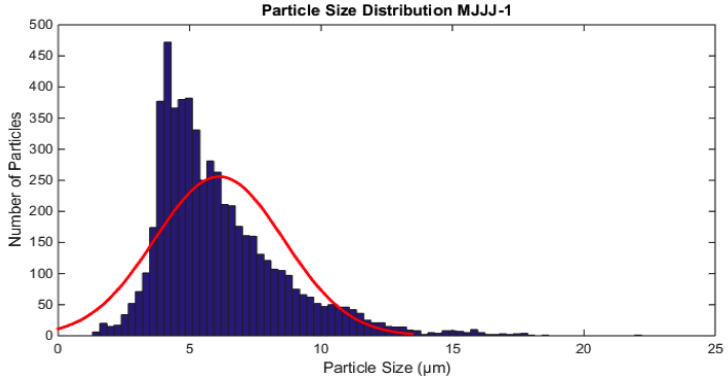

Figure D.2: Particle size distribution of particles synthesized by *Route I* with S2.

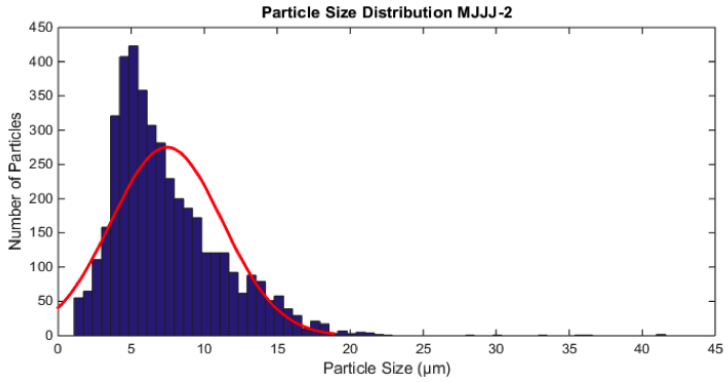

Figure D.3: Particle size distribution of particles synthesized by *Route I* with S2.

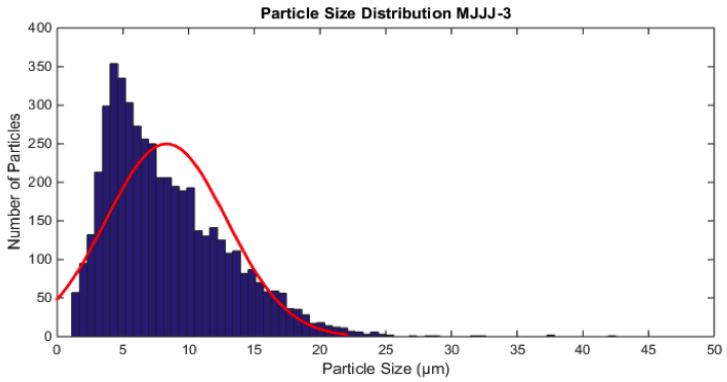

Figure D.4: Particle size distribution of particles synthesized by *Route I* with S2.

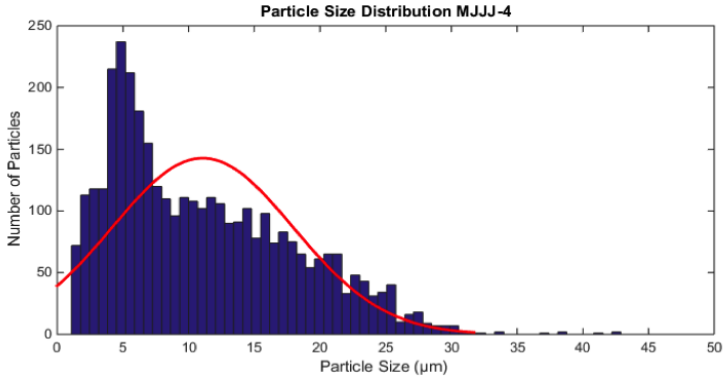

Figure D.5: Particle size distribution of particles synthesized by *Route I* with S2.

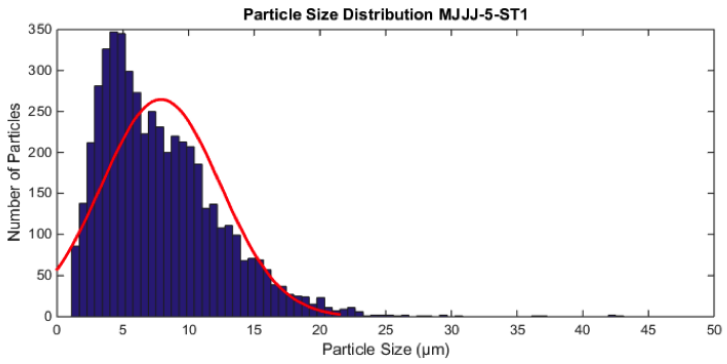

Figure D.6: Particle size distribution of particles synthesized by *Route IIIb* with S2 and 10 vol% of the silica exchanged for ST1.

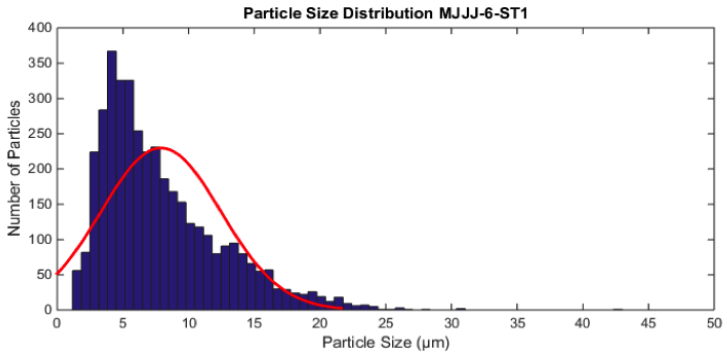

Figure D.7: Particle size distribution of particles synthesized by Route *IIIb* with S2 and 15 vol% of the silica exchanged for ST1.

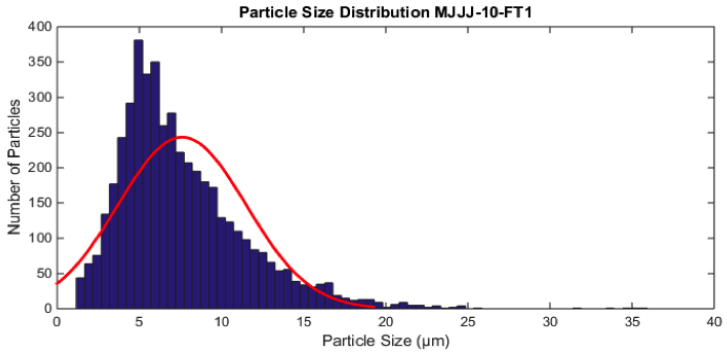

Figure D.8: Particle size distribution of particles synthesized by *Route IIIa* with S2 and 1 vol% of the silica exchanged for FT1.

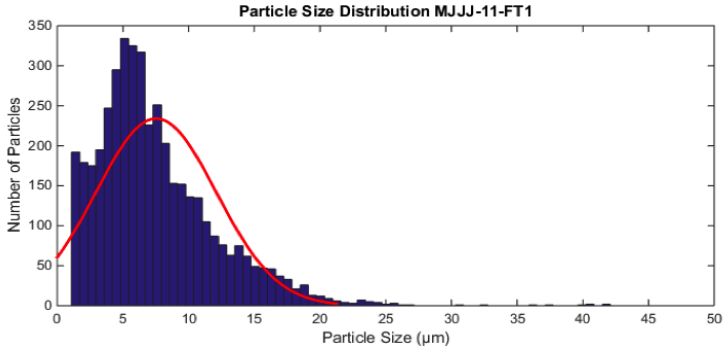

Figure D.9: Particle size distribution of particles synthesized by *Route IIIa* with S2 and 2 vol% of the silica exchanged for FT1.

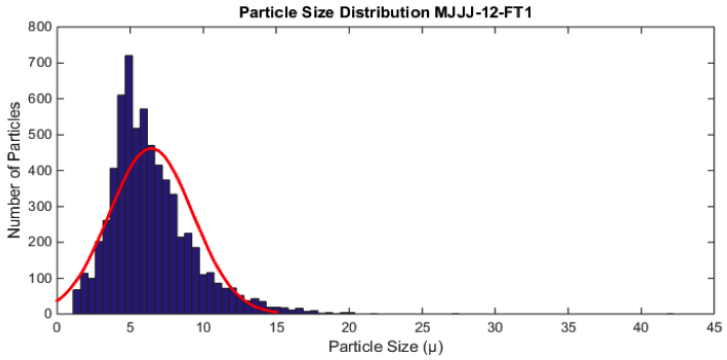

Figure D.10: Particle size distribution of particles synthesized by *Route IIIa* with S2 and 3 vol% of the silica exchanged for FT1.

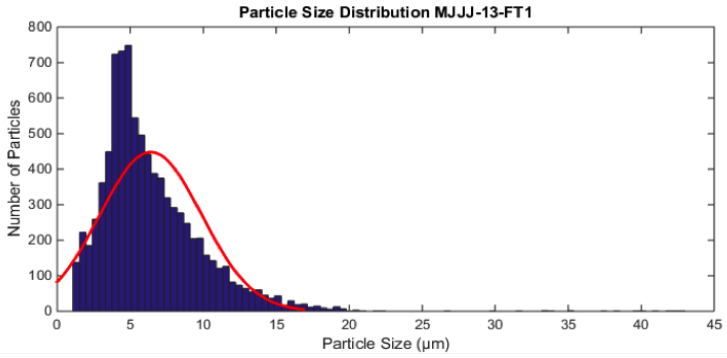

Figure D.11: Particle size distribution of particles synthesized by *Route IIIa* with S2 and 10 vol% of the silica exchanged for FT1.

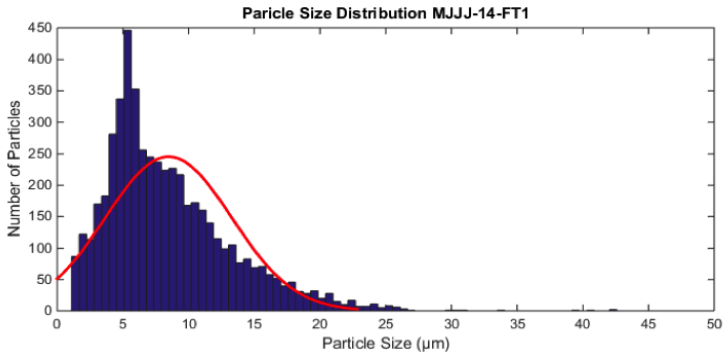

Figure D.12: Particle size distribution of particles synthesized by *Route IIIa* with S2 and 5 vol% of the silica exchanged for FT1.

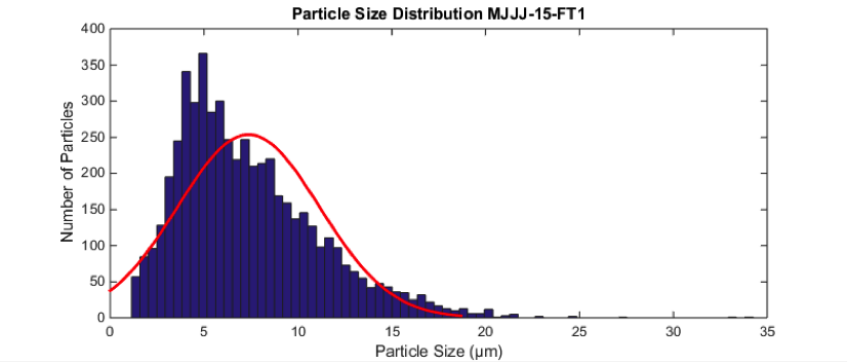

Figure D.13: Particle size distribution of particles synthesized by *Route IIIa* with S2 and 7 vol% of the silica exchanged for FT1.

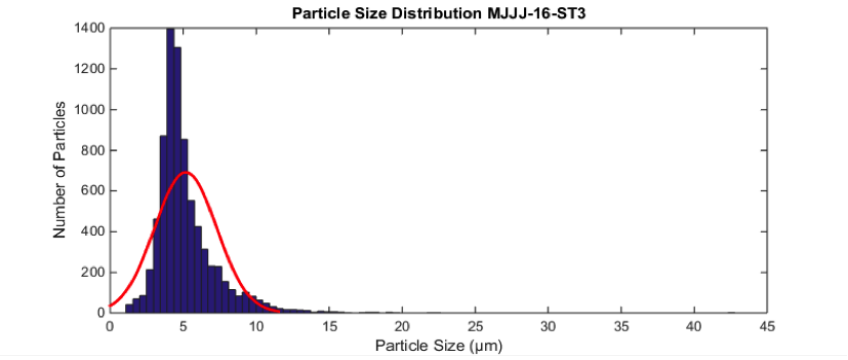

Figure D.14: Particle size distribution of particles synthesized by *Route IIIa* with S2 and 10 vol% of the silica exchanged for ST3.

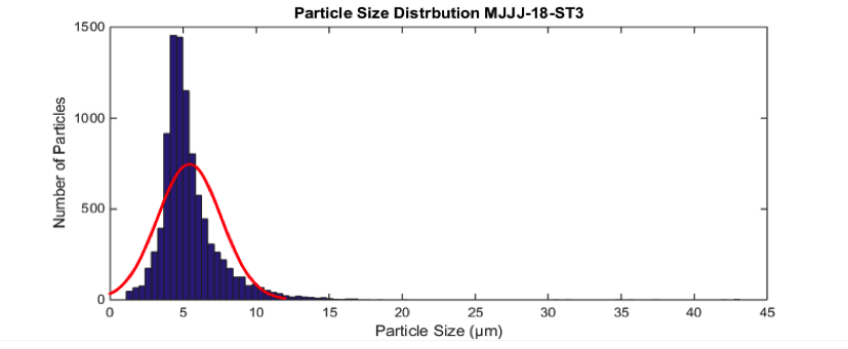

Figure D.15: Particle size distribution of particles synthesized by *Route IIIa* with S2 and 15 vol% of the silica exchanged for ST3.

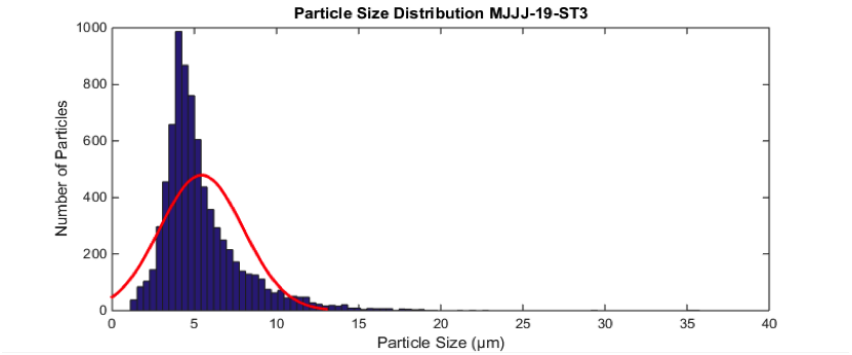

Figure D.16: Particle size distribution of particles synthesized by *Route IIIa* with S2 and 20 vol% of the silica exchanged for ST3.

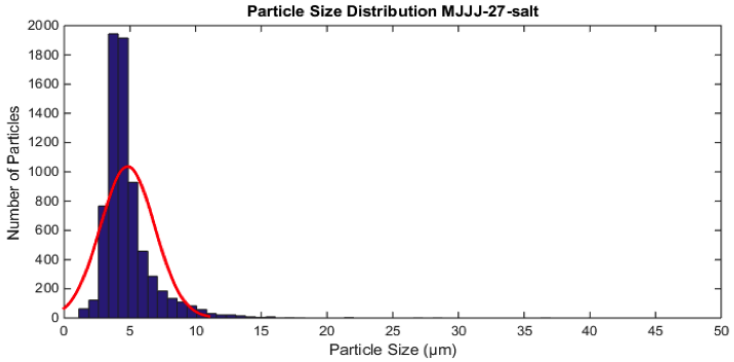

Figure D.17: Particle size distribution of particles synthesized by *Route IIb* with S2 and an ammonium acetate concentration of 0.46 M. The incubation time was set to 0 min.

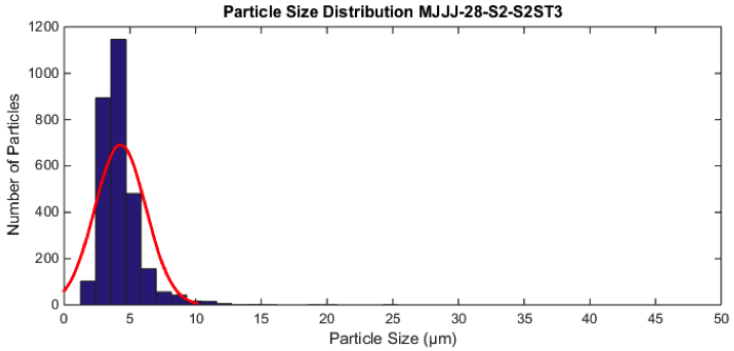

Figure D.18: Particle size distribution of particles synthesized by *Route VIa* with 1st batch being S2 dispersion and the 2nd batch being S2 dispersion with 15 vol% of the silica exchanged for ST3.

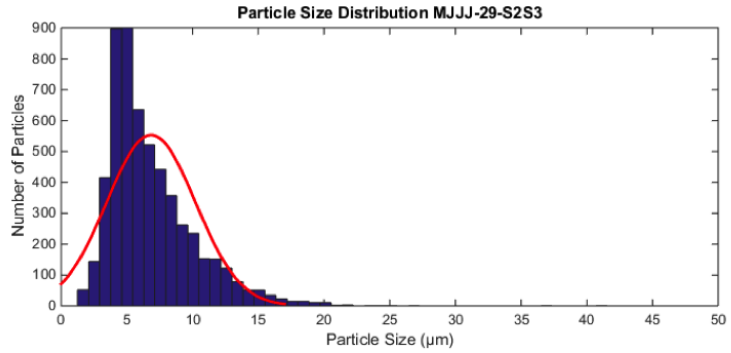

Figure D.19: Particle size distribution of particles synthesized by *Route Va* with a 1:1 mixture of S2 and S3.

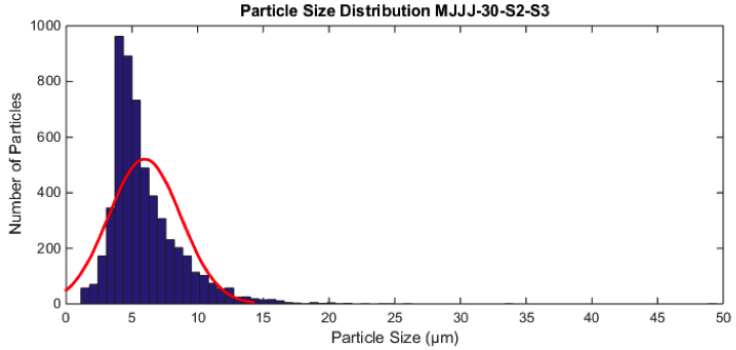

Figure D.20: Particle size distribution of particles synthesized by *Route VIa* with 1st batch being S2 dispersion and the 2nd batch being S3 dispersion with 15 vol% of the silica exchanged for ST3.

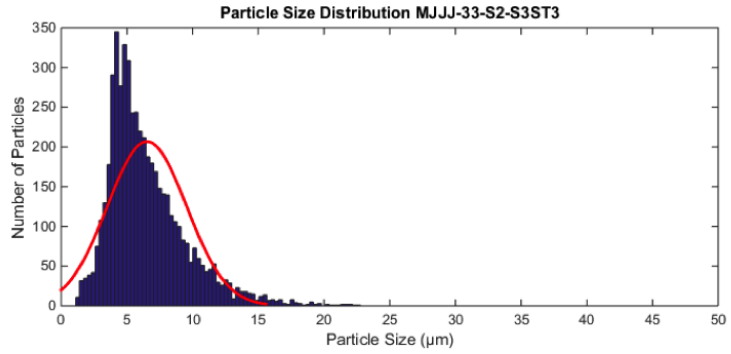

Figure D.21: Particle size distribution of particles synthesized by *Route IIb* with S2 and an ammonium acetate concentration of 0.6 M. The incubation time was set to 0 min.

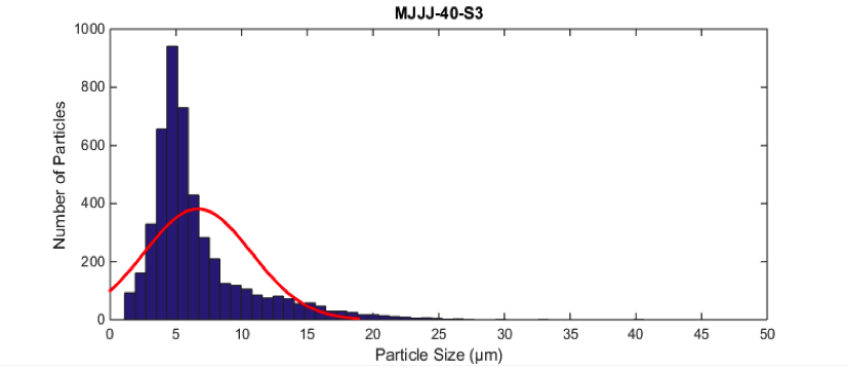

Figure D.22: Particle size distribution of particles synthesized by *Route I* with S3.

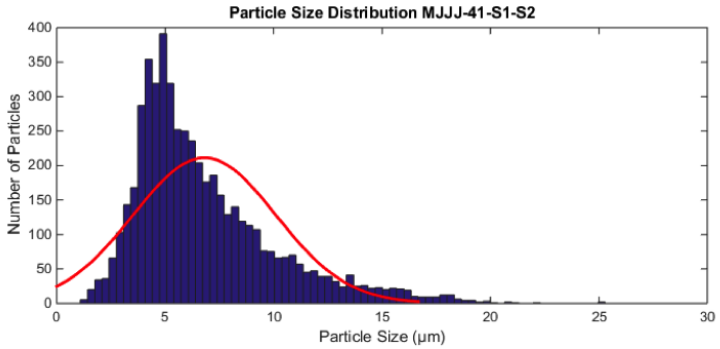

Figure D.23: Particle size distribution of particles synthesized by *Route Vd* with 1st batch being S1 dispersion and the 2nd batch being S2 dispersion.

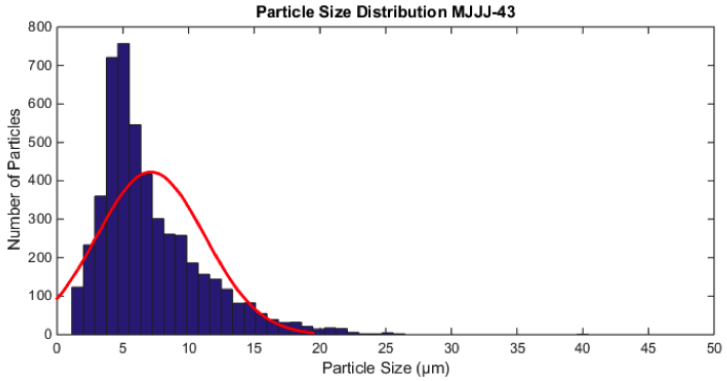

Figure D.24: Particle size distribution of particles synthesized by *Route I* with S2.